I. A NEW ELASTIC POTENTIAL FUNCTION FOR RUBBERS

II. THERMOELASTIC BEHAVIOR OF RUBBERS

Thesis by

Satish C. Sharda

In Partial Fulfillment of the Requirements

for the Degree of

Doctor of Philosophy

California Institute of Technology

Pasadena, California

1974

(Submitted January 18, 1974)

to my parents

ACKNOWLEDGEMENT

In concluding my research at California Institute of Technology, I am most grateful to Professor N. W. Tschoegl for the privilege of closely working with him. I deeply appreciate his guidance, encouragement and help concerning my research as well as advancements in my personal life. Most of all, I wish to thank Dr. Tschoegl for numerous efforts on my behalf and for a deep interest in the professional and private lives of his students.

I am grateful to Dr. P. J. Blatz for guidance and extremely helpful suggestions in my research. I also wish to thank Dr. Blatz for his time and many long and pleasant discussions.

Special thanks are extended to Robert W. Fillers for a close friendship we share. I am equally thankful to my office-mate Robert E. Cohen for a very fruitful companionship. Thanks are due to Wenji V. Chang, R. Bloch, K. Yagii and M. Okuyama for helpful suggestions and discussions.

Above all I am grateful to Mrs. Eileen Finke, not only for typing parts of this thesis and various other manuscripts, but also for all the help she provided during my residence at Caltech. Finally, it is a pleasure to acknowledge the skillful assistance of Mrs. Jennifer Burkhart and Ms. Judith Dedmon for typing parts of this manuscript.

ABSTRACT

The internal energy and the entropy components of the elastic restoring force in rubbers were determined for natural rubber up to an extension ratio of about 3.0. Four different experimental measurements were necessary to determine these components: (1) the force-temperature coefficient at constant temperature and length; (2) the force-pressure coefficient at constant temperature and length; (3) the thermal expansion coefficient at constant length; and (4) the isothermal compressibility at constant length. The force-temperature and the force-pressure coefficients were functions of strain whereas the expansion coefficients and the isothermal compressibilities were independent of strain. These measurements gave an internal energy contribution of 23% for natural rubber independent of the strain over the range of extensions studied.

To describe the thermal as well as the elastic behavior of rubbers a new phenomenological description of elastomers based on a generalized measure of strain was developed. The incompressible form of the strain energy function correctly described the elastic data on various elastomers (natural rubber, styrene-butadiene rubber, chlorinated ethylene-propylene copolymer rubber) in both homogeneous and non-homogeneous deformation fields. For a given rubber the same set of parameters fitted the data in simple tension, simple compression, equal biaxial tension and pure shear up to the point of rupture.

The compressible form of the strain energy function also described

the thermoelastic data on natural rubber. The thermoelastic data on chlorinated ethylene-propylene copolymer rubber, taken out of the literature,were also predicted. From the new strain energy function it was possible to determine the interchain interactions. For natural rubber the interchain energy effects were found to be small (4%) as compared to the intrachain energy effects.

The experimental results on natural rubber established the range of validity of the statistical mechanical (molecular) and the continuum mechanical (phenomenological) theories. The temperature coefficient of the unperturbed dimensions of natural rubber determined from the internal energy component of the force yielded the conformational energies associated with the cis-polyisoprene chain.

TABLE OF CONTENTS

PART II

LIST OF FIGURES

LIST OF TABLES

PREFACE

From thermoelastic data on rubbers it is possible to derive information on the hindrance potentials governing the flexibility of the network chains. Such data permit the calculation of the temperature coefficient of the unperturbed dimensions of the network chains. This can be used to describe the conformational changes accompanying the deformation of the network.

The research reported here focuses on the thermoelastic behavior of rubberlike substances with emphasis on the energetic and the entropic components of the elastic retractive force. The elasticity of rubbers is studied from the thermodynamical, the continuum mechanical (phenomenological) and the statistical mechanical (molecular) viewpoints.

The first part of this thesis describes a new elastic potential function (or strain energy function) capable of describing the deformation behavior of an elastomer when it can be considered to be incompressible. The applicability of this phenomenological function is demonstrated in various deformation fields. The study also includes the effect of temperature on the parameters of the potential function.

The second part considers the thermodynamic behavior of elastomers. A general analysis of the large principal deformation of a homogeneous isotropic elastomer is presented. The thermodynamics of the retractive force in elastomers is discussed from the viewpoint of the statistical mechanical theory. The strain energy function described in

the first part is here extended to account for compressibility. Experiments necessary to determine the energetic and the entropic components of the retractive force based on classical thermodynamics are detailed. The results are compared with the predictions of the phenomenological and the molecular theories. The most satisfactory fit is obtained with the compressible form of the new elastic strain energy function. It is shown that this new equation permits determination of the temperature coefficient of the unperturbed displacement length of long chain molecules by relatively simple experiments.

PART I

A NEW ELASTIC POTENTIAL FUNCTION FOR RUBBERS

1. INTRODUCTION

The mechanical deformation of rubberlike materials has been widely considered in the literature using both the molecular (statistical) and the phenomenological (continuum) approaches. The most widely accepted statistical theory is the well known network theory of rubber elasticity (1, 2, 3, 4). The equation of state which this theory furnishes, however, is at best applicable to small deformations. The other widely used approach is the phenomenological theory of large deformations. The development of the phenomenological theory, in contrast to the statistical theory, has been quite general (5, 6) and more successful (2).

The ultimate goal of these theories is to predict the state of strain in a body deformed by applied stresses. This is customarily achieved through a function known as the strain energy density, or elastic potential, or increase in Helmholtz free energy, accompanying the deformation. Once the strain energy function is known, the elastic properties of the material are completely defined. In the forthcoming discussion, a new elastic potential for the mechanical deformation of rubberlike materials is introduced and the application of this function in various modes of deformation is demonstrated.

The stress-strain relation is derived from the strain energy function by the principle of virtual work (6). For an isotropic material it is known that the elastic potential depends implicitly on the strain through three invariants of the strain tensor. The open problem in characterizing rubberlike materials is how best to express the elastic

potential in terms of the state of strain in the material. There are essentially two options available in approaching this problem. One may choose a given measure of strain (such as the Cauchy, Green, Almansi, Hencky, etc., strain), and then construct a strain energy function which best fits mechanical data in divers stress fields, regardless of the mathematical complexity of this function. Alternatively, one may search for a more generalized measure of strain (one which contains within itself one or more free parameters), and construct a mathematically less complex strain energy density which fits the data equally well or better. The latter approach is adopted here.

A general measure of strain based on an arbitrary power of the stretch ratio was first introduced by Seth (7). We call this the n-measure. Hsu (8) applied this measure successfully to various metallic materials. Blatz, Chu, and Wayland (9) and later Chu and Blatz (10) applied the same measure to rubberlike materials and elastic animal tissues. In a recent paper Ogden (11) used a similar approach and constructed a strain energy density which is a linear combination of terms involving various powers of the stretch ratios. In his paper no reference was made to the earlier work of Blatz, Chu, and Wayland. Specifically, Ogden used a combination of three terms of the form first introduced by Blatz et al.

The proposed new potential is based on a nonlinear combination of terms involving a single power of the stretch ratio (12, 13, 14). The final form of the strain energy function is quite different from that of Ogden and contains fewer parameters.

2. THE GENERALIZED MEASURE OF STRAIN

A rubberlike material may be assumed to be isotropic in the undeformed state; the strain energy density therefore depends on the strain implicitly through three symmetric functions of the principal stretch ratios λ_1, λ_2, and λ_3.

It is customary to associate with the stretch field two strain fields.

$$E_\alpha = (\lambda_\alpha^2 - 1)/2 \tag{2.1}$$

in a *material* (or *Lagrangean*) coordinate system, and by

$$e_\alpha = (1 - \lambda_\alpha^{-2})/2 \tag{2.2}$$

in a *spatial* (or *Eulerian*) system. Here ($\alpha = 1, 2, 3$) denotes the three principal directions. These have been widely used in continuum mechanics to formulate the constitutive theories of materials and to solve problems involving finite strains.

Seth suggested a more general measure to characterize the deformation field. His measure of strain is based on the realization that there is no unique definition of strain; rather, the most convenient strain measure is a property of the material and of the geometry of the deformation. This measure of strain is

$$E_\alpha = (\lambda_\alpha^{\,n} - 1)/n \tag{2.3}$$

in the material description, and

$$e_\alpha = (1 - \lambda_\alpha^{\,-n})/n \tag{2.4}$$

in the spatial description of the deformation. We note that $e_\alpha(-n) = E_\alpha(n)$. For $n = 2, 1, 0, -1, -2$, Eq. (2.3) yields Green's, Cauchy's, Hencky's, Swainger's, and Almansi's strain measure. However, the coefficient of strain measure $\underline{n}$ need not be an integer (8). By introducing a degree of freedom in the coefficient $\underline{n}$, it is possible to incorporate more of the nonlinear behavior of the material in the definition of strain, and less of the nonlinear behavior in the constitutive relation between the strain energy density and the strain. Indeed, it is possible to represent the stress-strain behavior of several rubberlike materials, each in several deformation fields, by a very simple stress-strain relation in which the strain is based on the n-measure, $\underline{n}$ being adjusted for the best fit to the data. The coefficient $\underline{n}$ is thus a material constant, and the strain measure becomes a material as well as a kinematic quantity.

3. THE ISOTROPIC STRAIN ENERGY DENSITY

It is expedient to represent the strain dependence of an isotropic strain energy function in terms of three invariants of the deformation. Rivlin (5) pioneered the use of the principal invariants of the right Cauchy-Green deformation tensor

$$I_1 = \sum_\alpha \lambda_\alpha^2 \tag{3.1}$$

$$I_2 = \frac{1}{2} \sum_\alpha \sum_\beta \lambda_\alpha \lambda_\beta \qquad (\alpha \neq \beta) \tag{3.2}$$

and

$$I_3 = \prod_\alpha \lambda_\alpha^2 \tag{3.3}$$

which have since been widely used. One is free, however, to choose any set of three symmetric functions. We elect to work with the principal invariants of the strain tensor defined in Eqs. (3.4) through (3.6). These invariants are

$$I_E = \sum_\alpha E_\alpha \tag{3.4}$$

$$II_E = \frac{1}{2} \sum_\alpha \sum_\beta E_\alpha E_\beta \qquad (\alpha \neq \beta) \tag{3.5}$$

and

$$III_E = \Pi_\alpha E_\alpha \tag{3.6}$$

We note that I_E, II_E, and III_E are the invariants of linear theory, but are based on a nonlinear measure of strain. However, this choice is not unique. One may choose any three symmetric functions of the stretch ratios. In a general sense, one can define invariants on perfectly arbitrary functions of the stretch ratios, namely:

$$I = \sum_\alpha w(\lambda_\alpha) \tag{3.7}$$

$$II = \frac{1}{2} \sum_{\alpha,\beta} w(\lambda_\alpha)\ w(\lambda_\beta) \tag{3.8}$$

$$III = \Pi_\alpha w(\lambda_\alpha) \tag{3.9}$$

Thus, the most general elastic potential, therefore, is

$$W = W(I, II, III) \tag{3.10}$$

In the particular case, where I, II, and III are replaced by I_E, II_E, and III_E, respectively, we may rewrite Eq. (3.10) as

$$W = W(I_E, II_E, III_E) \tag{3.11}$$

According to the principle of virtual work, the Cauchy principal stress is obtained as

$$\bar{\sigma}_\alpha = \lambda_\alpha \frac{\partial W}{\partial \lambda_\alpha} = \lambda_\alpha \frac{dE_\alpha}{d\lambda_\alpha} \frac{\partial W}{\partial E_\alpha} = \lambda_\alpha^n \frac{\partial W}{\partial E_\alpha} = (1 + n\, E_\alpha) \frac{\partial W}{\partial E_\alpha} \tag{3.12}$$

where the bar on σ denotes true stress. The form of Eq. (3.12) in general coordinates is given in the Appendix (1). Because the deformation behavior of rubberlike materials is very nearly isochoric, it is convenient to invoke the assumption of incompressibility and impose a constraint among the three invariants. From Eq. (2.3) we have

$$\lambda_\alpha^{\,n} = 1 + n\, E_\alpha \tag{3.13}$$

and

$$\Pi_\alpha \lambda_\alpha^{\,n} \equiv J^n = 1 + n\, I_E + n^2\, II_E + n^3\, III_E \tag{3.14}$$

The assumption of incompressibility, $J = 1$, then establishes the relation

$$(J^n - 1)/n = I_E + n\, II_E + n^2\, III_E = 0 \tag{3.15}$$

between the three invariants. Because of this constraint, it is necessary to rewrite the strain energy density function as

$$W(I_E, II_E, III_E) = \bar{W}(I_E, II_E) + k\,(J^n - 1)/n \tag{3.16}$$

where k is a Lagrangean multiplier. The leading term of $\bar{W}$ will, of course, be limited in the sense that Eq. (3.16) must reduce to Hooke's law for small strains.

We now proceed to eliminate the Lagrangean multiplier k, and then rewrite Eq. (3.16) in terms of $\bar{W}$. Since $\bar{W}$ is a function of I_E and II_E, we may write

$$\frac{\partial \bar{W}}{\partial E_\alpha} = \bar{W}_I \frac{\partial I_E}{\partial E_\alpha} + \bar{W}_{II} \frac{II_E}{\partial E_\alpha} \tag{3.17}$$

where

$$\bar{W}_I = \frac{\partial \bar{W}}{\partial I_E} \tag{3.18}$$

and

$$\bar{W}_{II} = \frac{\partial \bar{W}}{\partial II_E} \tag{3.19}$$

From Eqs. (3.4) and (3.5) we have

$$\frac{\partial I_E}{\partial E_\alpha} = 1 \tag{3.20}$$

$$\frac{\partial II_E}{\partial E_\alpha} = I_E - E_\alpha \tag{3.21}$$

Substituting Eq. (3.16) into Eq. (3.12), differentiating, and using Eq. (3.15) yields

$$\bar{\sigma}_\alpha = k + (1 + n\, E_\alpha)\left[\bar{W}_I + (I_E - E_\alpha)\,\bar{W}_{II}\right] \tag{3.22}$$

Equation (3.22) is perfectly general within the validity of the assumption of incompressibility. Elimination of k gives the principal stress differences as

$$\bar{\sigma}_\alpha - \bar{\sigma}_\beta = (\lambda_\alpha^{\,n} - \lambda_\beta^{\,n})\left[\bar{W}_I + (\lambda_\gamma^{\,n} - 2)\,\bar{W}_{II}/n\right] \tag{3.23}$$

After expanding $\bar{W}(I_E, II_E)$ in a Taylor series, retaining the first term only, and identifying

$$\bar{W}_I(0, 0) = 2G/n \tag{3.24}$$

to satisfy the requirement of Hooke's law, we obtain

$$\bar{W} = \frac{2G}{n} I_E \tag{3.25}$$

This simple elastic potential is general enough to fit most data on rubberlike materials up to about 200% strain in simple tension, and to equivalent deformations in other stress fields, with a suitable choice of the constant n. It contains the neo-Hookean potential for n = 2, and the potential of Dickie and Smith (15) for n = 1.

A particularly simple form of Eq. (3.10), namely

$$W = I \tag{3.26}$$

was chosen by Valanis and Landel (16) to represent data on natural rubber. The same approach has since been used by Dickie and Smith (15) and by Kawabata (17).

Equation (3.26), when written out explicitly, becomes

$$W = w(\lambda_1) + w(\lambda_2) + w(\lambda_3) \tag{3.27}$$

This equation was found (15, 16, 17) to represent data in different deformation fields up to about the same stretch ratios for which Eq. (3.25) also gives an adequate description of the data. Equation (3.27) implies separability of the elastic potential into three principal contributions based on the single function, $w(\lambda_\alpha)$. Equation (3.25) contains the same feature and it is, in fact, easily shown that

$$w(\lambda_\alpha) = 2G(\lambda_\alpha^{\,n} - 1)/n \tag{3.28}$$

One can evaluate $w(\lambda_\alpha)$ as a function of λ_α experimentally (15, 16, 17, 18). In moderate deformations, therefore, the two approaches represented by Eqs. (3.25) and (3.27), respectively, are equivalent and a choice can be made only on the grounds of simplicity. There is no known basis in thermodynamics or statistical mechanics for concluding that the elastic potential must be separable.

Before studying the new strain energy function in various deformation fields, the theoretical predictions of Eq. (3.25) for different values of n may be considered.

For simple tension Eqs. (3.12) and (3.25) give

$$\bar{\sigma} = (2G/n)\ (\lambda^n - \lambda^{-n/2}) \tag{3.29}$$

Plots of $\bar{\sigma}/G$ vs. λ or λ^{-1} are shown in Fig. 1 for values of n ranging from 0 to 10. It is evident that the n-measure of strain contributes an important degree of freedom in describing the behavior of incompressible nonlinear elastic materials.

To achieve a satisfactory fit of the data at deformations higher than those which the simple strain potential, Eq. (3.25), can handle, higher terms in the expansion are needed. Rather than adding higher terms in the second, third, etc., powers of the invariants we found it more convenient to write our strain energy density function in the form

$$\bar{W} = \frac{2G}{n} I_E + B\ I_E^{\ m} \tag{3.30}$$

where B and m are two additional material parameters.

As previously stated, Eq. (3.30) is a nonlinear combination of terms based on the n-measure of strain. Hill suggested that a strain energy density obey his inequality (19). For Eq. (3.30) this leads to $n > 0$ and $m > 1$ (Appendix 2).

It will now be shown that this strain energy function provides an excellent fit to data obtained in various deformation fields (both homogeneous and inhomogeneous) up to the point of rupture with the same

material constants G, n, B, and m for a given material. Equation (3.30) thus leads to true constitutive relations.

4. HOMOGENEOUS DEFORMATION FIELDS

We now examine the form of our constitutive equation, Eq. (3.30), in several different deformation fields. Substitution of Eq. (3.30) into Eq. (3.23) gives

$$\bar{\sigma}_\alpha - \bar{\sigma}_\beta = (\lambda_\alpha^{\,n} - \lambda_\beta^{\,n})\ (2G/n + m\ B\ I_E^{\,m-1}) \tag{4.1}$$

Eq. (4.1) can now be specialized.

4.1 Simple Tension

In simple tension $\lambda_1 = \lambda$, $\lambda_2 = \lambda_3 = \lambda^{-1/2}$ $\bar{\sigma}_1 = \bar{\sigma}$, and $\bar{\sigma}_2 = \bar{\sigma}_3 = 0$. Hence, from Eq. (4.1)

$$\bar{\sigma} = (\lambda^n - \lambda^{-n/2})\ (2G/n + m\ B\ I_E^{\,m-1}) \tag{4.2}$$

where

$$I_E = (\lambda^n + 2\lambda^{-n/2} - 3)/n \tag{4.3}$$

4.2 Equibiaxial Tension or Simple Compression

In equibiaxial tension $\lambda_1 = \lambda_2 = \lambda$, $\lambda_3 = \lambda^{-2}$, $\bar{\sigma}_1 = \bar{\sigma}_2 = \sigma$, and $\bar{\sigma}_3 = 0$. Hence

$$\bar{\sigma} = (\lambda^n - \lambda^{-2n})\ (2G/n + m\ B\ I_E^{m-1}) \tag{4.4}$$

where

$$I_E = (2\lambda^n + \lambda^{-2n} - 3)/n \tag{4.5}$$

For an incompressible material the state of deformation in simple compression and in equibiaxial tension is the same. Hence, the behavior in simple compression can be calculated from that in equibiaxial tension. Letting subscript c denote the former, and subscript t the latter, we have $\lambda_c = \lambda_t^{-2}$ and $\sigma_c = -\lambda_t^{3}\ \sigma_t$.

4.3 Pure Shear

In pure shear $\lambda_1 = \lambda$, $\lambda_2 = 1$, $\lambda_3 = \lambda^{-1}$, $\bar{\sigma}_1 = \bar{\sigma}$, $\bar{\sigma}_2 = \bar{\sigma}'$, and $\bar{\sigma}_3 = 0$, where $\bar{\sigma}$ is the maximum, and $\bar{\sigma}'$ is the intermediate true stress. We have

$$\bar{\sigma} = (\lambda^n - \lambda^{-n})\ (2G/n + m\ B\ I_E^{m-1}) \tag{4.6}$$

and

$$\bar{\sigma}' = (1 - \lambda^{-n})\ (2G/n + m\ B\ I_E^{m-1}) \tag{4.7}$$

where

$$I_E = (\lambda^n + \lambda^{-n} - 2)/n \tag{4.8}$$

It is often difficult to keep $\lambda_2 = 1$ in experiments in pure shear. If λ_2 can be measured, $\lambda_3 = (\lambda_1\lambda_2)^{-1}$, and Eqs. (4.6) through (4.8) can be modified to describe the state of stress as

$$\bar{\sigma} = (\lambda_1{}^n - \lambda_1{}^{-n}\,\lambda_2{}^{-n})\ (2G/n + m\ B\ I_E{}^{m-1}) \tag{4.9}$$

and

$$\bar{\sigma}' = (\lambda_2{}^n - \lambda_1{}^{-n}\,\lambda_2{}^{-n})\ (2G/n + m\ B\ I_E{}^{m-1}) \tag{4.10}$$

where

$$I_E = (\lambda_1{}^n + \lambda_2{}^n + \lambda_1{}^{-n}\,\lambda_2{}^{-n} - 3)/n \tag{4.11}$$

4.4 Simple Shear

The shear stress, $\bar{\sigma}_{12} = \sigma_{12}$, is obtained by differentiating $\bar{W}$ with respect to the amount of shear, t, given by (2)

$$t = \tan\gamma = \lambda - \lambda^{-1} \tag{4.12}$$

where γ is the angle of shear. The principal stretch ratios in simple shear are the same as those in pure shear. Hence, I_E is given by Eq. (4.8). Differentiation leads to

$$\sigma_{12} = \frac{\lambda^n - \lambda^{-n}}{\lambda + \lambda^{-1}} (2G/n + m\ B\ I_E^{m-1}) \tag{4.13}$$

for the shear stress.

4.5 Experimental Evidence

We now demonstrate the applicability of our proposed new strain energy density function, Eq. (3.30), to experimental data on natural rubber (NR) and on styrene-butadiene rubber (SBR), in homogeneous deformations.

Natural Rubber.

We used Treloar's data (20) in simple tension, pure shear (maximum stress only), and equibiaxial tension at 20°C, and Forster's data (30) in simple compression at 25°C. In both cases the shear modulus, G, was taken from the original work. The coefficient of strain measure, n, was obtained on a computer from a least squares fit of the data of Treloar in simple tension below about $\lambda = 3$. The constants B and m were obtained next, again from a computer least squares fit of Treloar's data in simple tension. The constants are listed in Table I. The same constants were used to predict the behavior in the other deformation fields. The results for the data of Treloar are shown in Fig. 2. The data in equibiaxial tension were calculated for simple compression. The

fit near the unstretched state ($\lambda = 1$) in both tension and compression is shown in an enlargement in Fig. 2. The fit to the simple tension data is excellent up to break. The prediction of the observed behavior in pure shear (maximum stress) and equibiaxial tension (compression) is also good up to break, the maximum error being about 10%.

Figure 3 shows the same data in a plot of the normal true stress differences, $\bar{\sigma}_\alpha - \bar{\sigma}_\beta$, against the prediction given by Eq. (4.1). As expected, the data lie on a straight line with a unit slope. The same figure also contains the data of Forster in simple compression. These data were obtained in an actual compression experiment. Except for the shear modulus, G, they were fitted with the constants obtained from Treloar's data in simple tension on another sample of natural rubber. Nevertheless, the fit is very good over the entire range.

Styrene-Butadiene Rubber

We examined the data of Dickie and Smith (15) in simple tension, pure shear (both maximum and intermediate stress), and equibiaxial tension. The authors reported the data in a time- and temperature-independent reference state for which the modulus is unity. For comparison with other data, a modulus of 75 psi, i.e., 5.27 kg/cm^2, at 25°C is appropriate (21).

The constants shown in Table I for SBR were again determined from the data in simple tension as explained above for NR. The same parameters were then used to predict the behavior in pure shear and in equibiaxial tension calculated as simple compression. The results are shown in Fig. 4 by the solid lines.

Again, the fit is excellent in simple tension. In pure shear, only the constants G and n were needed. The fit is excellent for the maximum stress. Some deviation appears at large values of λ in the intermediate stress. This deviation can be attributed to the fact that the stretch ratio in the direction of the intermediate stress did not remain unity, but changed appreciably as discussed in detail by Smith and Frederick (22). The predicted curve for $\bar{\sigma}'/3G$ in Fig. 4 was obtained from Eq. (4.7) assuming $\lambda_2 = 1$. Equation (4.10) which would undoubtedly have improved the fit, could not be used because the actual values of λ_2 are not known.

In equibiaxial tension the constants B and m determined in simple tension did not fit the data well. They begin to contribute around $1/\lambda = 12$. The broken line indicates the fit with the values of B and m shown in the last row of Table 1. These were obtained directly from the equibiaxial tension data and provide an excellent fit. Figure 5 shows the same plot as Fig. 3. The unfilled squares correspond to the four points fitted by the broken line in Fig. 4.

The points shown in Fig. 4 were taken from Table 1 of reference (15). The entries in that table for equibiaxial tension were read from Fig. 4 of the same reference. The last point, corresponding to a reduced strain of 5.0, appears to have been extrapolated in an inconsistent way from the figure and was, therefore, omitted from our calculations and plot.

The differences in the constants B and m for the uniaxial and equibiaxial tension data of Dickie and Smith is probably explained by the fact that the materials for the separate studies were prepared at

different times with minor variations in the preparative procedures (15). This may affect not only G (which was divided out by authors for this reason) but also B/3G and / or m. The parameter n appears to be insensitive to such variations as witnessed by the satisfactory fit to all NR data with the same value of n, and of the SBR data for values of the strain which do not require B and m.

5. INHOMOGENEOUS DEFORMATION FIELDS

5.1 Introduction

The application of the new strain energy function in various homogeneous stress fields was demonstrated in the preceding section. In this section we consider an inhomogeneous stress field for which the data are available in literature. The problem of simple torsion and torsion combined with extension are solved with the aid of the new strain energy function. Since the second term in Eq. (3.30) only contributes significantly beyond about 250% strain for natural rubber, and the available data in torsion do not exceed 150% strain, the form of the strain energy function used in this section is given by Eq. (3.25).

The torsion of a right circular cylinder, both with and without superimposed stretch, was considered by Rivlin (24). Rivlin and Saunders (25) measured the torsional couple on natural rubber (NR) in simple torsion, and in combined torsion and extension. The normal loads were also obtained in the simple torsion experiment. Ogden and Chadwick (26) predicted the torsional couple data of Rivlin and Saunders in combined torsion and extension using a new six parameter equation. The torsional couple data in simple torsion were recently predicted by Valanis (27) using the approach of Valanis and Landel (16). Equation (3.25) is used to predict the data in both the simple torsion and the torsion with extension. The principal Cauchy stresses corresponding to Eq. (3.25) are given by

$$\bar{\sigma}_\alpha = - k + 2G \left(E_\alpha - \frac{I_E}{3} \right) \tag{5.1}$$

where k is an arbitrary hydrostatic pressure.

5.2 Combined Torsion and Stretch of a Right Circular Cylinder

Consider a right circular cylinder of length L and radius A. The cylinder is capped by rigid plates, one of which is simultaneously displaced in the axial direction and twisted. The deformed length is denoted by $\ell (= \lambda L)$ and the deformed radius by $a (= A/\sqrt{\lambda})$. The inverse mapping in cylindrical coordinates is given by

$$R = \sqrt{\lambda} r \tag{5.2}$$

$$\Theta = \theta - \frac{kz}{\lambda} \tag{5.3}$$

$$Z = \frac{z}{\lambda} \tag{5.4}$$

where k is the angle of twist per unit undeformed length. R, Θ, Z are the material coordinates (X^K) and r, θ, z are the spatial coordinates (x^k). The Cauchy deformation tensor is given by

$$c^k_{\ m} = g^{k\ell} X^K_{\ ,\ell} G_{KL} X^L_{\ ,m} = \begin{pmatrix} \lambda & 0 & 0 \\ 0 & \lambda & - k \\ 0 & - kr^2 & \dfrac{1 + \lambda k^2 r^2}{\lambda^2} \end{pmatrix} \tag{5.5}$$

where $g^{k\ell}$ and G_{KL} are the metric tensors and $X^K{}_{,\ell}$ is the deformation gradient. The eigenvalues of the deformation tensor are given by

$$c^k{}_\ell \, n^\ell{}_\alpha = \lambda_\alpha^{-2} \, n^k{}_\alpha \tag{5.6}$$

which leads to the secular equation as

$$(\lambda - \lambda_\alpha^{-2}) \left[\lambda_\alpha^{-4} - 2(\lambda^{-1/2} \cosh \gamma) \, \lambda_\alpha^{-2} + \lambda^{-1}\right] = 0 \tag{5.7}$$

The solution of this equation gives the eigenvalues as

$$\lambda_1 = \lambda^{-1/2} \tag{5.8}$$

$$\lambda_2 = \lambda^{1/4} \exp(-\gamma/2) \tag{5.9}$$

$$\lambda_3 = \lambda^{1/4} \exp(\gamma/2) \tag{5.10}$$

where

$$\gamma = \cosh^{-1}\left\{\frac{\lambda^2 + \frac{1}{\lambda} + k^2 r^2}{2\sqrt{\lambda}}\right\} \tag{5.11}$$

The matrix of the eigenvectors corresponding to these three eigenvalues is given by

$$n^{k}_{\alpha} = \begin{pmatrix} 1 & 0 & 0 \\ 0 & \dfrac{\sqrt{\lambda^{3/2} - e^{-\gamma}}}{r\sqrt{e^{\gamma} - e^{-\gamma}}} & \dfrac{\sqrt{e^{\gamma} - \lambda^{3/2}}}{r\sqrt{e^{\gamma} - e^{-\gamma}}} \\ 0 & -\dfrac{\sqrt{e^{\gamma} - \lambda^{3/2}}}{\sqrt{e^{\gamma} - e^{-\gamma}}} & \dfrac{\sqrt{\lambda^{3/2} - e^{-\gamma}}}{\sqrt{e^{\gamma} - e^{-\gamma}}} \end{pmatrix} \tag{5.12}$$

The principal stresses are obtained from Eqs. (5.1), (5.8), (5.9), and (5.10) as

$$\bar{\sigma}_1 = -k - \frac{2G}{3n}\left[-2\lambda^{-n/2} + \lambda^{n/4}\left(e^{n\gamma/2} + e^{-n\gamma/2}\right)\right] \tag{5.13}$$

$$\bar{\sigma}_2 = -k - \frac{2G}{3n}\left[\lambda^{-n/2} + \lambda^{n/4}\left(e^{n\gamma/2} - 2e^{-n\gamma/2}\right)\right] \tag{5.14}$$

$$\bar{\sigma}_3 = -k - \frac{2G}{3n}\left[\lambda^{-n/2} + \lambda^{n/4}\left(e^{-n\gamma/2} - 2e^{n\gamma/2}\right)\right] \tag{5.15}$$

One can now combine the last three equations with the tensor of the eigenvectors [Eq. (5.11)] to obtain the Cauchy stresses given by

$$t^{k}_{\ell} = \sum_{\alpha} n^{k}_{\alpha}\, \bar{\sigma}_{\alpha}\, n^{\alpha}_{\ell} \tag{5.16}$$

from which the following stress tensor is obtained

$$t^{(k)}_{(\ell)} = \begin{Bmatrix} \bar{\sigma}_1 & 0 & 0 \\ 0 & \dfrac{(\lambda^{3/2}-e^{-\gamma})\,\bar{\sigma}_2 + (e^{\gamma}-\lambda^{3/2})\bar{\sigma}_3}{2\sinh\gamma} & \dfrac{(\bar{\sigma}_3-\bar{\sigma}_2)\sqrt{(e^{\gamma}-\lambda^{3/2})(\lambda^{3/2}-e^{-\gamma})}}{2\sinh\gamma} \\ 0 & \dfrac{(\bar{\sigma}_3-\bar{\sigma}_2)\sqrt{(e^{\gamma}-\lambda^{3/2})(\lambda^{3/2}-e^{-\gamma})}}{2\sinh\gamma} & \dfrac{(\lambda^{3/2}-e^{-\gamma})\bar{\sigma}_3 + (e^{\gamma}-\lambda^{3/2})\bar{\sigma}_2}{2\sinh\gamma} \end{Bmatrix} \tag{5.17}$$

where $t^{(k)}_{(\ell)}$ are the physical components of t^{k}_{ℓ}.

The components of Eq. (5.16) are undetermined with respect to an arbitrary hydrostatic pressure. We therefore solve the radial equilibrium equation (6)

$$r\frac{\partial\bar{\sigma}_r}{\partial r} = \bar{\sigma}_\theta - \bar{\sigma}_r \tag{5.18}$$

where

$$\bar{\sigma}_r = t^{(1)}_{(1)},\ \bar{\sigma}_\theta = t^{(2)}_{(2)} \text{ and } \bar{\sigma}_3 = t^{(3)}_{(3)} \tag{5.19}$$

subject to the boundary condition

$$\text{at} \qquad r = a,\ \bar{\sigma}_r = 0 \tag{5.20}$$

Equation (5.18) may be rewritten as

$$r\frac{\partial \bar{\sigma}_1}{\partial r} + \bar{\sigma}_1 = \frac{(\lambda^{3/2} - e^{-\gamma})\,\bar{\sigma}_2 + (e^{\gamma} - \lambda^{3/2})\,\bar{\sigma}_3}{2 \sinh \gamma} \tag{5.21}$$

Equation (5.21) may be integrated numerically by replacing r by γ by means of Eq. (5.11), and the result can be used to correlate normal stress data for various values of λ and k. Such data are available only in simple torsion (i.e., no superimposed stretch), the solution for which is given in the next section. There are, however, data available for the torque M vs. the amount of torsion for various values of the extension ratio. From Eq. (5.11)

$$r^2 = (e^{\gamma} - \lambda^{3/2})(\lambda^{3/2} - e^{-\gamma})/\lambda k^2 \tag{5.22}$$

which in conjunction with

$$M = 2\pi \int_0^a \bar{\tau}_{\theta z}\, r^2\, dr \tag{5.23}$$

yields

$$M = \frac{4\pi G \lambda^{n/4}}{nk^3} \int_{\gamma_o}^{\gamma_a} (e^{\gamma} - \lambda^{3/2})\,(\lambda^{3/2} - e^{-\gamma}) \sinh \frac{n\gamma}{2}\, d\gamma \tag{5.24}$$

where

$$\bar{\tau}_{\theta z} = t^{(2)}_{(3)} \tag{5.25}$$

$$\cosh \gamma_o = \frac{\lambda^2 + \frac{1}{\lambda}}{2\sqrt{\lambda}} \tag{5.26}$$

and

$$\cosh \gamma_a = \frac{\lambda^2 + \frac{1}{\lambda} + k^2a^2}{2\sqrt{\lambda}} \tag{5.27}$$

For the special case of n = 2, the above result reduces to

$$M = \frac{\pi}{2} \frac{G A^4 k}{\lambda} \tag{5.28}$$

which is a result obtained by Rivlin (28) for neo-Hookean materials.

5.3 Simple Torsion

This is a special case of torsion with superimposed elongation, where now the stretch ratio is unity. Thus, the principal extension ratios are given by

$$\lambda_1 = 1 \tag{5.29}$$

$$\lambda_2 \equiv \lambda^{-1} = \sqrt{1 + (kr/2)^2} - kr/2 \tag{5.30}$$

and

$$\lambda_3 \equiv \lambda = \sqrt{1 + (kr/2)^2 + kr/2} \tag{5.31}$$

Proceeding in a fashion similar to the one described in the previous section it is easily shown that the normal axial force N and the torsional couple M are given by

$$N = 2\pi \int_0^A r\,\bar{\sigma}_z\,dr = -\frac{2\pi G}{k^2 n}\left[-\frac{3}{n}\left(\lambda_A^{n/2} - \lambda_A^{-n/2}\right)^2 - \frac{1}{2}\left(\lambda_A - \lambda_A^{-1}\right)^2 + \frac{1}{n+2}\left(\lambda_A^{n/2+1} - \lambda_A^{-n/2-1}\right)^2 + \frac{2}{n-2}\left(\lambda_A^{n/2-1} - \lambda_A^{-n/2+1}\right)^2\right] \tag{5.32}$$

and

$$M = \frac{4\pi G}{nk^3}\left[\frac{\left(\lambda_A^{n/2+1} - \lambda_A^{-n/2-1}\right)^2}{n+2} - \frac{2\left(\lambda_A^{n/2} - \lambda_A^{-n/2}\right)^2}{n} + \frac{\left(\lambda_A^{n/2-1} - \lambda_A^{1-n/2}\right)^2}{n-2}\right] \tag{5.33}$$

where $\lambda_A = \lambda\big|_{r=A}$.

5.4 Experimental Results

Since the original data were obtained on two samples with slightly different moduli we used our equation in a normalized form. For the parameter n we used 1.64 as in our treatment of other data on NR.

5.41 Simple Torsion

The details of the simple torsion experiment are given in the original paper (25). The dimensionless torsional couple M is plotted against the amount of torsion in Fig. 6. The points represent the experimental data, given both as an increasing and decreasing load cycle. The solid line is the predicted curve using Eq. (5.33). The theory and

the observed behavior are in good agreement. In Fig. 7 the dimensionless normal axial load N is plotted against the square of the amount of torsion. As should be noted, the axial force is compressive, since to apply a torsion of amount k in a cylinder bonded with rigid plates to its plane ends, we must apply a torsional couple and a thrust parallel to the cylinder axis. The original data points predict an intercept as shown in Fig. 7. There is a finite value of thrust N even though there is no torsion. If we consider the material to be isotropic in the undeformed state, such an intercept cannot be expected. This can only be explained as an experimental error at this time. To circumvent this difficulty we have taken the mean of the intercepts of data points for increasing and decreasing loads and added it as a constant to the theoretical prediction as given by Eq. (5.32). Thus, the solid line in Fig. 7 represents the predicted curve shifted vertically by a constant amount. Hence, Eq. (5.27) predicts the normal axial force fairly well within the accuracy of the experiment. Since the parameter n was obtained from simple tension data, the results of Figs. 6 and 7 show that the strain energy function given by Eq. (3.25) correctly describes the simple torsion of a circular cylinder of a rubberlike material.

5.42 Combined Torsion and Simple Extension

To verify the theoretical results obtained for combined torsion and extension, we examined the dependence of the torque on the amount of torsion at each extension ratio. Figure 8 shows the dimensionless torsional couple M plotted against the amount of twist per unit deformed length at each extension ratio. A horizontal shift (indicated

by the intercept on the abscissa) was used for clearer representation. Using the parameters obtained earlier, the theoretical predictions of Eq. (5.24) are plotted as solid lines in Fig. 8. The predicted lines describe the experimental values of the torsional couple fairly well.

An important consequence of an experiment of torsion superposed on a stretch was pointed out by Rivlin and Saunders (25). They showed that the ratio of the load to torsional modulus for infinitesimal torsions is independent of the stored energy function. That is,

$$\frac{N\Big|_{k=0}\; a^2}{(M/k)\Big|_{k=0}} = 2(\lambda - \lambda^{-2}) \tag{5.34}$$

It can be shown easily that Eq. (5.24) reduces to

$$\frac{M}{k}\Bigg|_{k=0} = \frac{\pi G a^4}{n} \frac{\lambda^n - \lambda^{-n/2}}{\lambda - \lambda^{-2}} \tag{5.35}$$

and the normal load at zero torsion is given by

$$N\Big|_{k=0} = \frac{2G}{n} \pi a \, (\lambda^n - \lambda^{-n/2}) \tag{5.36}$$

Thus our theoretical analysis supports Eq. (5.34).

6. TEMPERATURE DEPENDENCE OF PARAMETERS

The dimensions of G and B are those of moduli while the constants n and m are dimensionless. To study the effect of temperature on these four parameters, we chose the natural rubber data of Anthony, Caston and Guth (29). The data are shown in Fig. 9 in which the stretch ratios are offset for clarity by an amount A as shown. We obtained the constants G, n, B, and m as described for the data of Treloar from the data at 30°C. Holding n and m fixed, we then determined G and B at the other three temperatures. The values are tabulated in Table I. We also determined G, n, B, and m separately for all temperatures. The variation in n and m was so slight that we feel justified to regard the exponential constants $\underline{n}$ and $\underline{m}$ to be independent of temperature in the range investigated. Figure 10 shows a plot of $\underline{G}$ and $\underline{B}$ as a function of temperature. It is seen that G and B vary linearly with temperature at least between 10° and 70°C for natural rubber.

7. CONCLUSIONS

The new strain energy function thus satisfactorily meets the requirements of a constitutive relation. The same parameters describe homogeneous as well as inhomogeneous modes of deformations up to the point of rupture. The strain energy function contains only four parameters and is quite simple to use. In comparison, Ogden's strain energy function (11) contains six parameters and is rather difficult to handle. Our treatment also offers advantages over the approach of Valanis and Landel (16) in which the function $\omega'(\lambda)$ has no analytic representation (12) and must be determined experimentally.

The concept of using an arbitrary power of the stretch ratio, although very useful, is completely empirical. No statistical thermodynamic argument exists which can substantiate the choice of such a strain measure. However, it is possible to look at the results in the light of the network theory of rubber elasticity. It is hoped that the n-measure may eventually be placed on a sound theoretical basis. Also, the importance of Seth's measure in viscosity and viscoelasticity can be anticipated since the power law has been widely used in these fields. This measure can be considered to be a modified power law and utilized to arrive at new constitutive relations in these fields.

A detailed summary of the results of the new strain energy function will be discussed in conjunction with Part II of this work. A number of suggestions for future work in the field of phenomenological behavior of elastomers is given in Chapter 6 of Part II.

APPENDIX 1

In general coordinates the matrix of the Lagrangean strain tensor is given by

$$E^K_{\ L} = \sum_\alpha N^K \ E_\alpha \ N^\alpha_{\ L} \tag{A-1.1}$$

where $N^K_{\ \alpha}$ is the matrix of the eigenvectors of the Green $\underset{\sim}{C}$-tensor. Introducing Eq. (2.3) and noting that $N^K_{\ \alpha}$ is an orthogonal matrix, we obtain

$$E^K_{\ L} = \sum_\alpha N^K_{\ \alpha} \frac{\lambda_\alpha^n - 1}{n} N^\alpha_{\ L} = \frac{(C^{n/2})^K_{\ L} - \delta^K_{\ L}}{n} \tag{A-1.2}$$

where

$$\underset{\sim}{C}^{n/2} = (\underset{\sim}{C})^{n/2} \tag{A-1.3}$$

and

$$C_{KL} = g_{k\ell} \ x^k{}_{,K} \ x^\ell{}_{,L} \tag{A-1.4}$$

where

$$x^k = x^k(X^K) \ . \tag{A-1.5}$$

The $\{\lambda_\alpha\}$ are the eigenvalues of the $\underset{\sim}{C}$-tensor; $\{x^k\}$ are the spatial coordinates while $\{X^K\}$ are the material coordinates.

The Cauchy stress in general coordinates is given by

$$t^k{}_\ell = \sum_\alpha n^k{}_\alpha \, \bar{\sigma}_\alpha \, n^\alpha{}_\ell \qquad \text{(A-1.6)}$$

where $n^k{}_\ell$ is the matrix of the eigenvectors of the $\underset{\sim}{c}$-tensor

$$c_{k\ell} = g_{KL} \, X^K{}_{,k} \, X^L{}_{,\ell} \qquad \text{(A-1.7)}$$

APPENDIX 2

Hill (19) suggested that any constitutive relation should obey the inequality

$$\dot{\bar{\sigma}}_\alpha \, \dot{e}_\alpha > 0 \tag{A-2.1}$$

where $\dot{\bar{\sigma}}_\alpha$ and $\dot{e}_\alpha$ are rates of stress and strain respectively. Hill's inequality is a sufficient but not a necessary condition.

The strain energy function

$$W = \frac{2G}{n} I_E + B \, I_E^{\,m} \tag{A-2.2}$$

implies

$$\bar{\sigma}_\alpha = \lambda_\alpha \frac{\partial W}{\partial \lambda_\alpha} = \lambda_\alpha^n \left[\frac{2G}{n} + m \, B \, I_E^{\,m-1}\right] \tag{A-2.3}$$

and

$$\dot{\bar{\sigma}}_\alpha = \dot{\lambda}_\alpha \, \lambda_\alpha^{n-1} \left[2G + n \, m \, B \, I_E^{\,m-1} + m(m-1) \, B \, I_E^{\,m-2} \, \lambda_\alpha^n\right] \tag{A-2.4}$$

The Eulerian strain e_α is defined by Eq. (2.4), from which

$$\dot{e}_\alpha = \dot{\lambda}_\alpha / \lambda_\alpha \tag{A-2.5}$$

PART II

THERMOELASTIC BEHAVIOR

OF RUBBERS

Now, combining Eqs. (A-2.4) and (A-2.5) yields

$$\dot{\bar{\sigma}}_\alpha \, \dot{e}_\alpha = \dot{\lambda}_\alpha^2 \, \lambda_\alpha^{n-2} \left[2G + n \, m \, B \, I_E^{m-1} + m(m-1) \, B \, I_E^{m-2} \, \lambda_\alpha^n \right] \qquad \text{(A-2.6)}$$

Thus Hill's inequality is always satisfied if $n \geq 0$ and $m \geq 1$. It may, however, also be satisfied for other values of n and m, depending on G and B.

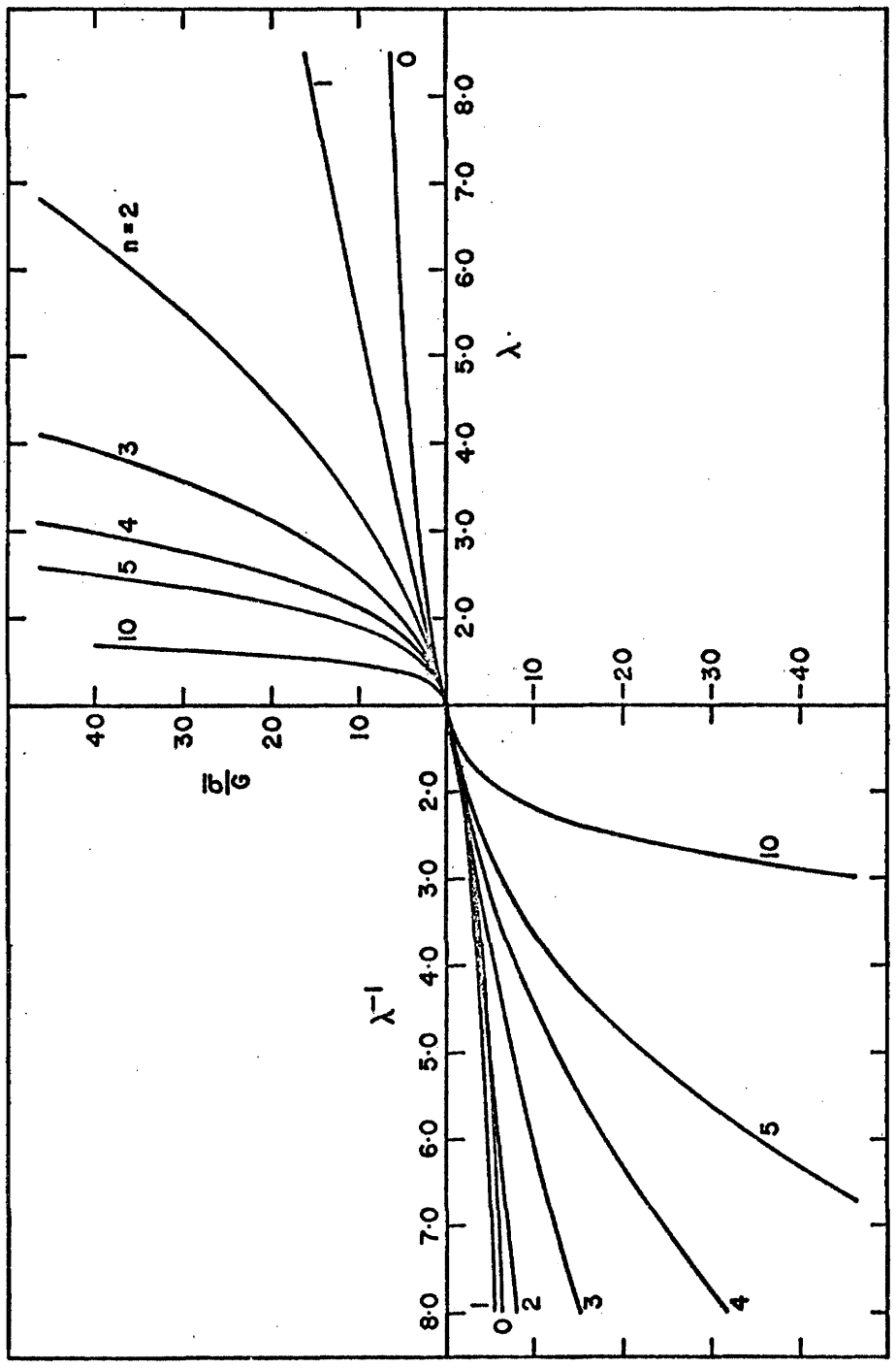

Figure 1 $\bar{\sigma}/G$ vs. λ or λ^{-1} for various values of n.

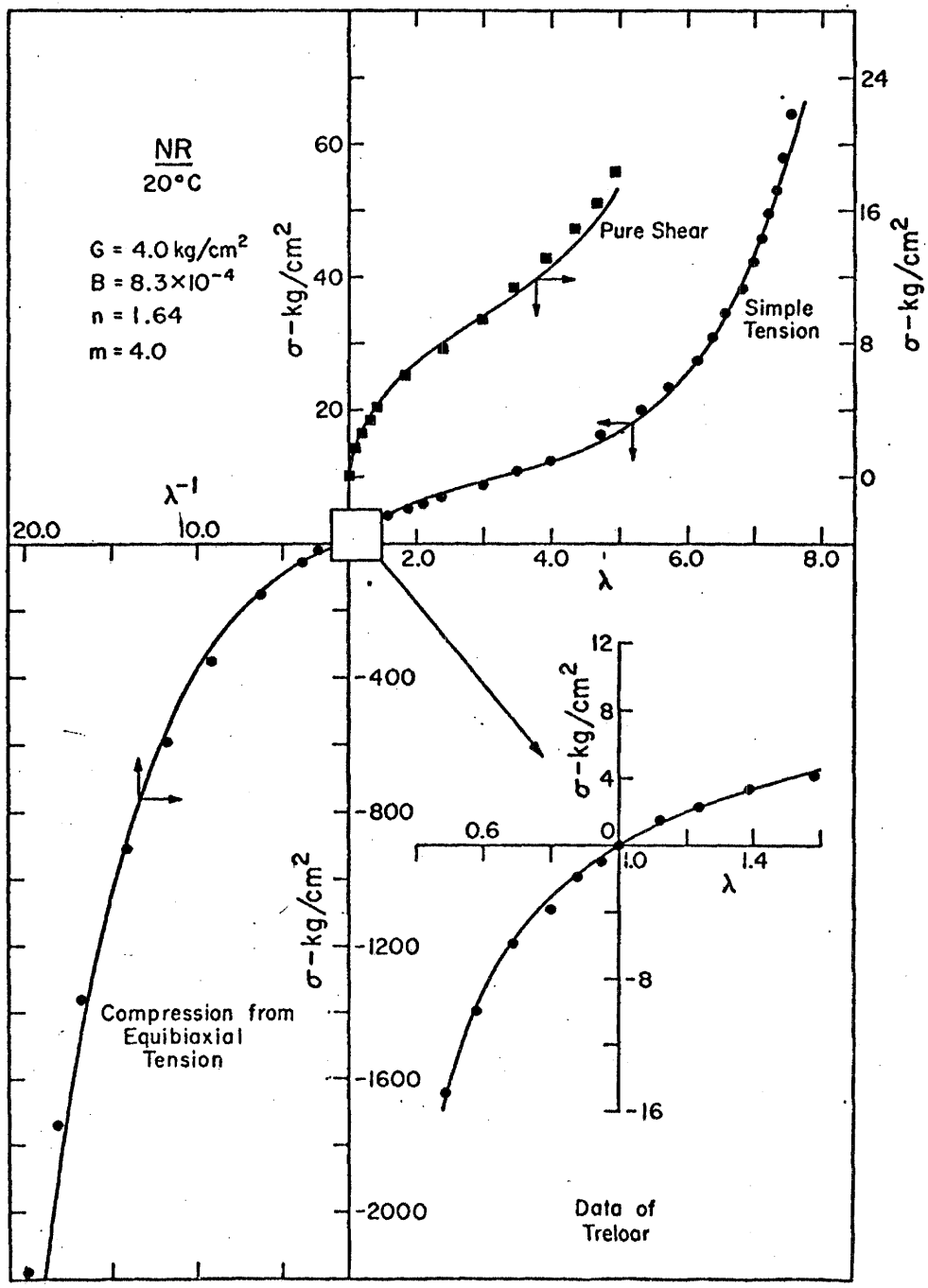

Figure 2 Data of Treloar on natural rubber at 27°C. Solid lines were calculated from Eq. (3.30) with parameters as indicated.

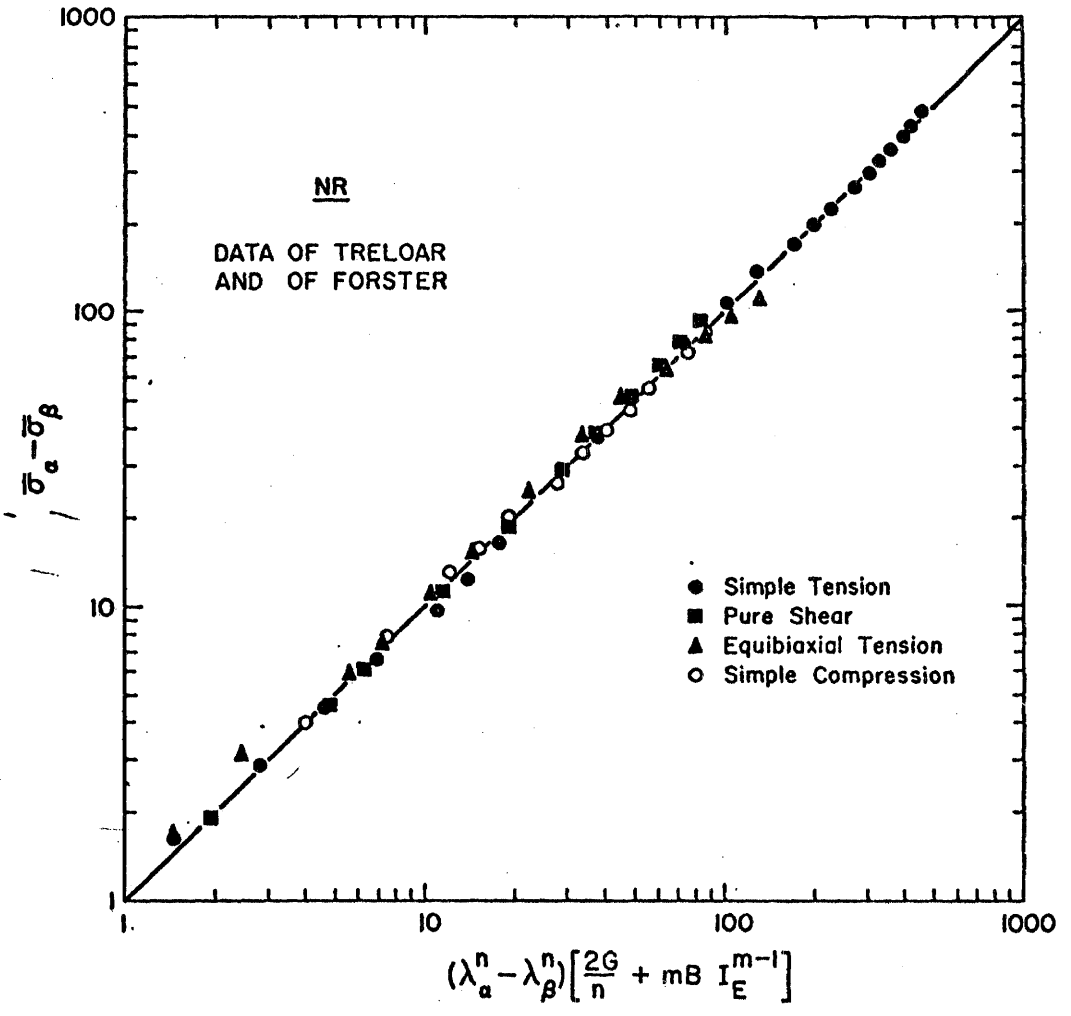

Figure 3 Data of Treloar on natural rubber at 20°C and of Forster at 25°C, plotted according to Eq. (4.1). Solid line is line of unit slope.

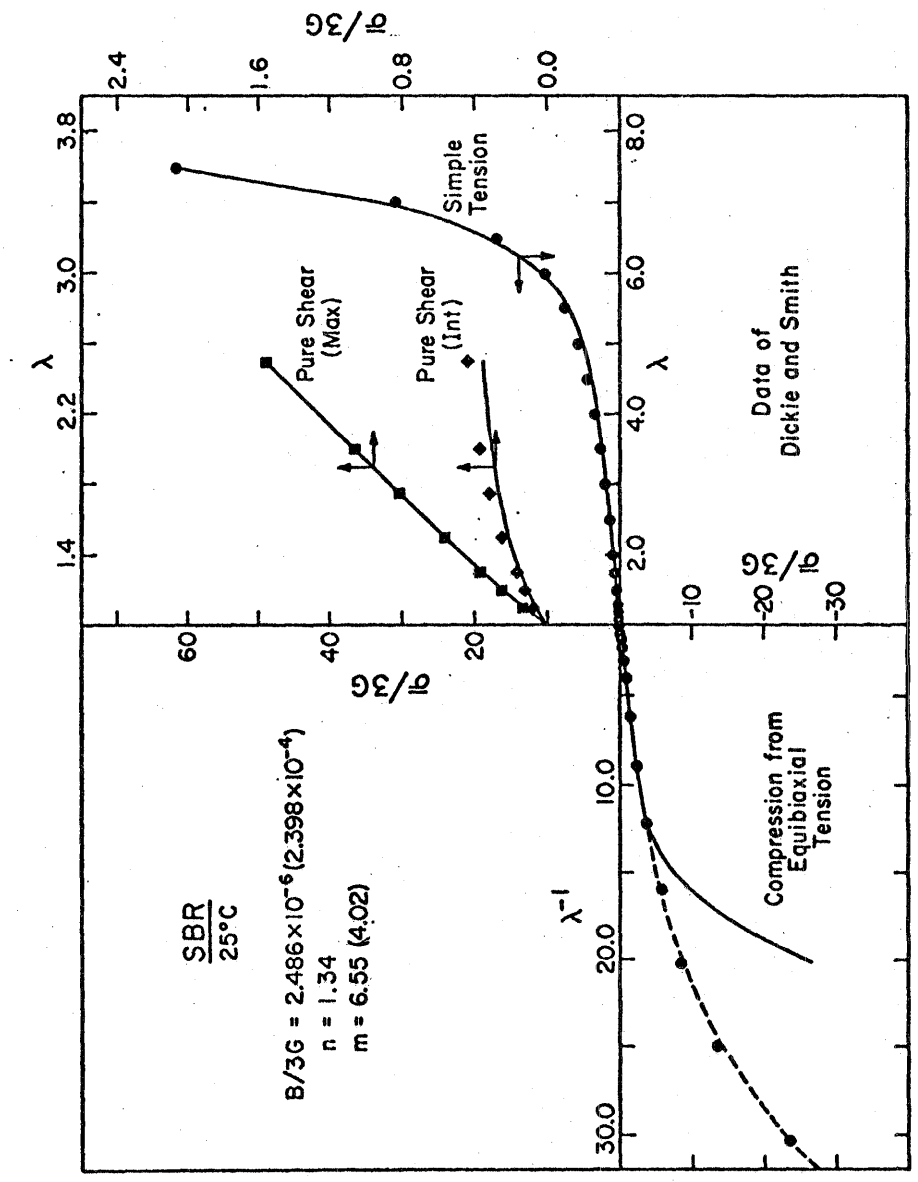

Figure 4 Data of Dickie and Smith on SBR at 25°C. Solid lines were calculated from Eq. (3.30) with parameters as indicated.

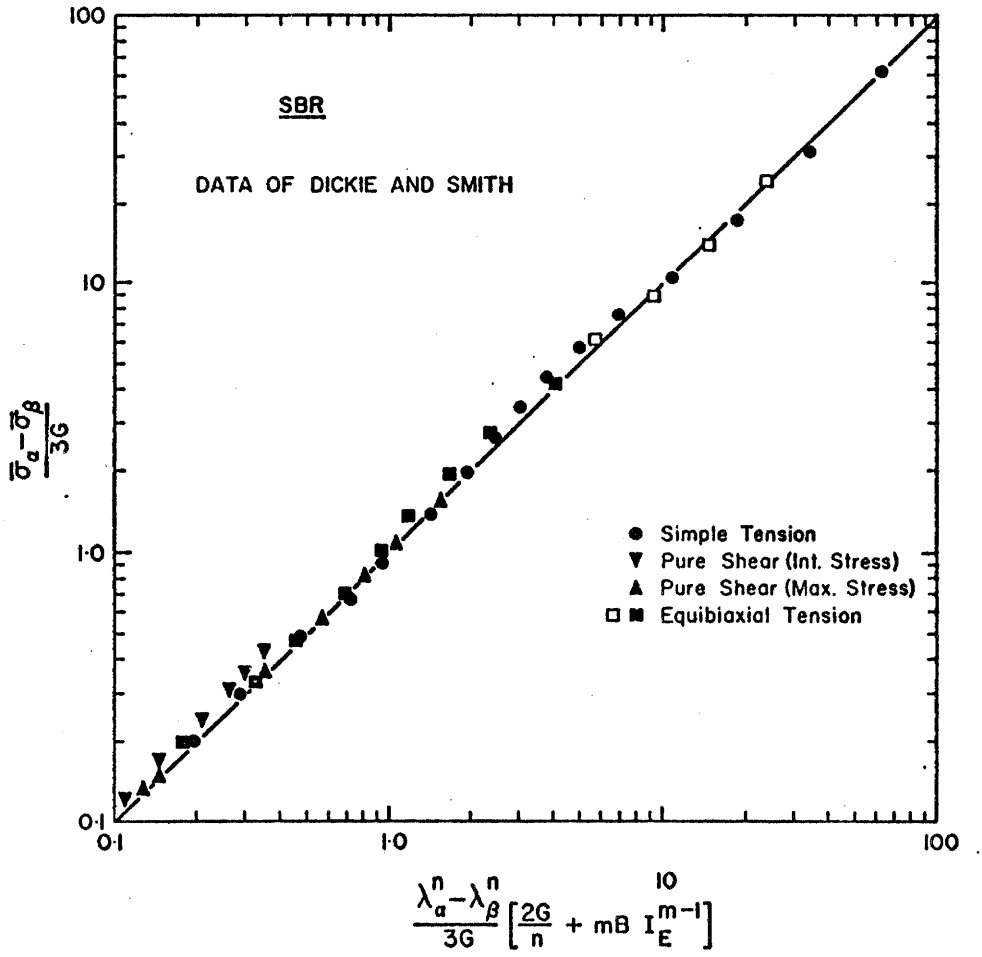

Figure 5 Data of Dickie and Smith on SBR at 25°C, plotted according to Eq. (4.1). Solid line is line of unit slope.

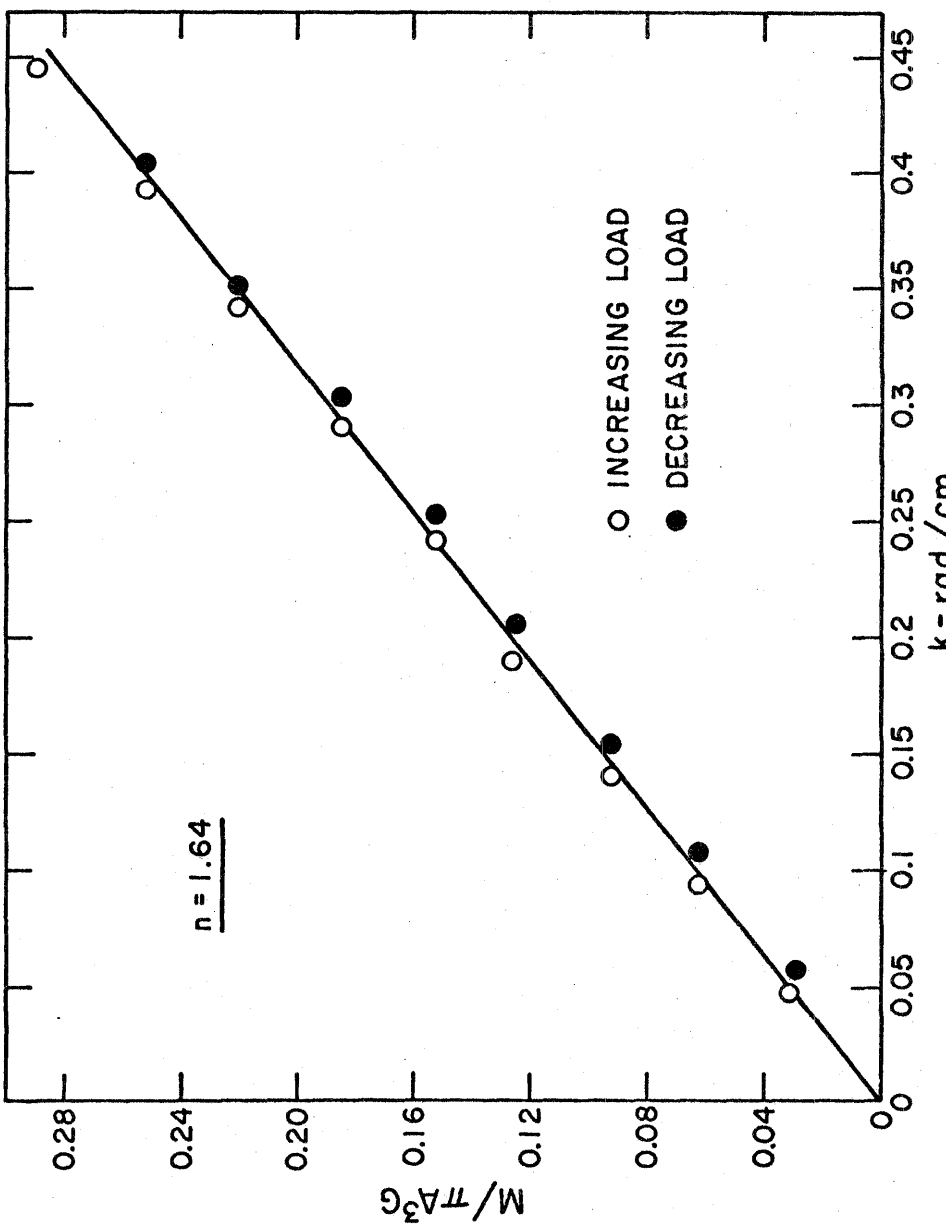

Figure 6 Plot of dimensionless torsional couple against amount of torsion for simple torsion experiment.

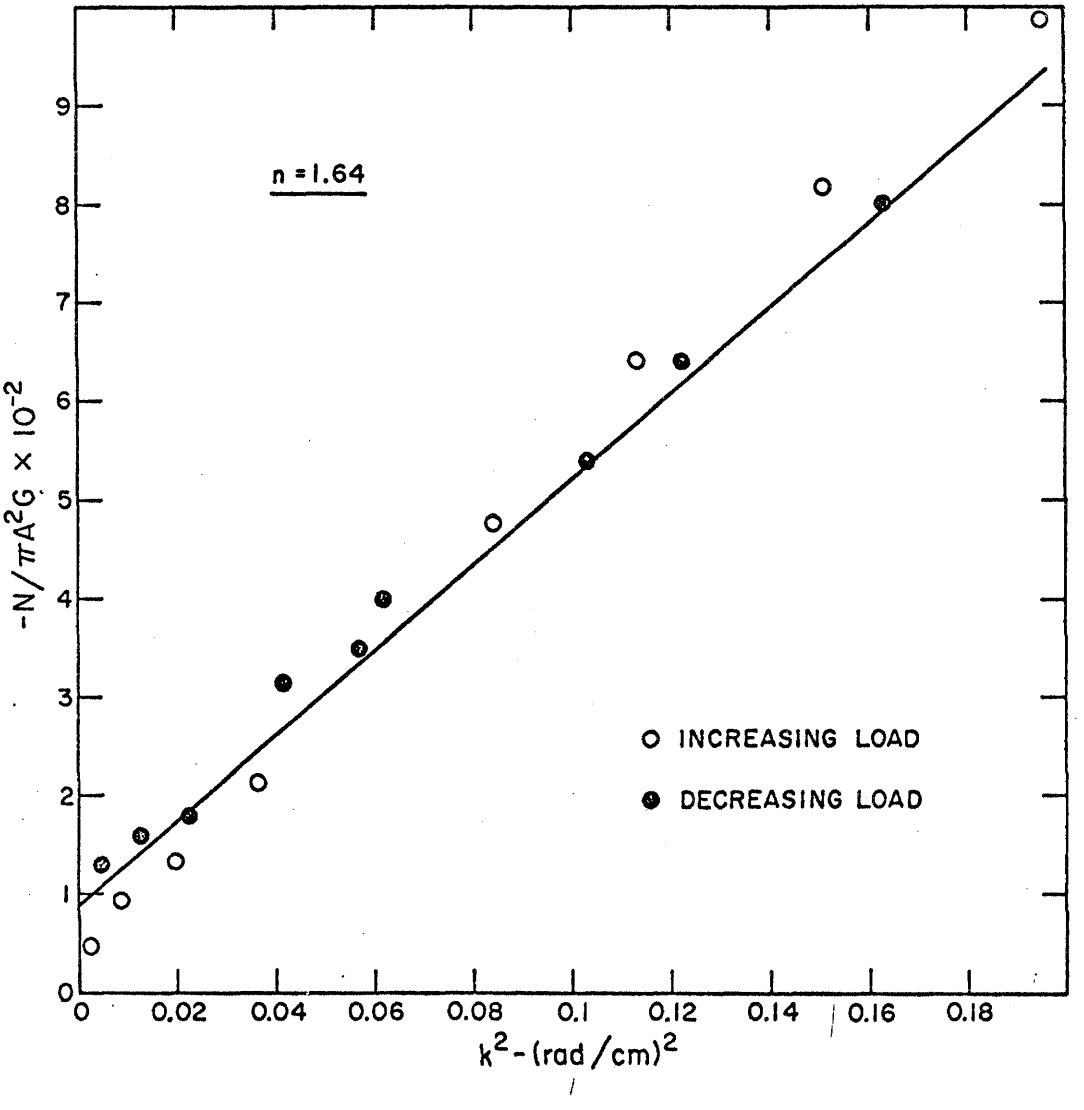

Figure 7 Plot of dimensionless normal load against the amount of torsion for the simple torsion experiment.

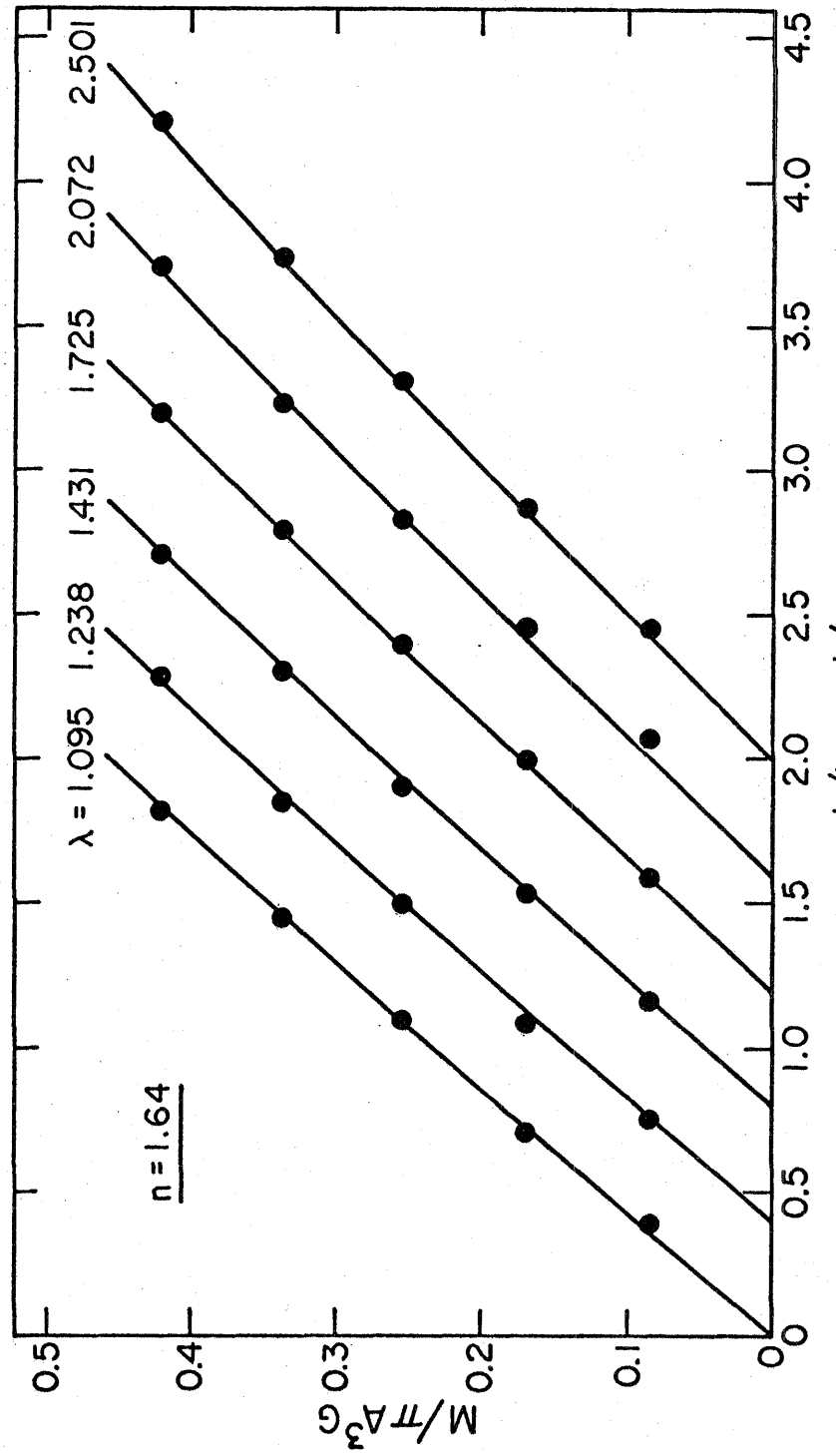

Figure 8 Plot of dimensionless torsional couple against amount of torsion for various values of extension ratio. Note the shift in origin.

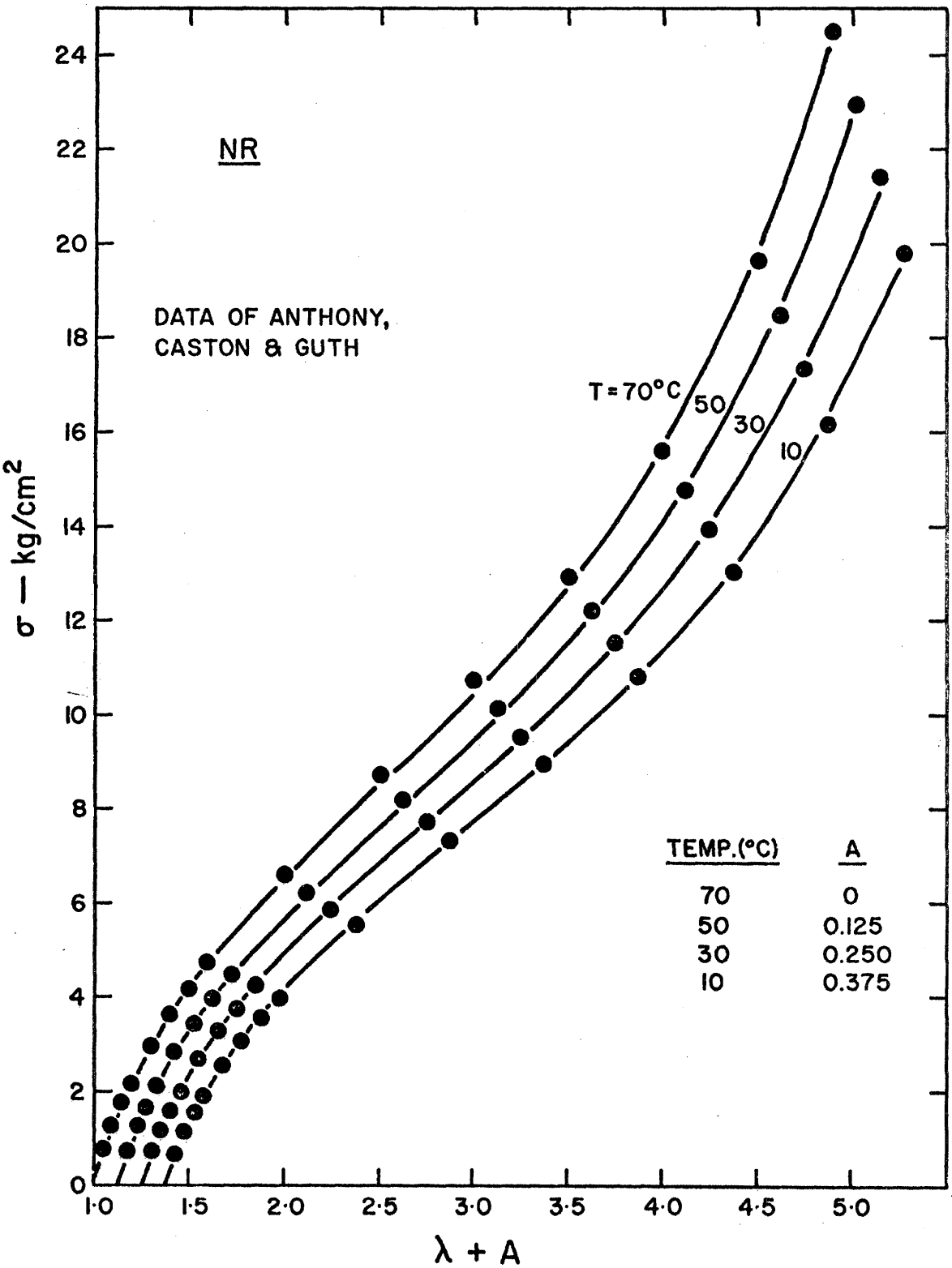

Figure 9 Simple tension data of Anthony, Caston and Guth on natural rubber at various temperatures.

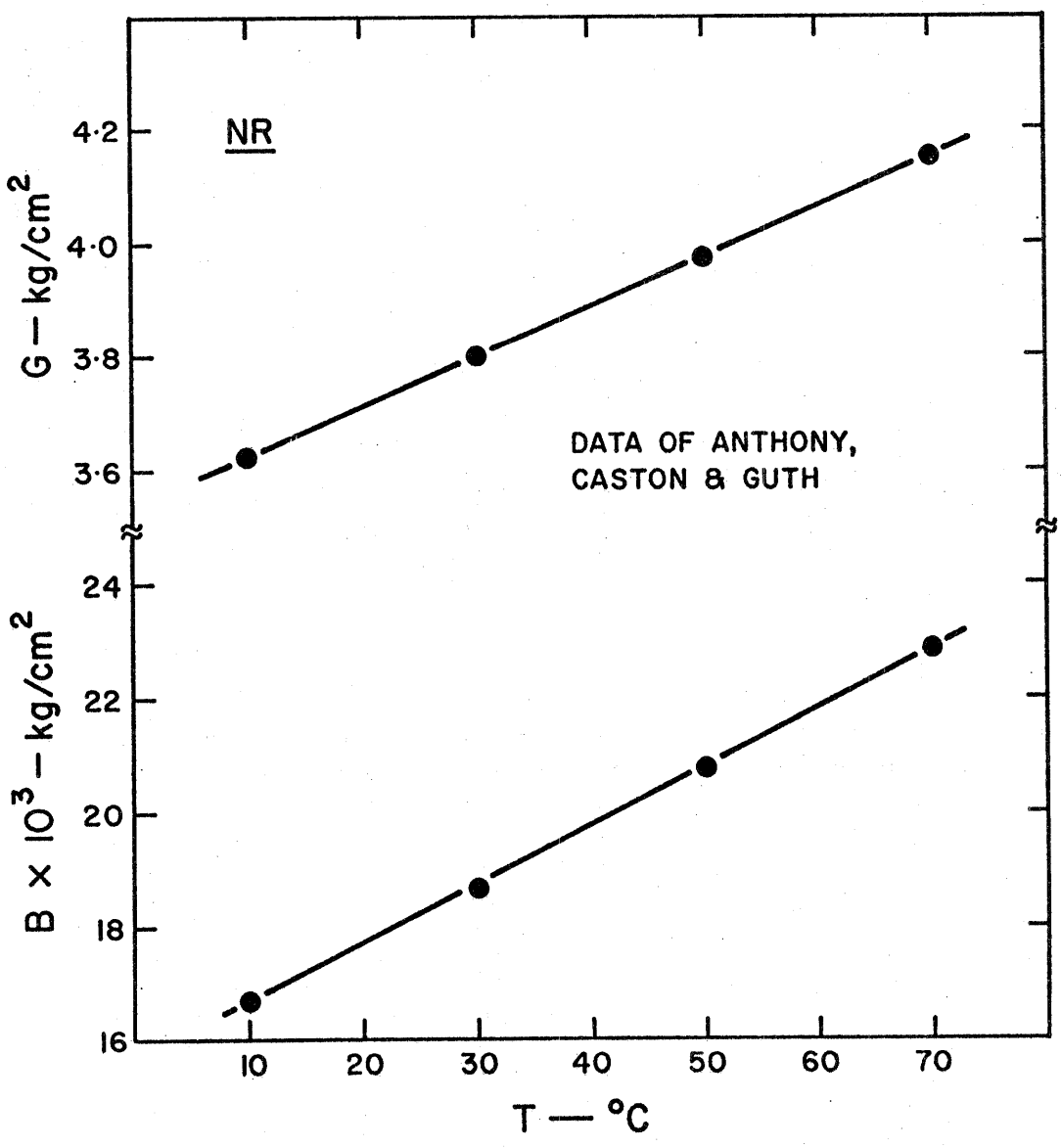

Figure 10 Temperature dependence of the constants G and B applied to data of Anthony, Caston and Guth on natural rubber.

TABLE I

Material Constants for Natural and Styrene-Butadiene Rubbers

Material	Temp.(°C)	G(kg/cm^2)	n	B × 10^3 (kg/cm^2)	m	Ref.
NR	20	4.0	1.64	0.83	4.0	20
NR	25	5.6	1.64	....	....	30
NR	10	3.62	1.64	16.67	3.1	29
NR	30	3.80	1.64	18.65	3.1	29
NR	50	3.97	1.64	20.73	3.1	29
NR	70	4.15	1.64	22.84	3.1	29
SBR[a]	25	....	1.34	0.00249[c]	6.55	15
SBR[b]	25	....	1.34	0.24[c]	4.02	15

[a] Simple tension and pure shear.

[b] Equibiaxial tension (compression).

[c] This value is actually B/3G (see the text).

References

1. P. J. Flory, "Principles of Polymer Chemistry", Cornell University Press, Ithaca, New York, 1953.

2. L. R. G. Treloar, "The Physics of Rubber Elasticity", Oxford at the Clarendon Press, London, 1958.

3. M. Shen, W. F. Hall and R. E. Dewames, J. Macromol. Sci. Revs. Macromol. Chem. C2(2), 183 (1968).

4. W. R. Krigbaum and R. J. Roe, Rubber Chem. Tech., 38, 1039 (1965).

5. R. S. Rivlin in "Rheology", F. Eirich, Ed., Academic Press, New York, 1956 Vol. 1.

6. A. C. Eringen, "Nonlinear Theory of Continuous Media", McGraw-Hill Book Co., New York, 1962.

7. a) B. R. Seth in, "Second Order Effects in Elasticity, Plasticity and Fluid Dynamics", M. Reiner and D. Abir, Eds., McMillan, New York, 1964, pp. 162-172.

   b) Proc. XI Int. Congr. Appl. Mech., Munich, Germany, 1964, pp. 383-389.

8. T. C. Hsu, S. R. Davies and R. Royales, J. Basic Eng., 89, 453 (1967).

9. P. J. Blatz, B. M. Chu and H. Wayland, Trans. Soc. Rheol., 13, 83 (1969).

10. B. M. Chu and P. J. Blatz, Ann. Biomed. Eng., 1, 204 (1972).

11. R. W. Ogden, Proc. Royal Soc. London, A326, 565 (1972).

12. P. J. Blatz, S. C. Sharda and N. W. Tschoegl, Proc. Nat'l. Acad. Sci., 70, 3041 (1973).

13. P. J. Blatz, S. C. Sharda and N. W. Tschoegl, Trans. Soc. Rheol., (in press).

14. S. C. Sharda, P. J. Blatz and N. W. Tschoegl, Letters in Appl. and Eng. Sci., (in press).

15. R. A. Dickie and T. L. Smith, Trans. Soc. Rheol., 15, 91 (1971).

16. K. C. Valanis and R. F. Landel, J. Appl. Phys., 38, 2297 (1967).

17. Y. Obata, S. Kawabata and H. Kawai, J. Poly. Sci., A-2, 8, 903 (1970).

18. T. J. Peng and R. F. Landel, J. Appl. Phys., 43, 3064 (1972).

19. R. Hill, Proc. Royal Soc. London, A314, 457 (1970).

20. L. R. G. Treloar, Trans. Faraday Soc., 40, 59 (1944).

21. T. L. Smith, private communication.

22. T. L. Smith and J. E. Frederick, Trans. Soc. Rheol., 12, 363 (1968).

23. R. A. Dickie and T. L. Smith, J. Poly. Sci., A-2, 7, 687 (1969).

24. R. S. Rivlin, Phil. Trans. Roy. Soc., London, A242, 173 (1949).

25. R. S. Rivlin and D. W. Saunders, Trans. Roy. Soc., London, A243, 251 (1951).

26. R. W. Ogden and P. Chadwick, J. Mech. Phys. Solids, 20, 77 (1972).

27. K. C. Valanis, J. Poly. Sci., 10, 1967 (1972).

28. R. S. Rivlin, Trans. Roy. Soc., London, A240, 589 (1948).

29. R. L. Anthony, R. H. Caston and E. Guth, J. Phys. Chem., 46, 826 (1942).

30. M. J. Forster, J. Appl. Phys., 26, 1104 (1955).

PART II

THERMOELASTIC BEHAVIOR

OF RUBBERS

1. INTRODUCTION

The establishment of relations between the bulk properties of macromolecules and their chemical structure has been a topic of major attention in polymer science. A number of general reviews of rubberlike elasticity are available in the literature (1, 2, 3, 4, 5, 6). These consider rubber elasticity from thermodynamics, molecular (statistical mechanical) and phenomenological (continuum mechanical) viewpoints. The objective of the work described here is the development of a phenomenological equation which permits the calculation of the temperature coefficient of the unperturbed displacement length of network chains over a wide range of extensions.

An effective way of examining the long range flexibility of macromolecules is to study the elastic retractive force in elastomers. Earlier theories of rubber elasticity have associated the retractive force with changes in the configurational entropy of the individual network chains. This has resulted in an equation of state applicable to what has been termed an ideal elastomer. In real elastomers, the elastic force arises not only from changes in the configurational entropy of the individual chains, but also contains significant contributions from the changes in internal energy due to intrachain and interchain interactions. Volkenstein (7), Flory et al. (8), and Volkenstein and Ptitsyn (9) have made important contributions to the statistical mechanics of polymer chains by incorporating the internal energy effects in the theory of

rubber elasticity. However, the range of validity of this equation is restricted to relatively low extensions ($\sim$40%).

The retractive force (f) in rubbers comprises the internal energy contribution (f_e) and the entropic contribution (f_s). From classical thermodynamics (see below), the relative change in the internal energy is given by:

$$f_e = f - T \left.\frac{\partial f}{\partial T}\right|_{P,L} - T \left.\frac{\partial P}{\partial T}\right|_{V,L} \left.\frac{\partial f}{\partial P}\right|_{T,L} \tag{1.1}$$

The entropic component of the force is then obtained by subtracting f_e from the total force. In order to determine f_e from Eq. (1.1) it is necessary to conduct four different experiments. These are the force temperature coefficient at constant pressure and length, the force-temperature coefficient at constant temperature and length and two components in $\gamma_{V,L}$:

$$\gamma_{V,L} \equiv \left.\frac{\partial P}{\partial T}\right|_{V,L} = - \left.\frac{\partial V}{\partial T}\right|_{P,L} / \left.\frac{\partial V}{\partial P}\right|_{T,L} \tag{1.2}$$

Due to difficulties in the determination of the force-pressure and the pressure-temperature coefficients, f_e/f has been determined traditionally by resorting to elastic equations of state which are subject to different assumptions. In this work, experimental measurements based on Eq. (1.1) have been generated.

In Chapter 2 the thermodynamics of a large principal deformation of a homogeneous isotropic elastomer is discussed. The analysis based on

different sets of independent variables is detailed. In Chapter 3 the theory of the retractive force is discussed from the thermodynamical, statistical mechanical, and the phenomenological viewpoints.

In Chapter 4 experiments on natural rubber conducted in connection with this study are described, and the data are presented. In Chapter 5 the results are compared with the predictions of the statistical and the phenomenological theories. Published data on a chlorinated ethylene-propylene copolymer rubber are also considered to extend this study. Calculation of hindrance potentials from f_e/f is demonstrated for the example of cis-polyisoprene chain. Finally in Chapter 6, the results and conclusions of this study are summarized.

2. THERMODYNAMICS OF ELASTOMERS

The thermodynamic description of the deformation of a solid system is more complex than that of a fluid (gas or liquid) system. In the latter, volume and pressure are the only mechanical parameters to be taken into account. In the former, the set of mechanical parameters must be enlarged, in the general case, to the 6+6=12 components of the strain and stress tensors (10). This section discusses the thermodynamic potential functions which are useful in describing the thermodynamics of large principal deformations of elastomers, and the general relations between their differentials and those of various sets of independent variables. Because an elastomer may be regarded as a homogeneous isotropic solid, its deformation can be described more simply than that of a general solid. The potential functions for the thermodynamics of elastomers introduced here are defined in a way which makes them consistent with the definitions of the potential functions in the thermodynamics of fluids.

2.1 Potential Functions

The first law of thermodynamics gives the change in the internal energy U as

$$dU = dQ - dW \tag{2.1}$$

where dQ is the element of heat absorbed, and dW is the element of work

done, by the system on its surroundings. If the process is conducted reversibly

$$dQ = T\ dS \tag{2.2}$$

where T is the (absolute) temperature and S is the entropy. Flory (11) has shown that the element of elastic work, dW, done by a homogeneous isotropic system in a large principal deformation is given by

$$dW = - V \sum_{i=1}^{3} t_i\ d\ell n\lambda_i \tag{2.3}$$

where V is the deformed volume, the t_i are the principal true stresses, and the λ_i are the principal extension ratios defined as the ratios of the stretched lengths, L_i, to the unstretched lengths, L_{io}.

Thus, the change in the internal energy is given by

$$dU = TdS + V \textstyle\sum_i t_i d\ell n\lambda_i \tag{2.4}$$

and the change in the associated free energy, defined by

$$A = U - TS \tag{2.5}$$

becomes

$$dA = - SdT + V \sum_i t_i d\ell n\lambda_i \tag{2.6}$$

The last terms in Eqs. (2.4) and (2.6) contain both the work of extension and the work of expansion. The two must be separated because changes in volume may be induced both by the application of forces or extensions, and by changes in temperature. We consider that the principal true stresses are

$$t_i = (L_i f_i/V) - P \tag{2.7}$$

where P is the external pressure and the f_i are the tractions along the three principal directions. Combining Eqs. (2.4) and (2.7), recognizing that

$$\sum_i d\ell n\lambda_i = d\ell nV \tag{2.8}$$

and using the summation convention for repeated indices from this point on, yields

$$dU = TdS - PdV + f_i dL_i \tag{2.9}$$

Similarly, from Eqs. (2.6) and (2.7),

$$dA = - SdT - PdV + f_i dL_i \tag{2.10}$$

Eq. (2.9) describes the elemental change in the internal energy, dU, in terms of their extensive parameters S, V, and L_i. By contrast, Eq. (2.10) has T, V, and L_i as the independent variables. The free energy (or Helmholtz free energy, or work content) A, therefore, is that partial Legendre transform (10) of U which replaces S by T as the independent variable.

The enthalpy, H, is defined in the thermodynamic of fluids as the thermodynamic potential summing the internal energy and the product of pressure and volume

$$H = U + PV \tag{2.11}$$

It is thus that partial Legendre transform of U which replaces V by P. Taking differentials and using Eq. (2.9) gives

$$dH = TdS + VdP + f_i dL_i \tag{2.12}$$

Now the Legendre transform of H which replaces S by T (or the transform of U which replaces S by T and V by P) is the free enthalpy (or Gibbs, or Lewis free energy), defined as

$$G = H - TS = U + PV - TS \tag{2.13}$$

Taking differentials and using Eq. (2.12) yields

$$dG = - SdT + VdP + f_i dL_i \tag{2.14}$$

The free enthalpy, G, is the free energy associated with the enthalpy, H.

The potential functions introduced so far simply parallel those in use in the thermodynamics of fluids and differ from them only in the additional $f_i L_i$ terms. It is because of the presence of these terms that A and G measure the work available in a reversible process from a homogeneous isotropic solid at constant temperature, and at constant temperature and pressure, respectively. Evidently, the work available at constant *forces* may also be of interest. Thus, we are led to consider those partial Legendre transforms in which L_i is replaced by f_i. As the first we introduce that thermodynamic potential which (algebraically) sums the internal energy and the products of the forces and lengths in the principal directions. Calling this potential D, we have

$$D = U - f_i L_i \tag{2.15}$$

which, proceeding as before, furnishes

$$dD = TdS - PdV - L_i df_i \tag{2.16}$$

Eq. (2.16) describes the elemental change in the thermodynamic potential D in terms of the independent variables S, V, and f_i. The corresponding

free energy, in which S is replaced by T as the independent variable, is

$$B = D - TS = U - f_i L_i - TS \tag{2.17}$$

from which we obtain

$$dB = - SdT - PdV - L_i df_i \tag{2.18}$$

If we assume the volume change to be negligible, we may set $dV = 0$, and D and B reduce to the "elastomer enthalpy", K, and its associated free energy, J, introduced by Wall (12) and elaborated by Reghi and Livingston (13). Wall derived these starting from the assumption that (in our notation)

$$dW = - f_i dL_i \tag{2.19}$$

i.e., that the elastomer is incompressible, in contrast to Eq. (2.3). However, even though the extension of an elastomer may not be accompanied by a noticeable change in volume, such a change may occur as function of temperature. In addition, at large pressures the incompressibility assumption is no longer tenable. Thus, Wall's potential functions are restricted to purely isochoric deformations. We prefer to bar the assumption of incompressibility from the definition of the potential functions.

With Eqs. (2.11) and (2.15) we have introduced potential functions which (algebraically) sum the internal energy and either the PV or the $f_i L_i$ term. The remaining potential to be introduced is

$$M = H - f_i L_i = U + PV - f_i L_i \tag{2.20}$$

which algebraically adds the internal energy to the PV as well as the $f_i L_i$ terms. We have

$$dM = TdS + VdP - L_i df_i \tag{2.21}$$

The associated free energy is

$$Z = M - TS = U + PV - f_i L_i - TS \tag{2.22}$$

from which we obtain

$$dZ = - SdT + VdP - L_i df_i \tag{2.23}$$

We call M the *elasthalpy* and Z the *free elasthalpy*. B and Z measure the work available in a reversible process from a homogeneous isotropic solid at constant temperature, and forces, and at constant temperature, pressure, and forces, respectively.

The choice of the appropriate thermodynamic potential with which

to describe the system depends on the experiment or the theoretical point one wishes to discuss. It should be noted, however, that the potentials U, A; H, G; D, B; and M, Z are the only transforms that need to be considered for the thermodynamic description of the principal deformation of an elastomer. In fact, for an elastomer, essentially the same thermodynamic information is obtained in uniaxial tension and in a more general deformation. Henceforth we shall, therefore, consider only simple tension, for which i = 1. For simplicity, we will write f, L, and λ for f_1, L_1, and λ_1. Thus we have

$$dU = TdS - PdV + fdL \tag{2.24}$$

$$dA = - SdT - PdV + fdL \tag{2.25}$$

$$dH = TdS + VdP + fdL \tag{2.26}$$

$$dG = - SdT + VdP + fdL \tag{2.27}$$

$$dD = TdS - PdV - Ldf \tag{2.28}$$

$$dB = - SdT - PdV - Ldf \tag{2.29}$$

$$dM = TdS + VdP - Ldf \tag{2.30}$$

$$dZ = - SdT + VdP - Ldf \tag{2.31}$$

We have here considered a closed system. Extension to an open system is straightforward. Consideration of an open single component system further elucidates the significance of the free energies associated with the deformation of a homogeneous isotropic solid. For an open single component system the Euler relation is

$$U = TS - PV + f_i L_i + \mu N \tag{2.32}$$

where μ is the chemical potential and N is the number of moles of the component. Inserting the Euler relation into Eqs. (2.5), (2.13b), (2.17b), and (2.22b) gives

$$A = - PV + f_i L_i + \mu N \tag{2.33}$$

$$G = f_i L_i + \mu N \tag{2.34}$$

$$B = - PV + \mu N \tag{2.35}$$

and

$$Z = \mu N \tag{2.36}$$

in turn. Thus, while the chemical potential is equal to the molar enthalpy in a fluid system, it is equal to the molar elasthalpy in a homogeneous isotropic solid.

In closing this subsection, we point out that the Gibbs-Duhem relation for such a solid is

$$SdT - VdP + L_i df_i = 0 \tag{2.37}$$

in a closed system. In an open single component system we have

$$d\mu = - sdT + vdP - (L_i/N)df_i \tag{2.38}$$

where s and v are the molar entropy and molar volume, respectively.

2.2 General Relations

Inspection of Eqs. (2.24) through (2.31) shows that S, V, and L are natural variables for U; T, V, and L are natural variables for A; etc. The differentials for these eight potential functions for a closed system, may, however, be expressed in terms of variables other than the natural ones and are often needed in such terms. In principle, the three independent variables can be chosen taking one variable from each of the three sets {S, T}, {V, P} and {L, f}, in which the first are extensive and the second are intensive variables. Thus, there are altogether $2^3 = 8$ sets of theoretically possible sets of variables. However, S is never used as an independent variable and, therefore, only the four sets

{T, V, L}

{T, V, f}

{T, P, L}

{T, P, f}

need to be obtained for each of the eight potential functions. Of these four sets, only the last two are convenient from the experimental standpoint. The first two sets are required, however, to correlate observations with theoretical considerations. Singling out U, A, M, and Z as the most important of the potentials, only 16 of the total of 32 relations will be derived here. To these may be added the "trivial" relations (2.25),

(2.27), (2.29), and (2.31). The remaining twelve are easily derived, when needed, by the procedures used in the following.

The derivations will make use of the Maxwell relations which are listed in the Appendix. Several of the partial derivatives have been designated by special symbols in the thermodynamics of fluids. These are redefined below as used in the thermodynamics of elastomers. They are:

(a) the specific heat at constants x and y

$$c_{x,y} = T \left.\frac{\partial S}{\partial T}\right|_{x,y} \tag{2.39}$$

where x represents either V or P, and y represents either f or L;

(b) the volumetric expansion coefficient at constant P and y

$$\beta_{P,y} = \frac{1}{V} \left.\frac{\partial V}{\partial T}\right|_{P,y} \tag{2.40}$$

where y is either f or L;

(c) the given expansion coefficient at constant P and f

$$\alpha_{P,f} = \frac{1}{L} \left.\frac{\partial L}{\partial T}\right|_{P,f} \tag{2.41}$$

(d) the isothermal compressibility at either constant force or constant length

$$\kappa_{T,y} = -\frac{1}{V}\left.\frac{\partial V}{\partial P}\right|_{T,y} \tag{2.42}$$

(e) and, finally,

$$\gamma_{V,y} = \left.\frac{\partial P}{\partial T}\right|_{V,y} = \frac{\beta_{P,y}}{\kappa_{T,y}} \tag{2.43}$$

with the previous meaning of y.

These partial derivatives differ from the definitions of specific heat, expansion coefficients, and isothermal compressibility in the thermodynamics of fluids because of the requirements of constant length or force.

2.21 T, V and L as independent variables

T, V, and L are the natural variables for the free energy, A. To obtain a relation for the internal energy change we need an expression for dS in terms of these variables. From S = S (T, V, L) we obtain

$$dS = \left.\frac{\partial S}{\partial T}\right|_{V,L} dT + \left.\frac{\partial S}{\partial V}\right|_{T,L} dV + \left.\frac{\partial S}{\partial L}\right|_{T,V} dL \tag{2.44}$$

With the aid of the appropriate Maxwell relations and Eqs. (2.39) and (2.43), Eq. (2.44) becomes

$$dS = T^{-1} c_{V,L} dT + \gamma_{V,L} dV - \left.\frac{\partial f}{\partial T}\right|_{V,L} dL \tag{2.45}$$

Equation (2.45) is not in a useful form because the partial derivatives in the first and third term on the right side must be determined at

constant volume which is difficult to do experimentally. We therefore change these partial derivatives at constant volume into the corresponding ones at constant pressure with the help of the general relation

$$\left.\frac{\partial Z}{\partial x}\right|_{W,U} = \left.\frac{\partial Z}{\partial x}\right|_{y,U} + \left.\frac{\partial Z}{\partial y}\right|_{x,U} \left.\frac{\partial y}{\partial x}\right|_{W,U} \tag{2.46}$$

using the Maxwell relations, if needed. This gives

$$dS = (T^{-1}c_{P,L} - TV\beta_{P,L}\gamma_{V,L})dT + \gamma_{V,L}dV - (\left.\frac{\partial f}{\partial T}\right|_{P,L} + \gamma_{V,L}\left.\frac{\partial f}{\partial P}\right|_{T,L})dL \tag{2.47}$$

Inserting this expression for dS into Eq. (2.24) and collecting terms, yields

$$dU = (c_{P,L} - TV\beta_{P,L}\gamma_{V,L})\ dT + (T\gamma_{V,L} - P)\ dV$$

$$+ (f - T\left.\frac{\partial f}{\partial T}\right|_{P,L} - T\ \gamma_{V,L}\left.\frac{\partial f}{\partial P}\right|_{T,L})\ dL \tag{2.48}$$

To obtain the desired expressions for the changes in the elasthalpy and free elasthalpy, we need, in addition to Eq. (2.45), expressions for dP and df. We obtain these from P = P(T, V, L) and f = f(T, V,L). Proceeding then as before, we obtain

$$dM = \left[c_{P,L} + (1 - T\beta_{P,L})\, V\gamma_{V,L} - L \left.\frac{\partial f}{\partial T}\right|_{P,L} - L\gamma_{V,L} \left.\frac{\partial f}{\partial P}\right|_{T,L} \right] dT$$

$$+ \left(T\gamma_{V,L} - \frac{1}{\kappa_{T,L}} + \frac{L}{V\kappa_{T,L}} \left.\frac{\partial f}{\partial P}\right|_{T,L} \right) dV$$

$$- \left[T \left.\frac{\partial f}{\partial T}\right|_{P,L} + L \left.\frac{\partial f}{\partial L}\right|_{T,P} + \left(T\gamma_{V,L} - \frac{1}{\kappa_{T,L}} + \frac{L}{V\kappa_{T,L}} \left.\frac{\partial f}{\partial P}\right|_{T,L} \right) \left.\frac{\partial f}{\partial P}\right|_{T,L} \right] dL$$

(2.49)

and

$$dZ = \left(V\gamma_{V,L} - S - L \left.\frac{\partial f}{\partial T}\right|_{P,L} - L\gamma_{V,L} \left.\frac{\partial f}{\partial P}\right|_{T,L} \right) dT - \frac{1}{\kappa_{T,L}} \left(1 - \frac{L}{V} \left.\frac{\partial f}{\partial P}\right|_{T,L} \right) dV$$

$$+ \left[\frac{1}{\kappa_{T,L}} \left(1 - \frac{L}{V} \left.\frac{\partial f}{\partial P}\right|_{T,L} \right) \left.\frac{\partial f}{\partial P}\right|_{T,L} - L \left.\frac{\partial f}{\partial L}\right|_{T,P} \right] dL \qquad (2.50)$$

2.22 T, P and L as independent variables

This set of independent variables is the natural set for the free enthalpy. To obtain a relation for the enthalpy H we have, from $S = S(T, P, L)$,

$$dS = \left.\frac{\partial S}{\partial T}\right|_{P,L} dT + \left.\frac{\partial S}{\partial P}\right|_{T,L} dP + \left.\frac{\partial S}{\partial L}\right|_{T,P} dL \qquad (2.51)$$

which can be rewritten by using the Maxwell relations and Eqs. (2.39) and (2.40) as

$$dS = \frac{1}{T}c_{P,L}dT - V\beta_{P,L}dP - \left.\frac{\partial f}{\partial T}\right|_{P,L}dL \tag{2.52}$$

Combining Eqs. (2.26) and (2.52) yields the change in enthalpy in terms of T, P and L as

$$dH = c_{P,L}dT + V(1 - T\beta_{P,L})dP + (f - T\left.\frac{\partial f}{\partial T}\right|_{P,L})dL \tag{2.53}$$

To obtain expressions for dU and dA, we use V = V(T, P, L) from which we obtain

$$dV = \left.\frac{\partial V}{\partial T}\right|_{P,L}dT + \left.\frac{\partial V}{\partial P}\right|_{T,L}dP + \left.\frac{\partial V}{\partial L}\right|_{T,P}dL \tag{2.54}$$

which leads to

$$dV = V\beta_{P,L}dT - V\kappa_{T,L}dP + \left.\frac{\partial f}{\partial P}\right|_{T,L}dL \tag{2.55}$$

Combining Eqs. (2.24), (2.52) and (2.55), and collecting terms, the change in internal energy results as

$$dU = (c_{P,L} - PV\beta_{P,L})dT + (P\kappa_{T,L} - T\beta_{P,L})VdP$$

$$+ (f - T\left.\frac{\partial f}{\partial T}\right|_{P,L} - P\left.\frac{\partial f}{\partial P}\right|_{T,L})dL \tag{2.56}$$

Inserting Eq. (2.55) into Eq. (2.25) yields

$$dA = -(S + PV\beta_{P,L})dT + PV\kappa_{T,L}dP + (f - P\left.\frac{\partial f}{\partial P}\right|_{T,L})dL \qquad (2.57)$$

To obtain expressions for dM and dZ we need df in terms of T, P, and L. From f = f(T, P, L)

$$df = \left.\frac{\partial f}{\partial T}\right|_{P,L} dT + \left.\frac{\partial f}{\partial P}\right|_{T,L} dP + \left.\frac{\partial f}{\partial L}\right|_{T,P} dL \qquad (2.58)$$

Substituting this into Eqs. (2.30) and (2.31) and using Eq. (2.52) in addition for dM, we find

$$dM = (c_{P,L} - L\left.\frac{\partial f}{\partial T}\right|_{P,L})dT + (V - VT\beta_{P,L} - L\left.\frac{\partial f}{\partial P}\right|_{T,L})\,dP$$

$$- (T\left.\frac{\partial f}{\partial T}\right|_{P,L} + L\left.\frac{\partial f}{\partial L}\right|_{T,P})dL \qquad (2.59)$$

and

$$dZ = -(S + \left.\frac{\partial f}{\partial T}\right|_{P,L})dT + (V - L\left.\frac{\partial f}{\partial P}\right|_{T,L})dP - L\left.\frac{\partial f}{\partial L}\right|_{T,P} dL \qquad (2.60)$$

2.23 T, V and f as independent variables

B is the natural function for this set of independent variables. An expression for dD is obtained by first finding dS from S = S(T, V, f). This gives

$$dS = \frac{1}{T} c_{V,f} dT + \gamma_{V,f} dV + L\alpha_{V,f} df \qquad (2.61)$$

where we have used the appropriate Maxwell relations to eliminate partial derivatives of S. Since the coefficients of dT and df are the inconvenient partial derivatives at constant volume, we change them to the corresponding ones at constant pressure using Eq. (2.46). This leads to

$$dS = \left(\frac{1}{T} c_{P,f} - V\beta_{P,f}\gamma_{V,f}\right)dT + \gamma_{V,f}dV + \left(L\alpha_{P,f} + \gamma_{V,f}\left.\frac{\partial L}{\partial P}\right|_{T,f}\right)df \tag{2.62}$$

Substituting this into Eq. (2.28) yields

$$dD = \left(c_{P,f} - TV\gamma_{V,f}\beta_{P,f}\right)dT + \left(T\gamma_{V,f} - P\right)dV + \left(TL\alpha_{P,f} + T\gamma_{V,f}\left.\frac{\partial L}{\partial P}\right|_{T,f} - L\right)df \tag{2.63}$$

To obtain dU and dA, we need an expression for dL. From L = L(T, V, f) we find

$$dL = \left(L\alpha_{P,f} + \gamma_{V,f}\left.\frac{\partial L}{\partial P}\right|_{T,f}\right)dT + \left.\frac{\partial L}{\partial V}\right|_{T,f}dV + \left(\left.\frac{\partial L}{\partial f}\right|_{T,P} + \left.\frac{\partial L}{\partial P}\right|_{T,f}\left.\frac{\partial L}{\partial V}\right|_{T,f}\right)df \tag{2.64}$$

To avoid derivatives at constant volume, we have used Eq. (2.46) for the coefficients of dT and df, and the Maxwell relation (A18) in the last

term on the right. Since the derivative $\partial L/\partial V$ is inconvenient experimentally, we eliminate it using the identity

$$\left.\frac{\partial L}{\partial V}\right|_{T,f} = -\frac{1}{V\kappa_{T,f}}\left.\frac{\partial L}{\partial P}\right|_{T,f} \tag{2.65}$$

Substituting the appropriate equations into Eqs. (2.24) and (2.25) furnishes

$$\begin{aligned} dU = {} & (c_{P,f} - TV\gamma_{V,f}\beta_{P,f} + f\gamma_{V,f}\left.\frac{\partial L}{\partial P}\right|_{T,f} + fL\alpha_{P,f})dT \\ & + (T\gamma_{V,f} - P - \frac{f}{V\kappa_{T,f}}\left.\frac{\partial L}{\partial P}\right|_{T,f})dV + \Bigg[TL\alpha_{P,f} + f\left.\frac{\partial L}{\partial f}\right|_{T,P} \\ & + (T\gamma_{V,f} - \frac{f}{V\kappa_{T,f}}\left.\frac{\partial L}{\partial P}\right|_{T,f})\left.\frac{\partial L}{\partial P}\right|_{T,f}\Bigg] df \end{aligned} \tag{2.66}$$

and

$$\begin{aligned} dA = {} & (-S + f\left.\frac{\partial L}{\partial T}\right|_{P,f} + f\gamma_{V,f}\left.\frac{\partial L}{\partial P}\right|_{T,f})dT - (P + \frac{f}{V\kappa_{T,f}}\left.\frac{\partial L}{\partial P}\right|_{T,f})dV \\ & + \Bigg[\left.\frac{\partial L}{\partial f}\right|_{T,P} - \frac{1}{V\kappa_{T,f}}(\left.\frac{\partial L}{\partial P}\right|_{T,f})^2\Bigg] f df \end{aligned} \tag{2.67}$$

For dM and dZ we require

$$dP = \gamma_{V,f}dT - \frac{dV}{\kappa_{T,f}} - \frac{1}{\kappa_{T,f}}\left.\frac{\partial L}{\partial P}\right|_{T,f} df \tag{2.68}$$

which results from P = P(T, V, f), using Eq. (A18) and then Eq. (2.65) to obtain the last term. With Eqs. (2.68) and (2.62) we then find

$$dM = \left[c_{P,f} + V\gamma_{V,f}\,(1 - T\beta_{P,f})\right] dT + (T\gamma_{V,f} - \frac{1}{\kappa_{T,f}})dV$$
$$- \left[L - TL\alpha_{P,f} - T\gamma_{V,f}\left.\frac{\partial L}{\partial P}\right|_{T,f} + \frac{1}{\kappa_{T,f}}\left.\frac{\partial L}{\partial P}\right|_{T,f}\right] df \qquad (2.69)$$

and

$$dZ = (-S + V\gamma_{V,f})dT - \frac{1}{\kappa_{T,f}}\,dV - (L + \frac{1}{\kappa_{T,f}}\left.\frac{\partial L}{\partial P}\right|_{T,f})df \qquad (2.70)$$

2.24 T, P, and f as independent variables

This set forms the natural variables of the free elasthalpy, z. To obtain dM, we seek dS from S = S(T, P, f). This yields

$$dS = \frac{1}{T}\,c_{P,f}dT - V\beta_{P,f}dP + L\alpha_{P,f}df \qquad (2.71)$$

and the change in the elasthalpy follows immediately as

$$dM = c_{P,f}dT + V(1 - T\beta_{P,f})dP - L(1 - T\alpha_{P,f})df \qquad (2.72)$$

To obtain the desired expressions for dU and dA we need expressions for both dV and dL. Proceeding as before, we find

$$dV = V\beta_{P,f}dT - V\kappa_{T,f}dP + \left.\frac{\partial L}{\partial P}\right|_{T,f} df \tag{2.73}$$

and

$$dL = L\alpha_{P,f}dT + \left.\frac{\partial L}{\partial P}\right|_{T,f} dP + \left.\frac{\partial L}{\partial f}\right|_{T,P} df \tag{2.74}$$

Substitution into Eqs. (2.24) and (2.25) then furnishes

$$\begin{aligned} dU = {} & (c_{P,f} + fL\alpha_{P,f} - PV\beta_{P,f})dT \\ & + (PV\kappa_{T,f} + f\left.\frac{\partial L}{\partial P}\right|_{T,f} - TV\beta_{P,f})dP \\ & + (TL\alpha_{P,f} + f\left.\frac{\partial L}{\partial f}\right|_{T,P} - P\left.\frac{\partial L}{\partial P}\right|_{T,f})df \end{aligned} \tag{2.75}$$

and

$$\begin{aligned} dA = {} & (-S + fL\alpha_{P,f} - PV\beta_{P,f})dT + (PV\kappa_{T,f} + f\left.\frac{\partial L}{\partial P}\right|_{T,f})dP \\ & + (f\left.\frac{\partial L}{\partial f}\right|_{T,P} - P\left.\frac{\partial L}{\partial P}\right|_{T,f})df \end{aligned} \tag{2.76}$$

3. INTERNAL ENERGY CONTRIBUTION TO THE ELASTIC FORCE

The elastic restoring force in rubbers results from deformational changes in the internal energy and the entropy of the rubber network. The internal energy changes are due to changes in the interchain and intrachain interactions in the network, whereas the entropy changes are associated with changes in the configurations of the network chains. From Eq. (2.25), the elastic force f is the change in the free energy with deformation at constant temperature and volume

$$f = \left.\frac{\partial A}{\partial L}\right|_{T,V} \tag{3.1}$$

which, from the definition of the free energy, Eq. (2.5), is also given by

$$f = \left.\frac{\partial U}{\partial L}\right|_{T,V} - T \left.\frac{\partial S}{\partial L}\right|_{T,V} \tag{3.2}$$

The total force f is thus resolved into entropic and energetic components defined by

$$f_s \equiv - T \left.\frac{\partial S}{\partial L}\right|_{T,V} = T \left.\frac{\partial f}{\partial T}\right|_{V,L} \tag{3.3}$$

$$f_e \equiv \left.\frac{\partial U}{\partial L}\right|_{T,V} \tag{3.4}$$

We obtain f_e from $f = f_e + f_s$, or by substituting Eq. (2.45) into Eq. (2.24) to obtain

$$dU = c_{V,L}dT + (T\gamma_{V,L} - P)dV + (f - T\left.\frac{\partial f}{\partial T}\right|_{V,L})dL \tag{3.5}$$

and then using Eq. (3.3). Either way results in

$$\frac{f_e}{f} = 1 - \frac{T}{f}\left.\frac{\partial f}{\partial T}\right|_{V,L} \tag{3.6}$$

An easily derived alternative form of Eq. (3.6) is

$$\frac{f_e}{f} = -T\left.\frac{\partial \ell n(f/T)}{\partial T}\right|_{V,L} \tag{3.7}$$

To determine f_e/f from Eq. (3.6), it is necessary to measure the changes in force with temperature at constant volume and length. Achievement of the constant volume condition requires applying hydrostatic pressure during the force temperature measurements. This experiment is extremely difficult in practice (14, 15). However, Eq. (2.48) directly provides the thermodynamically equivalent form of Eq. (3.6) given by

$$\frac{f_e}{f} = 1 - \frac{T}{f}\left.\frac{\partial f}{\partial T}\right|_{P,L} - \frac{T}{f}\gamma_{V,L}\left.\frac{\partial f}{\partial P}\right|_{T,L} \tag{3.8}$$

Instead of measuring the force-temperature coefficient at constant volume

and length, it is necessary to determine the four coefficients in Eq. (3.8) in order to calculate the relative internal energy component of the force. The four coefficients are the force-temperature coefficient at constant pressure and length, the force-pressure coefficient at constant temperature and length, the volumetric expansion coefficient, and the isothermal compressibility, both at constant lengths. The ratio of the last two is the pressure-temperature coefficient ($\gamma_{V,L}$), [cf., Eq. (2.43)].

An alternative approach to the determination of f_e/f consists in the simplification of Eq. (3.8) by resorting to an elastic equation of state. This procedure is subject to the validity of the assumptions made for the particular equation of state and, in addition, may be limited by the range within which the equation applies. Recently, Mark (16) has extensively reviewed the published data on f_e/f for a large number of elastomers. All the published works [except that of Allen et al. (14, 15) and of Dick and Mueller (17)] have used different equations of state in estimating f_e/f. Allen et al. have employed Eqs. (3.6) and (3.8), whereas Dick and Mueller obtained f_e/f from calorimetric methods. In the present work we determine the four coefficients in the thermodynamic Eq. (3.8) by employing new techniques. Also, we consider the statistical equation of state and the Blatz-Sharda-Tschoegl (BST) strain energy density function in estimating the relative internal energy component of the force.

3.1 Statistical Theory

The statistical theory of rubber elasticity considers the

changes in the free energy of an amorphous, cross-linked polymer. It is postulated (11, 18) that the free energy consists of two parts given by

$$A = A_1(T,V) + A_2(T,\Lambda) \tag{3.9}$$

where A_1 is the energy of interchain interactions and A_2 is the so-called "elastic" part of the free energy. It is assumed that A_1 depends only on T and V and is not a function of the state of strain. All the dependence of the free energy A on the deformation is through A_2 which is specified for a given temperature and displacement gradient tensor Λ. A_2 contains the contributions to the total free energy A arising from two factors. (1) the configurational entropy of the network chains, and (2) the hindrance to rotational potentials along the chain backbone (energy of intrachain interactions). In addition to assuming the addivity of free energies as given by Eq. (3.9), we require an explicit form for A_2. Since the elastic force as defined by Eq. (3.1) will have no contribution from A_1, it is not necessary to calculate this term. An expression for A_2 was given by Flory et al. (8) in the form

$$A_2 = \frac{\nu kT}{2}\left[\eta(\lambda_1^2 + \lambda_2^2 + \lambda_3^2)-3\right] - \nu kT\, \ell n(\eta^{3/2}\lambda_1\lambda_2\lambda_3) \tag{3.10}$$

ν is the number of network chains, k is Bolzmann's constant, and η is defined by

$$\eta \equiv \frac{\langle r^2 \rangle_i}{\langle r^2 \rangle_o} \tag{3.11}$$

To derive Eq. (13.10), Flory et al. have used the configurational integral of Volkenstein and Ptitsyn (9)

$$Z_f = \int \ldots \int \exp \left[(\vec{r} \cdot \vec{f} - \varepsilon\{\vec{\ell}\})/kT \right] d\vec{\ell}_1 \ldots . d\vec{\ell}_n \tag{3.12}$$

in which $\vec{f}$ is the external force applied to a chain, $\vec{\ell}_i$ (i = 1, 2, ...n) are the n bond vectors, $\vec{r}$ is the vector connecting the ends of the chain and $\varepsilon\{\vec{\ell}\}$ is the conformational energy (representing intrachain interactions) for the set of bond vectors $\{\vec{\ell}\}$. This is in contrast to the earlier statistical theories (19, 20) where the total free energy had been considered to consist of only the configurational entropy of the chains (i.e., $\varepsilon\{\vec{\ell}\} = 0$) thus in effect neglecting the changes in the internal energy. Equation (3.12) includes the contributions of intrachain energy and forms the basis for the network elasticity in the present form. The details of the derivation of Eq. (3.10) are given elsewhere (8, 18, 21).

In Eq. (3.11), $\langle r^2 \rangle_i$ is the mean square end-to-end distance for a network chain in the state of volume V, and $\langle r^2 \rangle_o$ is the corresponding "unperturbed" value for the free chain. $\langle r^2 \rangle_o$ depends on the potentials hindering the rotation and is therefore a function of temperature. On the other hand, $\langle r^2 \rangle_i$ depends only on the volume V of the network and is directly proportional to $V^{2/3}$. The various assumptions involved in Eq. (3.10) are

1. The chains in the network are long enough to assure the validity of the Gaussian distribution.
2. The free energy is the sum of two terms given by Eq. (3.9).
3. The intermolecular interactions are independent of deformation.
4. Cross-link junctions in the network transform in the same ratio as the macroscopic extension ratio (affine deformation).
5. Cross-link junctions are fixed at their mean positions. Needless to say, these assumptions are quite restrictive and oversimplify the physical nature of a rubbery network.

For the case of simple elongation, the retractive force in elastomers may now be obtained from Eq. (3.10) as

$$f = \left.\frac{\partial A}{\partial L}\right|_{T,V} = GA_o \left(\lambda - \frac{V}{V_o \lambda^2}\right) \tag{3.13}$$

where A_o is the initial cross-sectional area of the specimen, and the modulus G is defined by

$$G \equiv \frac{\nu kT}{V_o} \eta \tag{3.14}$$

Equation (3.13) is the statistical equation of state for elastomers (also referred to as the neo-Hookean equation). This equation provides the motivation for determining f_e/f. Combining Eqs. (3.7) and (3.13) yields

$$\frac{f_e}{f} = T \frac{d\ell n \langle r^2 \rangle_o}{dT} \tag{3.15}$$

Thus, f_e/f is directly related to the temperature coefficient of the dimensions of the chains in the network. Specifically, the temperature coefficient of the free chain can be used to interpret the difference in the energy levels present in the chain. For the purpose of illustration let us consider the chains in the network are of the polymethylene type so that their rotational potential energy curve is characterized by three minima at $\phi = \pi$ and $\pm \pi/3$, where ϕ is the angle of rotation. The dimension of such a chain consisting of n bonds each of length ℓ is given by (22, 23)

$$\langle r^2 \rangle_o = n\ell^2 \frac{1 + \cos\theta}{1 - \cos\theta} \frac{1 + \chi}{1 - \chi} \qquad (3.16)^*$$

where $\pi - \theta$ is the bond angle and χ depends upon the angle of rotation. For this particular chain, χ is given by (7, 23)

$$\chi = \langle \cos\phi \rangle_o = \frac{1 - \exp(-\Delta u/kT)}{1 + 2 \exp(-\Delta u/kT)} \qquad (3.17)$$

where Δu is the difference between the energies $u(\pi/3)$ and $u(\pi)$ of the gauche and transrotational isomers, i.e.

$$\Delta u = u(\pi/3) - u(\pi) \qquad (3.18)$$

*A large number of such relations for various types of chains are available in literature (7, 23, 24).

Now Eqs. (3.15) and (3.16) yield

$$\frac{f_e}{f} = \frac{T d\ell n\langle r^2\rangle_o}{dT} = \frac{-2\Delta u}{kT\left[2 + \exp\ (-\Delta u/kT)\right]} \tag{3.19}$$

Thus, f_e/f, which is determined from the physical properties of the bulk polymer, yields two important molecular characteristics of polymethylenic chains. Of course, the two quantities given by Eq. (3.19) may be determined from alternative procedures (measurements of light scattering, intrinsic viscosity, sedimentation velocity, diffusion constant, etc.), but the thermoelastic experiments are easier and more effective for cross-linked amorphous polymers.

Since Eq. (3.13) is a special case of the BST equation of state, we will consider the predictions of the statistical theory together with the predictions of the BST strain energy function.

3.2 Compressible BST Strain Energy Function

To describe thermoelastic behavior from the phenomenological viewpoint, it is necessary to modify the BST strain energy function to account for the compressibility of the material. An infinity of choices is possible for the compressible form of a strain energy function; the only restriction being that it satisfy Hooke's Law in the limit of small strain. The function we have chosen is similar in form to one suggested by Blatz (25, 26, 27) but is based on the BST equation, of which we use

only the first part, valid, for natural rubber, up to about 200% extension in simple tension. We write

$$W = \frac{2G}{n} I_E + \phi(J) \tag{3.20}$$

where $\phi(J)$ is a function to be determined. Once again, J is the ratio of the stretched volume to the unstretched volume of the rubber. The compressible stress-strain relation is obtained from Eq. (3.20) by differentiation

$$\bar{\sigma}_\alpha J = \frac{2G}{n}\lambda_\alpha^n + J\phi'(J) \tag{3.21}$$

To evaluate the function ϕ' we make use of the procedure developed by Blatz. To describe compressibility data on rubberlike materials he used the empirical expression

$$-P = \frac{K}{k}(1 - J^{-k}) \tag{3.22}$$

in which k is known as the Murnaghan exponent (28) and K is the bulk modulus. This equation was successfully used by Murnaghan to fit Bridgman's (29) high pressure data for solids. The same expression was found to hold for rubbers (25). The value of k for a number of rubbers was estimated to be around 10. Writing Eq. (3.21) for the case of hydrostatic pressure, we obtain

$$- P = \frac{2G}{n} J^{n/3-1} + \phi'(J) \tag{3.23}$$

Equating Eqs. (3.22) and (3.23) we obtain, upon integration between the limits 1 and J

$$\phi(J) = \frac{K}{k} \left(J + \frac{J^{1-k}}{k-1} - \frac{k}{k-1}\right) - \frac{6G}{n^2} \left(J^{n/3} - 1\right) \tag{3.24}$$

Substituting Eq. (3.24) into Eq. (3.20) gives a compressible strain energy function

$$W = \frac{2G}{n}\left[I_E - \frac{3(J^{n/3}-1)}{n}\right] + \frac{K}{k}\left[(J - 1) + \frac{J^{1-k} - 1}{k - 1}\right] \tag{3.25}$$

We expect Eq. (3.25) to describe the simple tension behavior of elastomers at high pressures.

Equation (3.25) assumes that the modulus is independent of the volume. Tobolsky and Shen (30) have shown that the shear modulus of rubbers is slightly volume dependent. To account for this dependence they introduced a parameter γ in the statistical theory. The effect of this is to render the statistical theory semi-empirical. This parameter can only be considered phenomenological since no reasons for its existence have been advanced on the ground of molecular considerations. Thus, whereas the parameter γ is perfectly legitimate in a phenomenological description, it is out of place in a rigorous statistical theory. We introduce it into the compressible form of the BST equation in anticipa-

tion of its possible use in describing the volume dependence of the modulus. Following Tobolsky and Shen, we modify Eq. (3.25) to

$$W_c = J^{\gamma}\left\{\frac{2G}{n}\left[I_E - \frac{3(J^{n/3} - 1)}{n}\right] + \frac{K}{k}\left[(J - 1) + \frac{J^{1-k} - 1}{k - 1}\right]\right\} \quad (3.26)$$

It will become clear later that the form of W_c given by

$$W_c = J^{\gamma}\frac{2G}{n} I_E \quad (3.26a)$$

is all that we need to deal with our data. However, at high pressure, Eq. (3.26a) is inadequate (25). We, therefore, prefer to carry out the analysis using the full Eq. (3.26).

The general stress-strain relation thus becomes

$$\bar{\sigma}_\alpha = \frac{\sigma_\alpha \lambda_\alpha}{J} = \frac{\lambda_\alpha}{J}\frac{\partial W_c}{\partial \lambda_\alpha} =$$

$$\gamma J^{\gamma-1}\left\{\frac{2G}{n}\left[I_E - \frac{3(J^{n/3} - 1)}{n}\right] + \frac{K}{k}\left[(J - 1) + \frac{J^{1-k} - 1}{k - 1}\right]\right\}$$

$$+ J^{\gamma-1}\left\{\frac{2G}{n}(\lambda_\alpha^n - J^{n/3}) + \frac{K}{k}(J - J^{1-k})\right\} \quad (3.27)$$

where $\bar{\sigma}_\alpha$ is the true stress.

For the special case of simple tension and superimposed hydrostatic pressure, we have $\bar{\sigma}_1 = \bar{\sigma} - P$, $\bar{\sigma}_2 = \bar{\sigma}_3 = P$, and $\lambda_1 = \lambda$, $\lambda_2 = \lambda_3 = \sqrt{J/\lambda}$

Substituting these into Eq. (3.27) yields

$$\sigma\lambda - PJ = \gamma J^{\gamma} \left\{\frac{2G}{n}\left[I_E - \frac{3(J^{n/3} - 1)}{n}\right] + \frac{K}{k}\left[(J - 1) + \frac{J^{1-k} - 1}{k - 1}\right]\right\}$$

$$+ J^{\gamma} \left\{\frac{2G}{n}(\lambda^n - J^{n/3}) + \frac{K}{k}(J - J^{1-k})\right\} \qquad (3.28)$$

But, from $\bar{\sigma}_2 = \bar{\sigma}_3 = -P$ and Eq. (3.27)

$$-PJ = \gamma J^{\gamma} \left\{\frac{2G}{n}\left[I_E - \frac{3(J^{n/3}-1)}{n}\right] + \frac{K}{k}\left[(J - 1) + \frac{J^{1-k}-1}{k - 1}\right]\right\}$$

$$+ J^{\gamma}\left\{\frac{2G}{n}\left(\frac{J^{n/2}}{\lambda^{n/2}} - J^{n/3}\right) + \frac{K}{k}(J - J^{1-k})\right\} \qquad (3.29)$$

so that

$$\sigma\lambda = \frac{2G}{n} J^{\gamma} (\lambda^n - J^{n/2}/\lambda^{n/2}) \qquad (3.30)$$

Equations (3.29) and (3.30) reduce to the incompressible equations introduced in the first part of this thesis by setting $J = 1$. Equation (3.30) may be rewritten in terms of the elastic force as

$$f = \frac{2G}{n} A_o J^{\gamma} \left(\lambda^{n-1} - J^{n/2}/\lambda^{n/2} + 1\right) \tag{3.31}$$

These equations are now used in conjunction with Eq. (3.7) to determine the relative internal energy component of the force. For the following analysis it is assumed that the parameters k and γ are independent of temperature and pressure, at least in the small range of temperature and pressure we will consider in this work. This assumption seems reasonable in the light of the temperature independence of the parameters n and m (see Part I). Equation (3.31) is rewritten here as

$$\begin{aligned} \ell nf = {} & \ell n(2/n) + \ell nG + \ell nA_o + \gamma \ell nJ + \ell n \left(\lambda^{3n/2} - J^{n/2}\right) \\ & - (n/2 + 1)\ell n\lambda \end{aligned} \tag{3.32}$$

Keeping in mind that V_o, A_o, and L_o change with temperature, the temperature derivative of Eq. (3.32) at constant V and L is given by

$$\left.\frac{\partial \ell nf}{\partial T}\right|_{V,L} = \frac{1}{G}\frac{dG}{dT} + \alpha_o(3 - n - 3\gamma) \tag{3.33}$$

where α_o is the linear expansion coefficient of the undeformed material. Hence, from Eqs. (3.7) and (3.33)

$$\frac{f_e}{f}(BST)^1 = 1 - \frac{T}{G}\frac{dG}{dT} - \alpha_o T(3 - n - 3\gamma) \tag{3.34}$$

where the superscript 1 distinguishes this expression from the one to be derived below.

An alternative expression for f_e/f may be obtained by considering the temperature derivative of Eq. (3.32) at constant P and L

$$\left.\frac{\partial \ell nf}{\partial T}\right|_{P,L} = \frac{1}{G}\frac{dG}{dT} + \alpha_o\left[\frac{(3-n)\lambda^{3n/2} - (3 + n/2)}{\lambda^{3n/2} - 1}\right] \tag{3.35}$$

where it has been assumed that $\beta_{P,L} = 3\alpha_o$. This assumption will be justified below. Combining Eqs. (3.33) and (3.35) yields

$$\frac{f_e}{f}(BST)^2 = 1 - \frac{T}{f}\left.\frac{\partial f}{\partial T}\right|_{P,L} - \left[\frac{n}{2(\lambda^{3n/2} - 1)} - \gamma\right]3\alpha_o T \tag{3.36}$$

Now, the statistical or neo-Hookean equation of state is the special case of Eq. (3.31), in which n = 2 and $\gamma = 0$. For this special case we obtain the following equations from Eqs. (3.34) and (3.36)

$$\frac{f_e}{f}(SB) = 1 - \frac{T}{G}\frac{dG}{dT} - \alpha_o T \tag{3.37}$$

$$\frac{f_e}{f}(FCH) = 1 - \frac{T}{f}\left.\frac{\partial f}{\partial T}\right|_{L,P} - \frac{3\alpha_o T}{\lambda^3 - 1} \tag{3.38}$$

In these equations SB stands for Shen and Blatz (31) and FCH stands for Flory, Ciferri and Hoeve (32) who first derived these equations. Equations

(3.37) and (3.38) are both based on the statistical theory but differ considerably in their estimation of f_e/f. Equation (3.37) claims f_e/f to be independent of strain, but this would be true according to Eq. (3.38) only if there were a compensating effect in the strain dependence of the force-temperature coefficients. The various equations will be compared in Chapters 4 and 5.

Before we close this section, however, we note that, from Eq. (2.46)

$$\gamma_{V,L} \left.\frac{\partial f}{\partial P}\right|_{T,L} = \left.\frac{\partial f}{\partial T}\right|_{V,L} - \left.\frac{\partial f}{\partial T}\right|_{P,L} \tag{3.39}$$

where the two terms of the right side are given by Eqs. (3.33) and (3.35) which were derived from Eq. (3.30). To check on the consistency of these expressions we can obtain $(\partial f/\partial P)_{T,L}$ also from Eq. (3.30), and $\gamma_{V,L} = (\partial P/\partial T)_{V,L}$ from Eq. (3.29). Simultaneously we will obtain justification for the earlier assumption that $\beta_{P,L} \simeq 3\alpha_o$.

To obtain the force-pressure coefficient at constant temperature and length, we differentiate Eq. (3.32) with respect to pressure to yield

$$\left.\frac{\partial \ell nf}{\partial P}\right|_{T,L} = \kappa_{T,L} \left[\frac{n}{2(\lambda^{3n/2}-1)} - \gamma\right] \tag{3.40}$$

Taking the temperature derivative of Eq. (3.29) at constant V and L, we get

$$-J^{1-\gamma}\left.\frac{\partial P}{\partial T}\right|_{V,L} = \gamma\left\{\frac{2G}{n}\ \alpha_o(J^{n/3}-\lambda^n - 2J^{-n/2}\lambda^{n/2})\right.$$

$$+\frac{2}{n}\frac{dG}{dT}\left[I_E - \frac{3(J^{n/3}-1)}{n}\right] + \frac{1}{k}\frac{dK}{dT}\left[(J-1) + \frac{J^{1-k}-1}{k-1}\right]$$

$$\left. - \frac{3K}{k}\alpha_o(J - J^{1-k})\right\}$$

$$+\frac{2}{n}\frac{dG}{dT}(\lambda^n - J^{n/3}) - 2G\alpha_o(\lambda^n + J^{n/3}) + \frac{1}{k}\frac{dK}{dT}(J - J^{1-k})$$

$$- 3\alpha_o\frac{K}{k}\left[J - (1-k)J^{1-k}\right] - 3P(1-\gamma)\alpha_o J^{1-\gamma} \qquad (3.41)$$

For ordinary pressures J will not change much, so that we may set J = 1. We also note that the bulk modulus K of rubbers is usually four orders of magnitude larger than the ~~other~~ modulus G, so that the terms containing K are dominant in Eq. (3.41) ($P \ll K$). This observation simplifies the above expression to

$$\gamma_{V,L} = \left.\frac{\partial P}{\partial T}\right|_{V,L} \simeq 3\alpha_o K \qquad (3.42)$$

Simil ly, we may differentiate Eq. (3.29) with respect to pressure at constant temperature and length, and with respect to temperature at constant pressure and length to obtain expressions for the isothermal compressibility and expansion coefficient, respectively, at constant length. The results thus obtained are

$$\kappa_{T,L} \simeq \frac{1}{K} \tag{3.43}$$

and

$$\beta_{P,L} = 3\alpha_o \tag{3.44}$$

which justifies the assumption made earlier in connection with Eq. (3.35). Once again, we have set J = 1 in Eqs. (3.43) and (3.44) and assumed that $K \ll G$, and $P \ll K$.

Combining Eqs. (3.40), (3.42), and (3.43) yields

$$\gamma_{V,L} \left.\frac{\partial \ell n f}{\partial P}\right|_{T,L} = 3\alpha_o \left[\frac{n}{2(\gamma^{3n/2}-1)} - \gamma\right] \tag{3.45}$$

But the right side of Eq. (3.45) equals the difference between the force-temperature coefficient at constant volume and length, and the force-temperature coefficient at constant pressure and length [cf., Eqs. (3.33) and (3.35)]. Hence, Eq. (3.39) is vindicated.

Equations (3.35), (3.40) and (3.42) give expressions for the partial derivatives in Eq. (3.8). These expressions predict that the force-temperature and force-pressure coefficients in Eq. (3.8) are functions of the strain but the volume-temperature and volume-pressure are not. The latter was postulated by Flory (5) and was later confirmed experimentally by Allen and coworkers (14).

3.3 Contributions to the Extension

As is the custom, we have discussed the contribution of the internal energy to the restoring force in elastomers. It should be noted, however, that the length may be considered just as well as the force in the extension of an elastomer specimen. In such an experiment, a constant force is applied to the test piece and the changes in equilibrium lengths are studied at various conditions of temperature and pressure.

From Eq. (2.31), the lengths at constant temperature and pressure are obtained as

$$L = \left.\frac{\partial Z}{\partial f}\right|_{T,P} \tag{3.46}$$

i.e., as the partial derivative, with respect to force, of the free elasthalpy defined in Chapter 2. From Eq. (2.22a) then,

$$L = \left.\frac{\partial M}{\partial f}\right|_{T,P} - T \left.\frac{\partial S}{\partial f}\right|_{T,P} \tag{3.47}$$

where M is the elasthalpy. The length (or, more meaningfully, the extension $\Delta L = L - L_o$) can, therefore, likewise be resolved into elasthalpic and entropic components

$$\Delta L_M = \left.\frac{\partial M}{\partial f}\right|_{T,P} - L_o \tag{3.48}$$

and

$$\Delta L_S = - T \left.\frac{\partial S}{\partial f}\right|_{T,P} - L_o = -T \left.\frac{\partial L}{\partial T}\right|_{P,f} - L_o = LT\alpha_{P,f} - L_o \quad (3.49)$$

thus

$$L_M = L(1 + T\alpha_{P,f}) \quad (3.50)$$

The linear thermal expansion coefficient at constant pressure and force, $\alpha_{P,f}$ is easily determined experimentally by the method detailed in Section 4.4. We remark parenthetically that similar decompositions can be made from

$$f = \left.\frac{\partial H}{\partial L}\right|_{T,P} \quad (3.51)$$

and

$$L = \left.\frac{\partial B}{\partial f}\right|_{T,V} \quad (3.52)$$

The first splits the force into an enthalpic and entropic component, while the second resolves the extension into components linked to the functions D and S. The two entropic components of the force or the extensions are, of course, not identical. We suspect that the elasthalpic and entropic components of the extension could be useful parameters, particularly in practical applications.

It is, naturally, also possible to obtain the extension con-

tributed by internal energy. This is easily obtained from Eq. (2.74) as

$$\Delta L_E = \left.\frac{\partial U}{\partial f}\right|_{T,P} - L_o = TL\alpha_{P,f} + f \left.\frac{\partial L}{\partial f}\right|_{T,P} - P \left.\frac{\partial L}{\partial P}\right|_{T,f} - L_o \qquad (3.53)$$

The expressions involving changes with length and changes with force are interchangeable and, in principle, would yield exactly the same molecular information. However, the choice of one set of independent variables over the other may be dictated by experimental convenience. With the recent development of new techniques for measuring dimensional changes (33), the constant force experiment may prove to be of some importance. Shen and coworkers (34, 35) have studied some thermoelastic behavior at constant force.

4. EXPERIMENTAL

Natural rubber latex was chosen as the material for studying the internal energy component of the restoring force in natural rubber.

4.1 Natural Rubber Latex (NR) Samples

Natural rubber samples were prepared from a rubber latex using the following formula

Firestone S-5 Hevea Latex	100.0 parts
AZ-64	16.78 parts
Setsit-5	1.5 parts

AZ-64 is a dispersion prepared by Aztec Chemical Division of American Mineral Spirits Company, Los Angeles. It consists of five parts of zinc oxide, two parts of sulfur and two parts of Wingstay-L antioxidant. The rubber and the dispersion were stirred for about fifteen minutes and the slurry-like mixture was dried under vacuum for two days. Setsit-5, supplied by Vanderbilt Chemical Corporation, Bethel, Connecticut, was used as an accelerator. It was milled into the dry mixture which was cured in the mold for eight hours at 95°C. Ring specimens of 1.5 in. outer and 1.35 in. inner diameters were cut from a 0.175 in. thick sheet.

The density of the rubber at 23°C was 0.921 gm/cc. The average cross-link density was determined by swelling in benzene as 3.46×10^{-4} moles/cc.

4.2 Ring Specimens

Before describing the experimental procedures for the determination of the four coefficients in Eq. (3.8), it is important to define the manner in which stress and strain are calculated from the measured variables, force and displacement, in a ring specimen. Let the ring specimen have the following dimensions

t_o = initial thickness of the sheet from which the ring is cut

w_o = initial width of the ring = $(D_o - D_i)/2$

D_o = outside diameter of the ring

D_i = inside diameter of the ring

The stress, σ, based on the undeformed cross-section of the ring is given by

$$\sigma = \frac{f}{2t_o w_o} \tag{4.1}$$

where f is the observed force.

At any extension, the shape of the deformed ring is as shown in the following figure

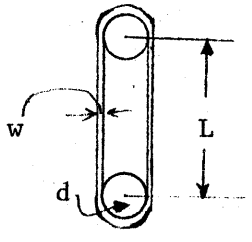

Here, L represents the separation of two hooks holding the sample and

d is the diameter of these hooks. We will use the extension ratio based on the average diameter of the rings. This is given by

$$\lambda_{avg} = \frac{c}{c_o} \tag{4.2}$$

where c and c_o are the average circumferences of the deformed and the undeformed ring, respectively. From inspection of the figure

$$c = 2L + \pi(d + w) \tag{4.3}$$

and

$$c_o = \pi D_a \tag{4.4}$$

Thus,

$$\lambda_{avg} = \frac{2L + \pi(d + w)}{\pi D_a} \tag{4.5}$$

where D_a is the average diameter of the ring and w is the width of the deformed specimen. In practice, it is not always possible to measure the width of the deformed sample. In such a case, one may safely resort to the assumption of incompressibility (36, 37) to obtain an expression for w. However, in our case, we will use Eq. (4.5) as such, since the dimensions of the deformed sample will be measured. The stretch ratio,

λ, referred to in the remainder of the text denotes the average value given by Eq. (4.5). Since it is common practice to plot stress as a function of strain, henceforth we will consider the stress coefficient rather than the force coefficients.

4.3 Stress-Temperature Coefficient

To estimate the stress-temperature coefficient, the changes in force with temperature at various elongations are measured. A ring specimen was pulled to a desired elongation at room temperature in the Instron Tensile Tester. The initial force was allowed to come to an equilibrium value, and the output corresponding to this value was then suppressed electronically so as to observe the force changes on a more sensitive scale. The temperature of the system was now raised to 60°C and again the force was allowed to relax. The temperature was then lowered in steps of 10°C, and the relaxed force recorded at each temperature interval. This procedure was repeated at various elongations, both in cooling as well as heating cycles. In general, it took two to three hours to obtain equilibrium at a given temperature. A plot of stress against temperature at various elongations is shown in Figure 1. The data are also given in Table 1. The solid lines represent the least squares fits. The slopes of these lines are the stress-temperature coefficients, shown in Figure 2.

To check the predictions of the new strain energy function, a cross-plot of Figure 1 is shown in Figure 3. The solid lines are ob-

tained from Eq. (3.30) with J = 1 and n = 1.64 for all temperatures. The results of the stress temperature experiments once again confirm (38, 39) that only the modulus in the new strain energy function depends upon temperature. The variation in modulus with temperature is linear (Figure 4) and the slope, dG/dT, of the line is 13×10^{-3} bars/°C.

4.4 Pressure-Temperature Coefficient

Two experimental procedures for determining the pressure-temperature coefficient have been described in the literature. Allen et al. (14, 15) have calculated $\gamma_{V,L}$ from the ratio of $\kappa_{L,T}$ and $\beta_{L,P}$ which were determined using a special dilatometer. Bianchi and Pedemonte (40) have measured the internal pressure for elastomers from which the pressure-temperature coefficient was estimated. Here we employ an entirely different technique. A highly sensitive thickness sensor based on the Hall effect measures the width of the specimen as a function of temperature and pressure at constant length. $\gamma_{V,L}$ is calculated from the width-temperature and width-pressure coefficients, both at constant lengths

$$\gamma_{V,L} = - \left.\frac{\partial w}{\partial T}\right|_{P,L} \Big/ \left.\frac{\partial w}{\partial P}\right|_{T,L} \tag{4.6}$$

The theory and experimental details concerning the thickness sensor are given by Yagii (37) and by Okuyama, Yagii, Sharda and Tschoegl (33).

To demonstrate briefly the working of the sensor, a typical

arrangement is shown in Figure 5. Here, S is the specimen, H is the Hall device and M is a small but powerful magnet. The whole assembly is held by a spring (Sp). The clamp (C) installs the device on the specimen. The thickness sensor was constructed from a F. W. Bell, Inc. Model BH-700 Hall effect device. A constant input current (I_c) was supplied to the Hall device from a Hewlett-Packard Model 6218A power supply. The set-up is shown in Figure 6. The output voltage from the Hall device is directly recorded, and may be suppressed using the voltage suppressor (SUP). The experimental procedure consists of placing the thickness sensor across the specimen and supplying a constant input current to the Hall device. After an initial start-up period of about 30 minutes, the output voltage can be recorded.

4.41 Calibration of the Hall device

Before measurements can be made, the distance between the Hall device and the magnet must be calibrated against the Hall output voltage. Since the Hall output voltage also depends upon the conditions of the environment, the calibration needs to be carried out at various temperatures and pressures. The calibration is made with the use of phosphor bronze blocks, whose thickness was known accurately to one ten-thousandth of an inch. The expansion and the compressibility of the phosphor bronze blocks are neglected as compared to the rubber.

To obtain the required temperature calibration, the thickness sensor was placed on the parallel surfaces of a phosphor bronze block

which was suspended from the upper hook of the Instron Tensile Tester. The temperature of the chamber was now brought to 60°C and the initial Hall output voltage was recorded. This value was suppressed with the aid of the voltage suppressor. The changes in the Hall output voltage were now measured. The temperature of the Instron chamber was lowered in steps of 10°C down to 0°C, and the changes in voltage at each temperature was recorded. This procedure was repeated for the nine blocks ranging in thickness from 0.0391 in. to 0.08 in. A plot of the thickness against the Hall output voltage for seven temperatures is shown in Figure 7. The solid lines are lines of best fit. The data are well represented by a straight line relationship.

The pressure calibration of the thickness sensor was conducted in the Pressurized Tensile Tester (PTT), which has been described elsewhere (41). A calibration block with the thickness sensor was suspended inside the PTT chamber. This was then pressurized to about 138 bars (2000 PSI) and the temperature of the environment was brought to 25°C. The initial Hall output was again suppressed and the voltage changes were recorded in decreasing steps of 34.5 bars (500 PSI). The results of the pressure calibration are shown in Figure 8. The solid lines are drawn using a least squares fit. A horizontal shift is employed for clarity.

4.42 Expansion coefficient at constant length

A ring specimen was pulled to the highest extension ($\lambda \simeq 3.0$) in the Instron Tensile Tester. The thickness sensor was carefully placed

across the width of the specimen. The temperature of the environment was brought to 60°C. The initial Hall ouput voltage was recorded and then suppressed. The temperature was now lowered to 0°C in steps of 10°C and the output voltage was recorded at each temperature. To achieve a steady output, it was found necessary to allow 10 to 15 minutes at each temperature.

After having completed the measurements at one extension ratio, the specimen was brought to a lower extension and the same procedure was repeated. During the experiment it was observed that the specimen in the vicinity of the Hall device was being heated due to excessive input current. An input current of 160 mA produced a large enough change in output voltage so that amplification of the signal was not needed. Amplification had been tried previously, but was found to be impractical since the output of the amplifier could not be kept steady over the long period of time required to conduct this experiment. The slight rise in the temperature of the sample at the point of contact with the Hall device was calibrated by inserting a thermocouple between the specimen and the Hall device. The output of this thermocouple was then compared with the output of the thermocouple in the environmental chamber. The difference in the emf of the two thermocouples was added as a correction to the emf values of the environmental thermocouple. No heating was detected in the case of phosphor bronze blocks where the excessive heat was apparently quickly dissipated through the metal.

For a given temperature and extension ratio, the Hall output

voltage is easily converted to width with the aid of the calibration curve (Figure 7). Thus, the width of the specimen at various temperatures and extension ratios was computed. A plot representing the change in width with extension ratio at 25°C is shown in Figure 9. The data lie on a smooth line with negligible scatter. The change in width with temperature at various elongations is plotted in Figure 10, where w_T is the width at the lowest temperature. The data have been shifted vertically by 0.1 units per successive elongation for clarity. The slopes of the lines in Figure 10 represent the linear expansion of natural rubber at constant length. The linear expansion coefficients at constant length as a function of extension ratios are given in Table 2. The results imply that strain has no effect on the value of $\frac{1}{w}\frac{\partial w}{\partial T}\Big|_{P,L}$, at least up to about $\lambda = 3.0$ for NR. The standard deviation for the values of the expansion coefficient is 4.5×10^{-6}/°C and the average over the range of λ(1.0 to 3.0) is 3.48×10^{-4}/°C.

4.43 Isothermal compressibility at constant length

The procedure followed to measure the changes in width of the specimen with pressure was quite similar to the one described in the previous section. This experiment was conducted in the Pressurized Tensile Tester. The Hall voltage was recorded as a function of pressure at various elongations, while the temperature of the pressurized chamber was maintained at 25°C. The width of the specimen was then computed from the Hall voltage using the pressure calibration curves (Figure 8).

The results are plotted as changes in width against pressure in Figure 11. The values of $-\frac{1}{w}\frac{\partial w}{\partial P}\Big|_{T,L}$ are given in Table 2. Similar to the linear expansion coefficient, the linear compressibility is also independent of strain. The average of the values in Table 2 is 32×10^{-6}/bars and the standard deviation is 0.6×10^{-6}/bars.

The pressure-temperature coefficient at constant length is now obtained from the ratio of the linear expansion coefficient and the linear compressibility, both at constant length. This yields a constant value of $\gamma_{V,L} = 10.8$ bars/°C for NR over the range of the extensions (up to $\lambda = 3$) studied. This supports the original contention of Flory (5) who regarded the ratio of the expansion coefficient and the isothermal compressibility of amorphous cross-linked polymers to be independent of strain. The data on $\gamma_{V,L}$ also support the predictions of the BST compressible strain energy function. Equation (3.42) implies that at ordinary pressures the pressure-temperature coefficient at constant volume and length is independent of length. These results are also in agreement with the published dilatometric data of Allen et al. (14, 15). They observed the same behavior up to an extension of about 2.0. We have studied the behavior up to an extension ratio of about 3.0 which, incidentally, is a very convenient stretch ratio for NR. Beyond this value, this particular rubber starts crystallizing and the stress-temperature behavior is no longer reversible (Figure 1). Also, the one-term BST strain energy function adequately describes the stress-strain behavior within this range.

4.5 Stress-Pressure Coefficient

The experiments on the stress-pressure coefficients at constant length were conducted using the Pressurized Tensile Tester (Figures 12, 13). The apparatus consists of a chamber which can be pressurized to about 2000 PSI using silicone oil as the pressurizing fluid. Unlike changes in force with temperature, changes in force with pressure are quite small. To amplify the signal from a load cell, a Daytronic Model 300-D Transducer-amplifier is used. This is fitted with a suppression module where the initial value of the force may be suppressed. The changes in force can be detected on a very sensitive scale.

Before conducting the force pressure experiment, the effect of pressure on the various measuring devices in the pressure chamber was determined. It was observed by Lim, Sharda and Tschoegl (42) that there was no effect of pressure on the thermocouple readings at the pressures employed (< 2000 PSI). The thermocouples are housed in a metal sheath. These were checked by inserting one of the thermocouples inside the cooling coil in a spot where it saw essentially the same temperature as the other which remained at atmospheric pressure at all times. No change in the thermocouple readings could be detected in this way. The output from the load cell showed good linearity, reproducibility and no drift. The zero shift of the load cell due to the applied hydrostatic pressure was small, but not negligible. A correction of 1.61×10^{-4} N/bar was subtracted from the observed load.

The experimental procedure for determining the force-pressure

coefficient consisted of the following. A ring specimen was pulled to the highest extension ratio and allowed to stand for over a week at room temperature and atmospheric pressure. This allowed sufficient time for the initial load to relax to an equilibrium value. The system was now pressurized to 138 bars (2000 PSI). The temperature in the pressurized chamber was controlled at 25°C. The system was maintained at this temperature and pressure until an equilibrium value of the force was achieved, at which time the load was recorded and then suppressed. The pressure was now decreased, usually in steps of 34.5 bars (500 PSI). At each pressure the temperature was closely controlled at 25°C and the force was allowed to come to an equilibrium. In general, it took about two hours at each pressure. It was not found necessary to conduct the whole experiment for increasing pressure cycle since the force value could be checked from time to time for an intermediate pressure. After the force pressure experiment was completed at one extension ratio, the ring specimen was brought to a lower extension and the same procedure was repeated. The results of the change in stress with pressure at a given extension are given in Figure 14. The experimental data are also given in Table 3. The stress pressure coefficients are simply the initial slopes of the curves in Figure 14.

4.6 Intermolecular Interactions

The stress-pressure coefficients provide a way of estimating the contributions of intermolecular interactions in the elastomer network.

The thermoelastic equation (Eq. 3.37) based on the statistical equation of state assumes that the modulus of the elastomer can be represented by Eq. (3.14) so that G only depends on temperature. As previously mentioned, Tobolsky and Shen (30) postulated for the first time that the shear modulus in fact has a slight volume dependence. This idea seems to have been overlooked in the literature. We will show that this indeed is a significant contribution in the field of rubber elasticity. Although the postulate of Tobolsky and Shen is empirical, nevertheless, it allows one to correctly evaluate the effect of pressure on the retractive force in rubbers. Equation (3.40) is rewritten here as

$$\frac{1}{\kappa_{T,L} f}\left.\frac{\partial f}{\partial P}\right|_{T,L} = \frac{n}{2(\lambda^{3n/2} - 1)} - \gamma \qquad (4.7)$$

Figure 15 is a plot of $\frac{1}{f\kappa_{T,L}}\left.\frac{\partial f}{\partial P}\right|_{T,L}$ against $n/2(\lambda^{3n/2} - 1)$ from which a value of $\gamma = -0.2$ for NR is obtained. The same data are plotted in Figure 16 to show the importance of γ. In the same figure the predictions of the statistical theory (Flory's eq.)

$$\frac{1}{f\kappa_{L.T}}\left.\frac{\partial f}{\partial P}\right|_{T,L} = \frac{1}{\lambda^3 - 1} \qquad (4.8)$$

are also shown together with Eq. (4.7) with and without the parameter γ. Unlike Tobolsky and Shen, we have not incorporated γ in the statistical theory since the effect of γ would be to render the statistical theory empirical. It should be noted, however, that the FCH-equation comes

close to the predictions of the BST^2-equation if the factor γ is incorporated.

The force-pressure coefficients can also be transformed into the dilation coefficient by

$$\left.\frac{\partial f}{\partial P}\right|_{T,L} = \left.\frac{\partial V}{\partial L}\right|_{P,T} \tag{4.9}$$

Combining Eqs. (4.7), (4.9) and (3.31) and integrating the resulting equation yields the relative change in volume as

$$\frac{\Delta V}{V_o} = \frac{2G}{n}\kappa_{L,T}\left[1 - \lambda^{-n/2} - \frac{\gamma}{n}(\lambda^n + 2\lambda^{-n/2} - 3)\right] \tag{4.10}$$

To derive Eq. (4.10) we have set J = 1, i.e., we have, in effect, neglected terms of the order $\Delta V/V_o$ as compared to unity (43). Also, combination of Eqs. (4.8), (4.9) and (3.31) [with J = 1, n = 2, and γ = 0], gives

$$\frac{\Delta V}{V_o} = \kappa_{L,T}G(1 - \lambda^{-1}) \tag{4.11}$$

The results of Eq. (4.10) and (4.11) are plotted in Figure 17. The data points are obtained by graphical integration of data in Figure 16. Once again the results demonstrate the significance of the parameter γ. The deviations from Flory's equation have also been reported in the literature. Christensen and Hoeve (44) and Allen et al. (15) have measured

dilation coefficients and observed similar behavior. It can be easily shown that their data can be represented by Eq. (4.7). Recently Goebel and Tobolsky (45) have fitted the data of Christensen and Hoeve based on Eq. (4.7) but with n = 2.

To further interpret the parameter γ, we note that the volume dilates on extension in a real elastomer. To maintain the volume constant it is necessary to apply hydrostatic pressure. In a rubbery network, an applied pressure changes the average distance between the chains, thus altering the interchain forces that keep them apart. The statistical forces do not account for the changes in the interchain interactions and cannot be expected to describe the effect of pressure on the elastic force. The parameter γ is an indirect measure of these interactions.

4.7 Thermodynamic Equation

Table 2 lists experimental data calculated from the thermodynamic equation, Eq. (3.8). The results of Table 4 are plotted in Figure 18, where the stress, σ, and its energetic and entropic components, σ_e and σ_s, are shown. The circles and squares on the σ-curve represent stresses measured in the stress-temperature (Section 4.3) and the stress-pressure (Section 4.5) experiments, respectively. Evidently, most of the restoring force in natural rubber comes from the entropy, but a significant part also comes from the internal energy. The data indicate that the relative internal energy is, within the limits of the experimental error, a constant independent of the strain ($\lambda < 3$). The average value for natural rubber

in this region is 0.23, with a standard deviation of 0.02. Before comparing these results with the existing literature values, we will compare the predictions of the statistical and the phenomenological theories.

4.8 Range of Validity of the Statistical and BST Equations

In Chapter 3 we have shown that f_e/f may be determined from three sets of relations which are tabulated below for convenience.

I.
$$\frac{f_e}{f} = 1 - \frac{T}{f}\frac{\partial f}{\partial T}\bigg|_{L,P} - \frac{T}{f}\gamma_{V,L}\frac{\partial f}{\partial P}\bigg|_{T,L} \tag{3.8}$$

II.
$$\begin{cases} \dfrac{f_e}{f}\,(\mathrm{FCH}) = 1 - \dfrac{T}{f}\dfrac{\partial f}{\partial T}\bigg|_{L,P} - \dfrac{3\alpha_o T}{\lambda^3 - 1} & (3.38) \\[2ex] \dfrac{f_e}{f}\,(\mathrm{BST})^2 = 1 - \dfrac{T}{f}\dfrac{\partial f}{\partial T}\bigg|_{L,P} - \left[\dfrac{n}{2(\lambda^{3n/2} - 1)} - \gamma\right] 3\alpha_o T & (3.36) \end{cases}$$

III.
$$\begin{cases} \dfrac{f_e}{f}\,(\mathrm{SB}) = 1 - \dfrac{T}{G}\dfrac{dG}{dT} - \alpha_o T & (3.37) \\[2ex] \dfrac{f_e}{f}\,(\mathrm{BST})^1 = 1 - \dfrac{T}{G}\dfrac{dG}{dT} - \alpha_o T(3 - n - 3\gamma) & (3.34) \end{cases}$$

Most reported data on f_e/f have been obtained using the FCH-equation. No attempt was made in earlier work (4, 46) to determine the range of extensions over which this equation would be valid. It would therefore be of value to compare the range of validity of the FCH-equation,

derived from statistical mechanical considerations, with those of the related, but phenomenologically derived BST^2-equation on hand of experimental data calculated from the thermodynamic equation, Eq. (3.8). A moment's research shows, however, that such a comparison is of little value because the FCH - and BST^2- equations both only estimate the last term of the thermodynamic equation and share with this the numerically larger second term containing the experimentally determined $(\partial \ell nf/\partial \ell nT)_{P,L}$ term. The comparison is particularly poor at moderate-to-large values of λ because the last terms in both equations rapidly decrease as λ increases.

To evaluate the relative merits of the statistical mechanical and the phenomenological approach, one must therefore compare the SB - and related BST^1- equations. To do this, we must decompose the measured stress, σ, into its energetic and entropic components, σ_e and σ_s, on the grounds of the two theories. We use Eqs. (3.37) and (3.34) for σ_e and obtain σ_s as $\sigma - \sigma_e$, where $\sigma = f/A_o$ and f is given by Eq. (3.31). Setting J = 1 again because of its closeness to unity, we obtain

$$\sigma_e(BST)^1 = \frac{2G}{n}\left(\lambda^{n-1} - \frac{1}{\lambda^{n/2+1}}\right)\left[1 - \frac{T}{G}\frac{dG}{dT} - \alpha_o T(3 - n - 3\gamma)\right] \quad (4.12)$$

$$\sigma_s(BST)^1 = \frac{2G}{n}\left(\lambda^{n-1} - \frac{1}{\lambda^{n/2+1}}\right)\left[\frac{T}{G}\frac{dG}{dT} + \alpha_o T(3 - n - 3\gamma)\right] \quad (4.13)$$

from the phenomenological approach, and

$$\sigma_e(SB) = G(\lambda - \frac{1}{\lambda^2})\ (1 - \frac{T}{G}\frac{dG}{dT} - \alpha_o T) \tag{4.14}$$

$$\sigma_s(SB) = G(\lambda - \frac{1}{\lambda^2})\ (\frac{T}{G}\frac{dG}{dT} + \alpha_o T) \tag{4.15}$$

from the statistical theory, where n = 2, $\gamma = 0$. Equations (4.12) through (4.15) are plotted in Figure 19, together with

$$\sigma(STAT) = G(\lambda - \lambda^{-2}) \tag{4.16}$$

and

$$\sigma(BST) = G(\lambda^{n-1} - \frac{1}{\lambda^{n/2+1}}) \tag{4.17}$$

Figure 19 clearly shows that the statistical theory does not predict the observed behavior beyond about 40% strain, whereas the BST[1]-equation does an excellent job over the entire range studied. The parameters used in Eqs. (4.12) to (4.15) are assembled in Table 5. As previously mentioned, only the one-term BST strain energy function was needed to describe these data. In the next chapter we shall demonstrate the application of the complete BST equation in describing the thermoelastic data on a chlorinated ethylene-propylene copolymer rubber.

5. MEASUREMENTS OF f_e/f

In this chapter we shall compare the values of f_e/f calculated from our experimental data on NR by the five equations listed in the previous section. We shall then discuss literature data on a chlorinated ethylene-propylene copolymer rubber which extend to much higher values of λ. The latter data are also interesting because the sign of f_e/f is positive for NR but negative for the copolymer rubbers.

5.1 Natural Rubber

The stress data calculated purely from experiments by the thermodynamic equation, Eq. (3.8) were discussed in Section 4.7 and are tabulated in Table 4 and shown in Figure 18. The data calculated from the SB- and the BST^1- equations are shown in Figure 19 with the parameters given in Table 5. The data calculated from the FCH- and the BST^2- equations are tabulated in Table 6 and shown in Figure 20. The results obtained for f_e/f at 25°C are summarized below.

	Equation	f_e/f	Eq. #
I.	Thermodynamic	0.23	(3.8)
II.	FCH	0.28	(3.38)
	BST^2	0.24	(3.36)
III.	SB	0.27	(3.37)
	BST^1	0.23	(3.34)

Tables 4 and 6 indicate that in the low to moderate strain region the relative internal energy contribution to the elastic force is a constant within experimental error. The predictions of the BST phenomenological equations agree remarkably well with the experimental data [Eq. (3.8)]. The statistical theory, which should not be used beyond 40% strain, also yields closely similar values for f_e/f but these are higher than the "experimental" value. The difference of about 0.04 arises solely from the neglect of the volume dependence of the modulus in the statistical theory. It is thus seen that introduction of the parameter γ into the compressible BST strain energy function provides an important degree of freedom in accounting for the interchain energy effects. The rather small contribution which this term makes to f_e/f suggests that the contribution of the interchain interactions is quite small as compared to the other components of the elastic force.

Our experimental data also explain why the FCH equation, which is based on the statistical theory, yields good values for f_e/f at strains where the statistical theory does not describe the deformation behavior. From the results in Tables 4 and 6, we conclude that as the strain increases, the force-pressure term in Eq. (3.8) becomes smaller and f_e/f is well approximated by the simple relation

$$\frac{f_e}{f} \simeq 1 - \frac{T}{f}\frac{\partial f}{\partial T}\bigg|_{L,P} \qquad \text{(Large } \lambda\text{)} \qquad (5.1)$$

Both the FCH-equation and the BST^2-equation reduce to Eq. (5.1) in the limit of large λ. Thus, it is not surprising that Eqs. (3.36) and (3.38) describe the f_e/f data quite well. As previously mentioned, the results of these equations should be cautiously interpreted. If the purpose is to obtain f_e/f values, these equations provide excellent results. However, for the purposes of determining the shortcomings of these theories, we must resort to equations of the type discussed in the previous section [Eqs. (4.12) to (4.16)].

A further reflection of Eqs. (3.34) and (3.37) indicates that f_e/f is independent of strain in both cases. This is true for the statistical theory over the entire range of strain and the BST strain energy function up to the point ($\lambda < 3$) where the parameters n and G adequately describe the deformation behavior. As will be shown in the next section, the BST theory predicts f_e/f to be strain dependent beyond this point.

The values of f_e/f calculated from Eq. (3.8) are compared in Figure 21 with the existing data on natural rubber. With the exception of the data of Allen et al. the published values were calculated by the FCH-equation. Figure 21 shows three distinct regions of f_e/f values for NR. In the region of small strains ($\lambda < 1.2$) f_e/f is a function of λ; in the region of moderate strains ($1.2 < \lambda < 3.0$) f_e/f is independent of λ and at large strains ($\lambda > 3.0$) f_e/f once again depends on the strain. The data in the small strain region (31, 46) do not agree with the predictions of either the SB- or the BST^1-equations, which we believe to be correct in this region. In this region the FCH-equation requires

extremely precise values of the force and the stretch ratio because of their appearance in the denominators of the second and third terms, respectively. As $\lambda^3 - 1$ goes to zero, so does f. Thus, at present, the value of f_e (and, therefore, f_s) at $\lambda = 1$ cannot be obtained by extrapolation of data in the small strain region. Furthermore, there does not seem to exist any theoretical argument from which it could be predicted.

5.2 Ethylene-Propylene Copolymer Rubber (Cℓ EPR)

In the case of natural rubber, only one term in the BST strain energy function was necessary for an adequate representation of the data since these did not exceed 200% strain. To check the applicability of the two-term BST strain energy function, the data of Natta, Crespi and Flisi, obtained on a chlorinated EPR (47) were used. These data extend to an extension ratio of nearly 7.

The two-term equation corresponding to the BST[1]-equation is

$$\frac{f_e}{f}(BST)^3 = 1 - (3-n-3\gamma)\alpha_o T - \frac{\frac{2T}{n}\frac{dG}{dT} + mT\frac{dB}{dT}I_E^{m-1} - m(m-1)B\alpha_o I_E^{m-2}(\lambda^n+2\lambda^{-n/2})}{\frac{2G}{n} + mBI_E^{m-1}} \qquad (5.2)$$

Equation (5.2) is obtained from the two-term analog of Eq. (3.30),

$$\sigma\lambda = J^\gamma\,(2G/n + mBI_E^{m-1})\,(\lambda^n - J^{n/2}/\lambda^{n/2}) \qquad (5.3)$$

and from that of Eq. (3.35),

$$\left.\frac{\partial \ell nf}{\partial T}\right|_{P,L} = \frac{(2/n)(dG/dT) + m(dB/dT)I_E^{m-1} - m(m-1)BI_E^{m-2}\alpha_o(\lambda^n - \lambda^{-n/2})}{2G/n + mBI_E^{m-1}}$$

$$+ \alpha_o \frac{(3 - n)\lambda^{3n/2} - (3 + n/2)}{\lambda^{3n/2} - 1} \qquad (5.4)$$

The data of Natta et al. are plotted in Figure 22. The solid line through the experimental points represents the least squares fit with the parameters n = 1.71, m = 4.84, B = 6.47 x 10^{-5} Kg/cm^2 and G = 2.71 Kg/cm^2. These parameters were then used in Eq. (5.4) to predict the stress-temperature slopes shown in Figure 23. The values of dG/dT and dB/dT were 14.2 x 10^{-3} Kg/cm^2°C and 5.54 x 10^{-7} Kg/cm^2°C, respectively, as found from the initial slopes of the stress-strain curves at different temperatures. Figures 22 and 23 indicate an excellent agreement of Eqs. (5.3) and (5.4) with the experimental data.

These parameters are now used to predict f_e/f for the copolymer rubbers. The results are shown in Figure 24 whereas the individual components are given in Figure 23. It is seen that for this rubber f_e/f is negative. It stays constant up to an extension ratio of about 3.0 and decreases beyond this point.

5.3 Comments on NR Chain Parameters

The value of f_e/f for natural rubber is positive in contrast to most rubbers. The sign of the internal energy contribution depends on

the relative magnitude of the various rotational potentials. In the following some comment will be made regarding these potentials in the light of the experimental results presented here.

A convenient parameter in characterizing the configuration of a polymer chain is the "characteristic ratio", $\langle r^2 \rangle_o / n\ell^2$. This is defined for a state of the molecule that remains invariant to the long range effects of the hydrodynamic interaction, the external force etc., and is subject only to the local constraints due to the bond structure (i.e., bond length, bond angle and rotational hindrance potentials). The characteristic ratio is usually obtained from viscosity measurements. Wagner and Flory (48) have determined a value of 4.7 for natural rubber.

In conjunction with the thermoelastic data we have obtained the characteristic ratio can be used in obtaining parameters that characterize the chain structure. From Eq. (3.15) we determine the temperature variation of $\langle r^2 \rangle_o$ for NR to be

$$\frac{d\ell n \langle r^2 \rangle_o}{dT} = \frac{f_e}{Tf} = 0.67 \times 10^{-3} \text{ deg}^{-1} \qquad (5.5)$$

where we have taken the average of all published values of f_e/f at 25°C, 0.2 (see Figure 21). We make use of these results to obtain rotational energy parameters for the cis - 1,4-polyisoprene (cis-PIP) chain shown below as Formula I

by two artificial bonds a and b obtained by extending bonds C-C to intersect at a point as shown in Formula II. This structure splits the cis - PIP unit into two parts: (1) the artificial bonds a and b whose rotations are interdependent; and (2) the CH_2 - CH_2 bond, c, whose rotation is independent of its neighbors.

The bond CH - CH_2 (a or b) is known to have distinct rotational minima at ± 60° and 180°, whereas the CH_2 - CH_2 bond (c) possesses minima at 0° and ± 120°. Since the rotational pairs a and b are interdependent, the rotational state 180° must be excluded because the cis conformation about these bonds results in large steric hindrance. However, intramolecular interactions between H and CH_3 across the double bond give rise to an additional minimum. Mark (49) has suggested that in the bond pair a-b occurence of one bond in the state of ±60° can give rise to an effective minimum at 0° for the other bond. Thus, only 0°, ± 60° and 0° rotational pairs are available to bonds a and b. Let us assign the energy E_γ to the rotational pairs ± 60°, ± 60° (or ± 60°, $\mp$ 60°). E_γ is relative to zero for the rotational pairs 0°, ± 60° and ± 60°, 0°. Let us also assign E_σ to the gauche-rotational state ± 120° relative to zero for the trans-rotational state 0°. Our purpose is to calculate the energies E_γ and E_σ which are consistent with the values:

$$\langle r^2 \rangle_o / n\ell^2 = 4.7 \qquad (5.6)$$

$$d\ell n \langle r^2 \rangle_o / dT = 0.67 \times 10^{-3} \quad deg^{-1} \qquad (5.7)$$

Since the random coil configurations of the cis - PIP chain have been computed by Mark based on the rotational isomeric model, we use the published results to determine E_γ and E_σ. The following figure (taken from Mark, 1.c.) gives the values of the characteristic ratio as a function of E_σ for various values of E_γ, based on the dimensions of the NR chain given in Formula II for a degree of pressurization (DP) of 120.

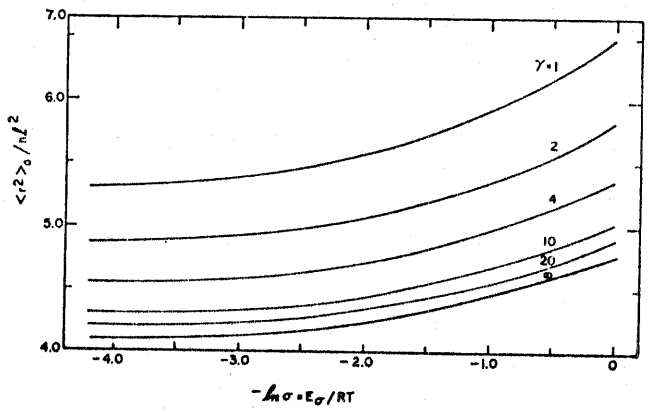

Characteristic ratio of cis - 1, 4 - PIP chain

Also, the temperature coefficient of $\langle r^2 \rangle_o$ is given by

$$- T \frac{d\ell n\langle r^2\rangle_o}{dT} = \ell n\sigma \frac{\partial \ell n\langle r^2\rangle_o}{\partial \ell n\sigma} + \ell n\gamma \frac{\partial \ell n\langle r^2\rangle_o}{\partial \ell n\gamma} \qquad (5.8)$$

where

$$\sigma = \exp\ (-E_\sigma/RT) \qquad (5.9)$$

and

$$\gamma = \exp\ (-E_\gamma/RT) \qquad (5.10)$$

To satisfy Eqs. (5.7) and (5.8) we must have

E_σ = - 0.5 Kcal/mole

E_γ = - 1.36 Kcal/mole

σ = 2.72

γ = 10

$\partial \ell n \langle r^2 \rangle_o / \partial \ell n \sigma$ = - 0.0665

$\partial \ell n \langle r^2 \rangle_o / \partial \ell n \gamma$ = - 0.059

These values were obtained by trial and error. The second term in Eq. (5.9) contributes nearly 75% of the temperature coefficient according to these parameters. From this it may be concluded that the transition from 0°, ± 60° to ± 60°, ± 60° (or ±60°, $\mp$ 60°) in bonds b and c in the natural rubber chain are more effective in changing the dimensions of the chain than the transition from 0° to ± 120°. The two energy parameters E_σ and E_γ calculated on the basis of rotational isomeric theory are consistent with optical anisotropy data on cis - 1, 4 - polyisoprene (52).

From Eq. (5.9) it is evident that the positive slope of $\langle r^2 \rangle_o$ with temperature for NR results directly from the negative values for the conformational energies E_σ and E_γ. The negative value of E_γ implies that the more extended conformation (0°, ± 60°) around the CH-CH_2-CH bond pair has a higher energy than the conformations ± 60°, ± 60° (or ± 60°, $\mp$ 60°).

Similarly, E_σ implies that the trans-conformation (0°) about CH_2-CH_2 bond possesses higher energy than the gauche-conformation (± 120°).

6. DISCUSSION

In the discussion below, the results of this study are summarized and suggestions for future work are given. The results of both Parts I and II will be reviewed from a general standpoint.

6.1 Phenomenological Theory

A new elastic potential function for rubbery materials was introduced. In Part I its application in both homogeneous and inhomogeneous deformation fields for two materials, natural rubber and styrene-butadiene rubber was successfully demonstrated. The same set of parameters was used in describing the behavior in various deformation fields (simple tension, equibiaxial tension, pure shear, torsion and torsion with extension) up to the point of rupture. In Part II this strain energy function was modified to account for the compressibility of the material. The compressible form of the strain energy function fitted the thermoelastic data on natural rubber and chlorinated ethylene-propylene copolymer rubber. For the different types of experimental data considered up to now the parameter n remained constant for a given rubber. The two moduli B and G depend on the degree of cross-linking and the procedure employed in preparing the samples, as expected. A study of the temperature dependence of the parameters based on two sets of data indicated that the moduli (G and B) were linearly dependent on temperature while the constants n and m remained unchanged over the range of temperatures studied.

The development of this strain energy function has raised interesting questions. The first important question that needs to be answered at present is the origin of the parameters n and m. The fact that n remains constant over the entire range of strain and over a large range of temperature suggests that it may be possible to explain or at least interpret this parameter from network or chain statistics.

A similar point may be made about the parameter γ in the compressible strain energy function. It was possible to relate γ to the intermolecular energy effects.

A number of uses for the new strain energy function suggest themselves in other phenomena in elasticity (e.g., stress-optical coefficient, failure data in filled and unfilled materials, swelling of rubbers, etc.). The n-measure of strain also offers a challenge in other fields of continuum mechanics (viscosity, viscoelasticity, etc.). A common problem in mechanics of viscoelastic flow is the description of the shear and the normal stresses. The success of the n-measure of strain in elasticity suggests employing these concepts in the rate-of-strain measure.

6.2 Thermoelasticity

A new scheme for the thermodynamics of elastomers is proposed. The newly introduced thermodynamic potential functions are given in terms of the appropriate sets of independent variables. It was shown that the decomposition into entropic and energetic components can be carried out in terms of length as well as force. The choice depends on theoretical

and experimental convenience.

A number of important results emerge from the thermoelastic measurements on natural rubber. The relative internal energy component of the elastic force remains constant up to an extension ratio of about 3.0. A contribution of 23 % is obtained for natural rubber in this range. The experimental data also indicates that the pressure-temperature coefficient at constant V and L as well as the temperature coefficient of $\langle r^2 \rangle_o$ remain constant in this region of strain.

The approach based on a compressible form of the Blatz-Sharda-Tschoegl elastic potential satisfactorily predicted the experimental results. It was also demonstrated that the statistical theory is applicable only up to an extension ratio of about 1.4. A test of the statistical theory based on the thermoelastic data is possible only through the Shen-Blatz equation but not through the Flory-Ciferri-Hoeve equation. The data clearly demonstrate the reasons for the validity of the latter equation beyond the range in which the statistical theory holds.

The new elastic potential function results in another important conclusion. This is that intermolecular interactions play a small but not negligible part in the flexibility of macromolecules. This is an encouraging observation since it indicates that in the development of a more general theory of rubber elasticity these interactions will not be particularly crucial.

The magnitude of the conformational energies E_σ and E_γ, as previously explained, account for a positive value of the temperature

coefficient of the unperturbed dimensions of NR chains. It is also concluded that in natural rubber chains the conformations about the CH-C_2H_2-CH bond pairs are more effective in changing the dimensions of the chain.

Finally, this work has provided a complete phenomenological description of the elastic retractive force in rubbers. For the first time the effects of strain, temperature and pressure (in turn volume) have been described with the aid of a single potential function.

APPENDIX

The mathematical equality of mixed second derivatives gives rise to the useful Maxwell relations. The relations for elastomers are listed below.

$$\left.\frac{\partial T}{\partial V}\right|_{S,L} = -\left.\frac{\partial P}{\partial S}\right|_{V,L} \tag{A1}$$

$$\left.\frac{\partial T}{\partial L}\right|_{S,V} = \left.\frac{\partial f}{\partial S}\right|_{V,L} \tag{A2}$$

$$-\left.\frac{\partial P}{\partial L}\right|_{S,V} = \left.\frac{\partial f}{\partial V}\right|_{S,L} \tag{A3}$$

$$\left.\frac{\partial S}{\partial V}\right|_{T,L} = \left.\frac{\partial P}{\partial T}\right|_{V,L} \tag{A4}$$

$$-\left.\frac{\partial S}{\partial L}\right|_{T,V} = \left.\frac{\partial f}{\partial T}\right|_{V,L} \tag{A5}$$

$$-\left.\frac{\partial P}{\partial L}\right|_{T,V} = \left.\frac{\partial f}{\partial V}\right|_{T,L} \tag{A6}$$

$$\left.\frac{\partial T}{\partial P}\right|_{S,L} = \left.\frac{\partial V}{\partial S}\right|_{P,L} \tag{A7}$$

$$\left.\frac{\partial T}{\partial L}\right|_{S,P} = \left.\frac{\partial f}{\partial S}\right|_{P,L} \tag{A8}$$

$$\left.\frac{\partial V}{\partial L}\right|_{S,P} = \left.\frac{\partial f}{\partial P}\right|_{S,L} \tag{A9}$$

$$-\left.\frac{\partial S}{\partial P}\right|_{T,L} = \left.\frac{\partial V}{\partial T}\right|_{P,L} \tag{A10}$$

$$-\left.\frac{\partial S}{\partial L}\right|_{T,P} = \left.\frac{\partial f}{\partial T}\right|_{P,L} \tag{A11}$$

$$\left.\frac{\partial V}{\partial L}\right|_{T,P} = \left.\frac{\partial f}{\partial P}\right|_{T,L} \tag{A12}$$

$$\left.\frac{\partial T}{\partial V}\right|_{S,f} = -\left.\frac{\partial P}{\partial S}\right|_{V,f} \tag{A13}$$

$$\left.\frac{\partial T}{\partial f}\right|_{S,V} = -\left.\frac{\partial L}{\partial S}\right|_{V,f} \tag{A14}$$

$$\left.\frac{\partial P}{\partial f}\right|_{S,V} = \left.\frac{\partial L}{\partial V}\right|_{S,f} \tag{A15}$$

$$\left.\frac{\partial S}{\partial V}\right|_{T,f} = \left.\frac{\partial P}{\partial T}\right|_{V,f} \tag{A16}$$

$$\left.\frac{\partial S}{\partial f}\right|_{T,V} = \left.\frac{\partial L}{\partial T}\right|_{V,f} \tag{A17}$$

$$\left.\frac{\partial P}{\partial f}\right|_{T,V} = \left.\frac{\partial L}{\partial V}\right|_{T,f} \tag{A18}$$

$$\left.\frac{\partial T}{\partial P}\right|_{S,f} = \left.\frac{\partial V}{\partial S}\right|_{P,f} \tag{A19}$$

$$\left.\frac{\partial T}{\partial f}\right|_{S,P} = - \left.\frac{\partial L}{\partial S}\right|_{P,f} \tag{A20}$$

$$\left.\frac{\partial V}{\partial f}\right|_{S,P} = - \left.\frac{\partial L}{\partial P}\right|_{S,f} \tag{A21}$$

$$\left.\frac{\partial V}{\partial T}\right|_{P,f} = - \left.\frac{\partial S}{\partial P}\right|_{T,f} \tag{A22}$$

$$\left.\frac{\partial S}{\partial f}\right|_{T,P} = \left.\frac{\partial L}{\partial T}\right|_{P,f} \tag{A23}$$

$$\left.\frac{\partial L}{\partial P}\right|_{T,f} = - \left.\frac{\partial V}{\partial f}\right|_{T,P} \tag{A24}$$

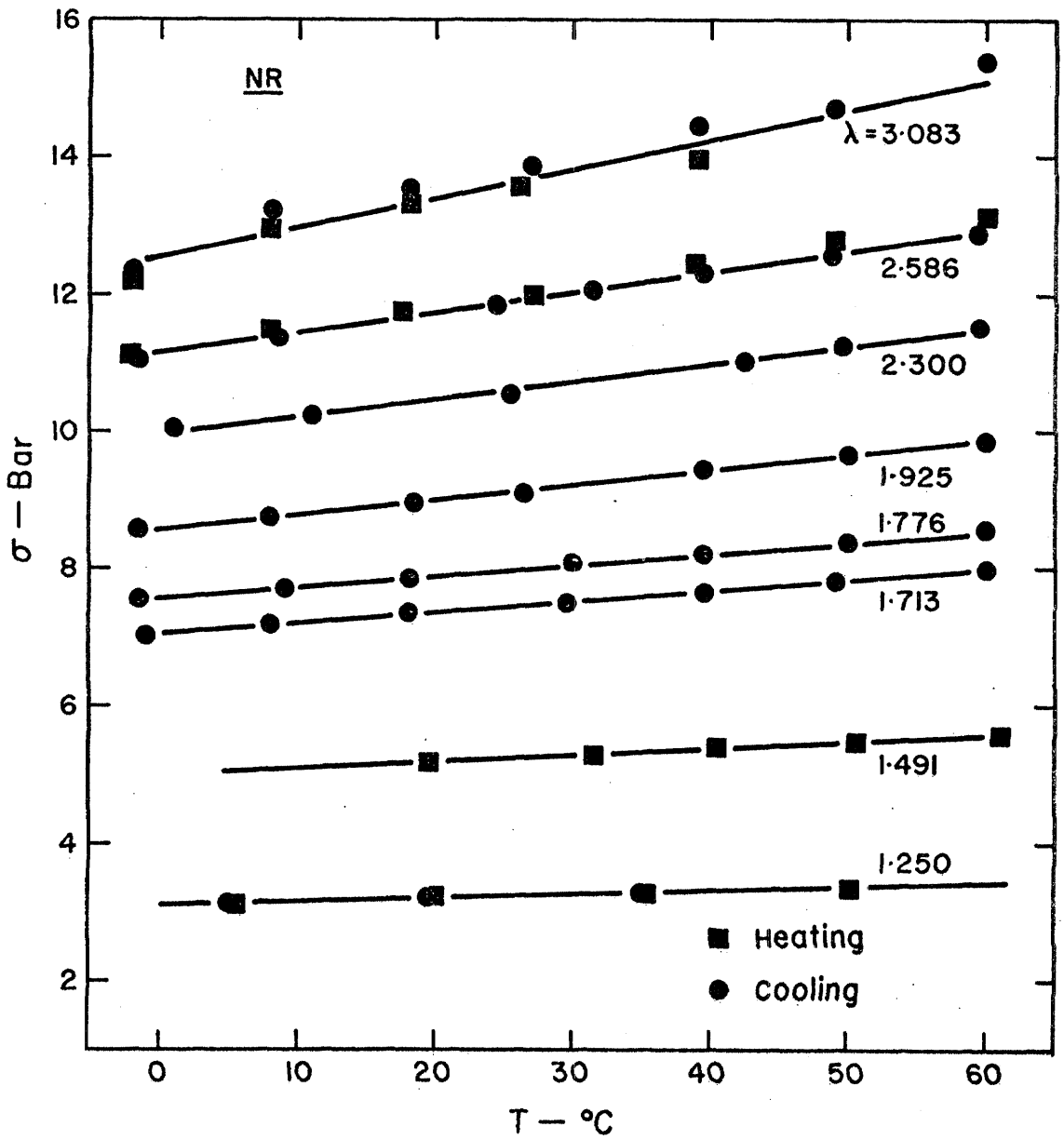

Figure 1 Plot of stress vs. temperature on natural rubber for various values of extension ratio.

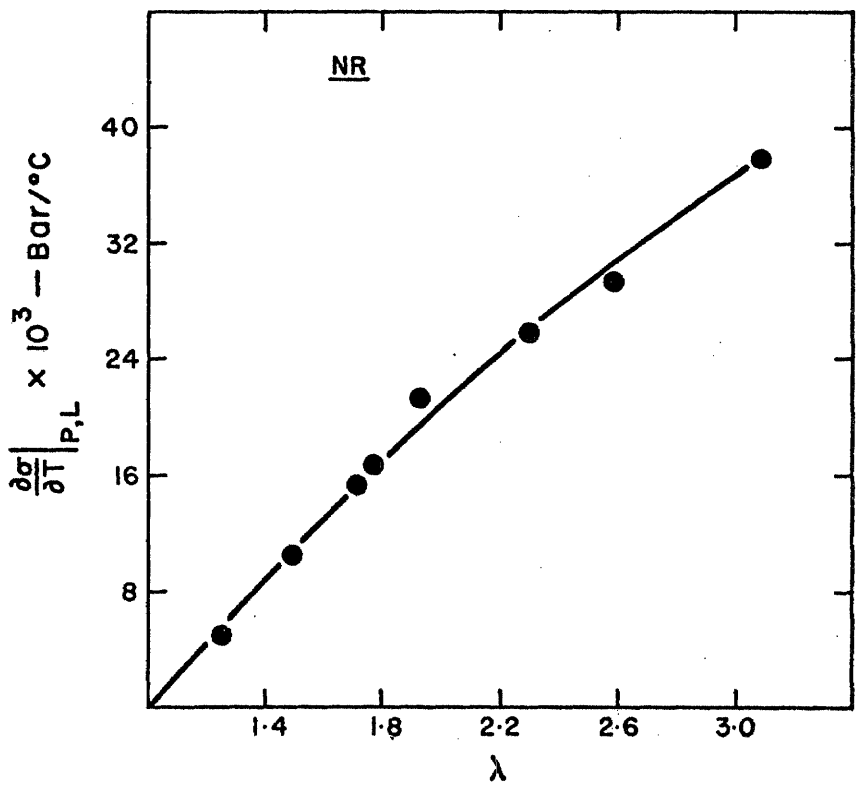

Figure 2 Stress-temperature coefficients of natural rubber.

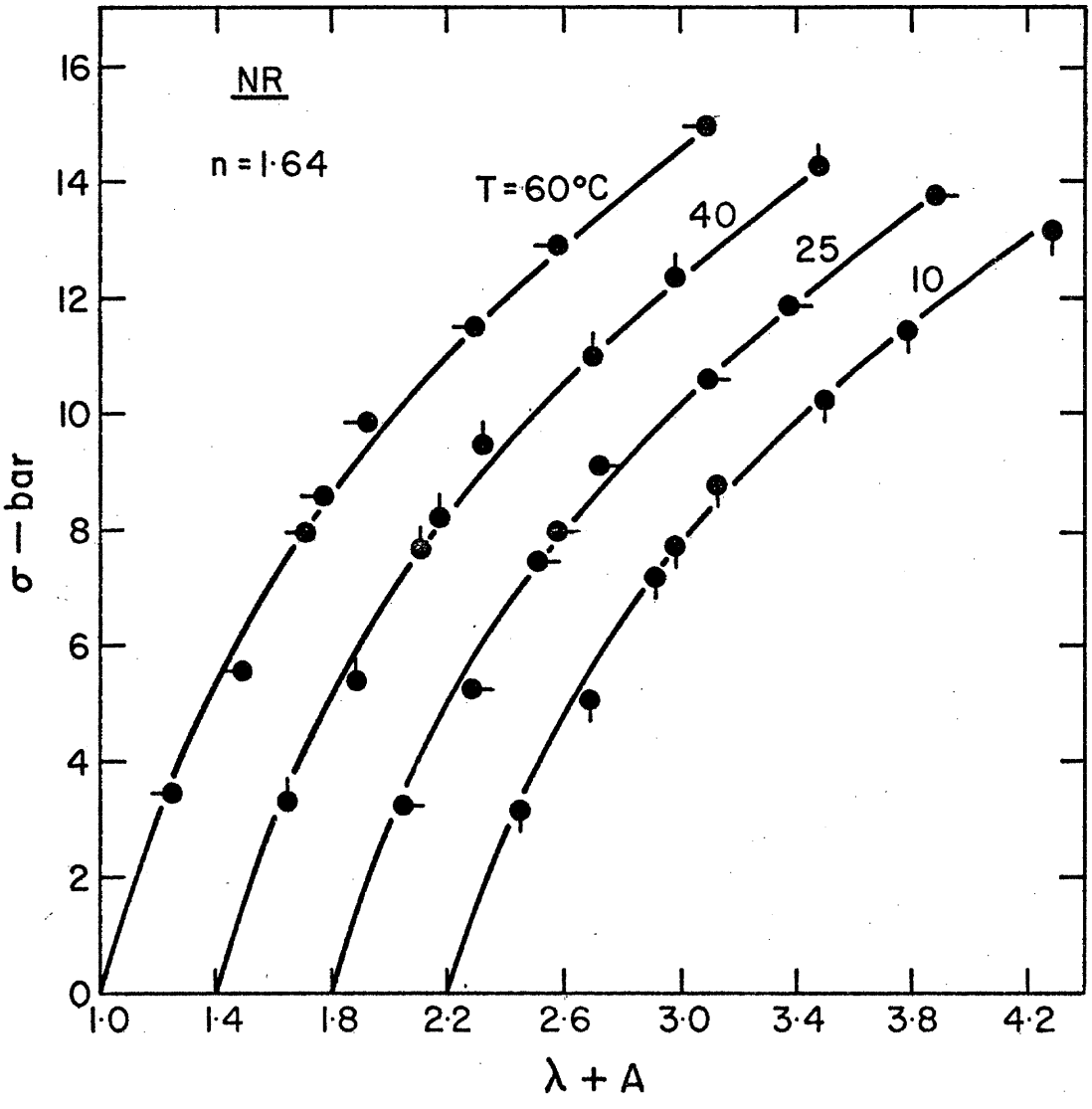

Figure 3 Stress-strain data at various temperatures. Solid lines were calculated from Eq. (3.30).

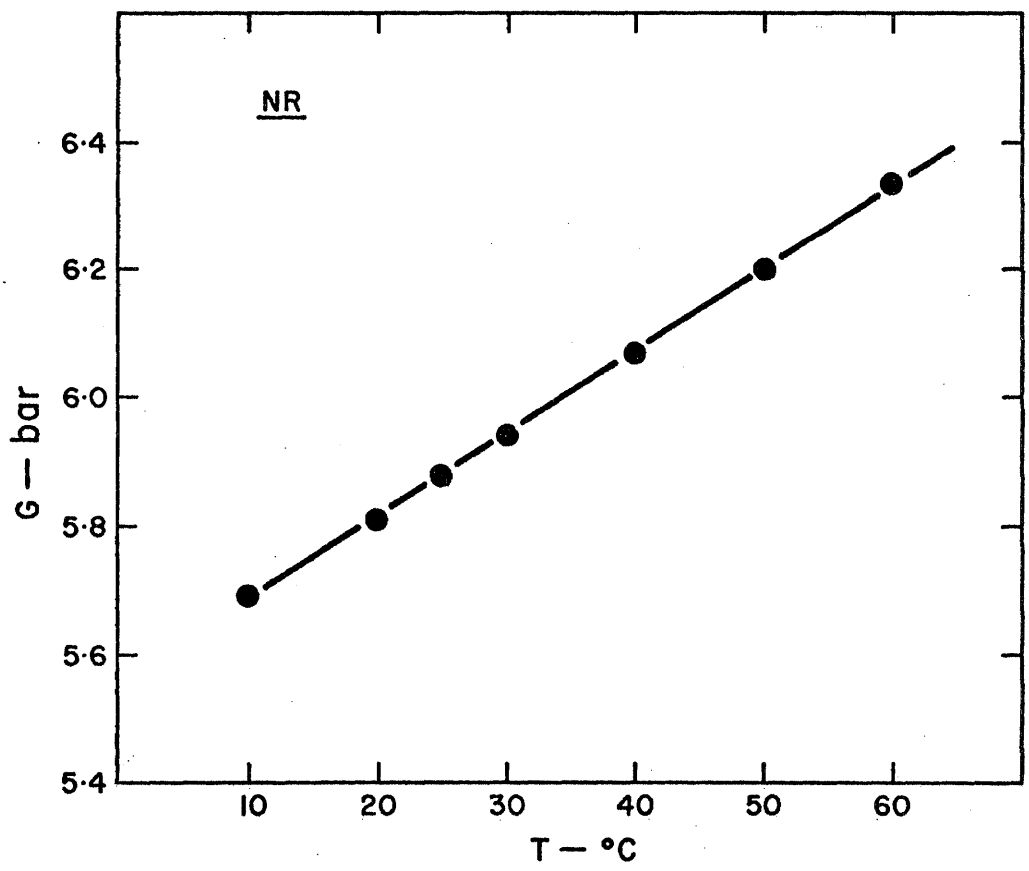

Figure 4 Temperature dependence of the modulus G.

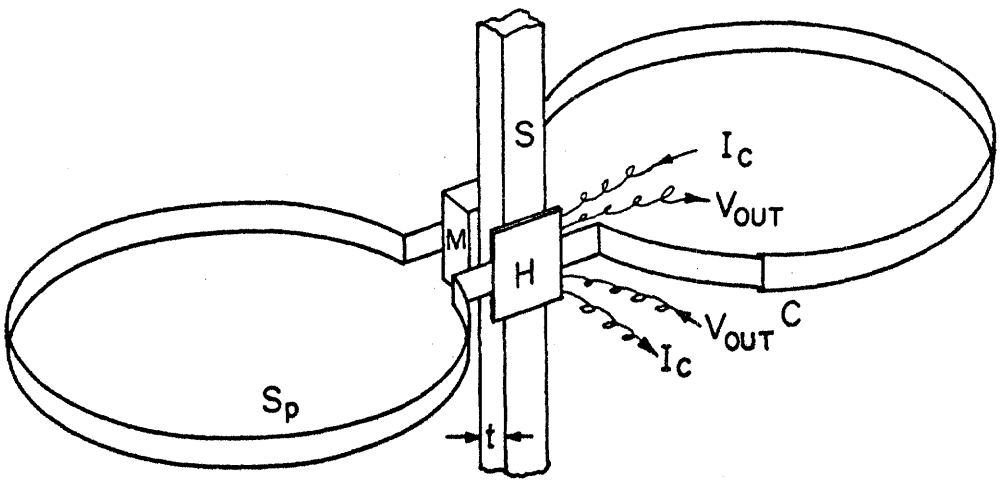

Figure 5 Schematic of Hall effect thickness sensor.

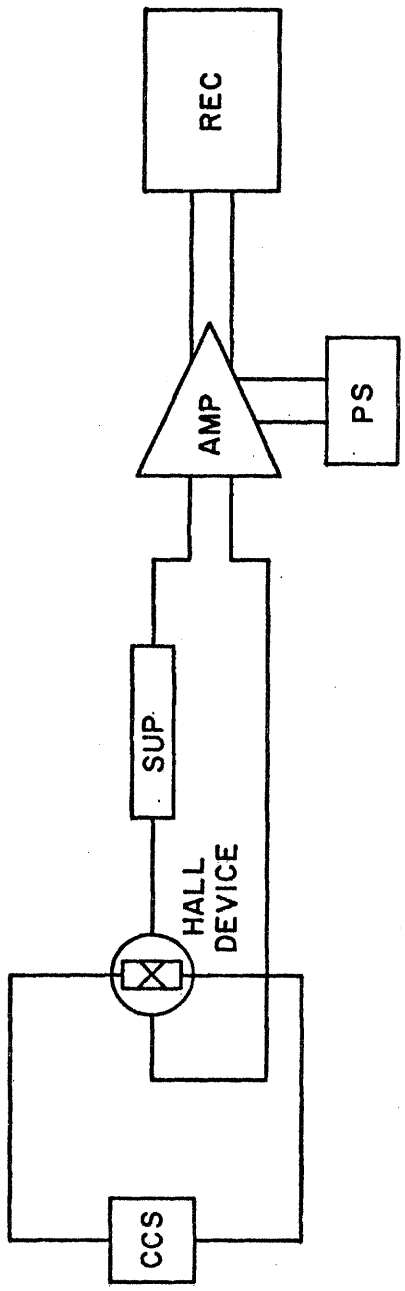

Figure 6 Block diagram showing interconnection of electronic components of thickness sensor.

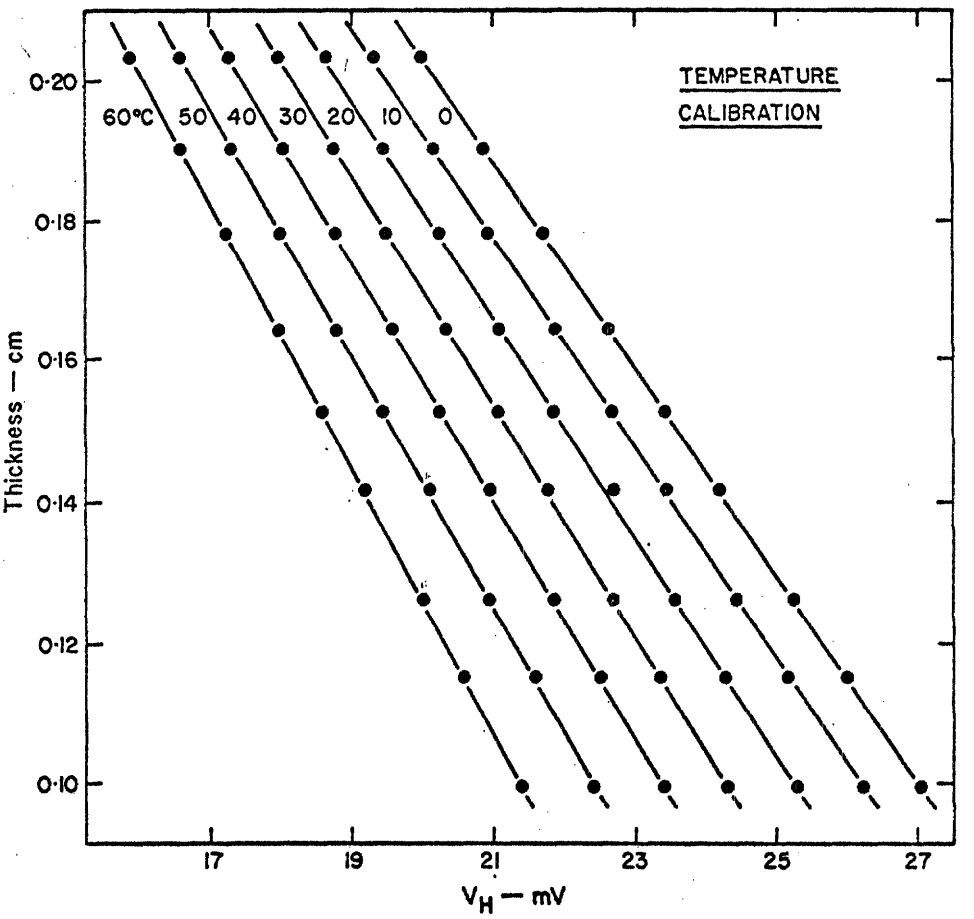

Figure 7 Calibration curves of thickness vs. Hall output voltage at various temperatures.

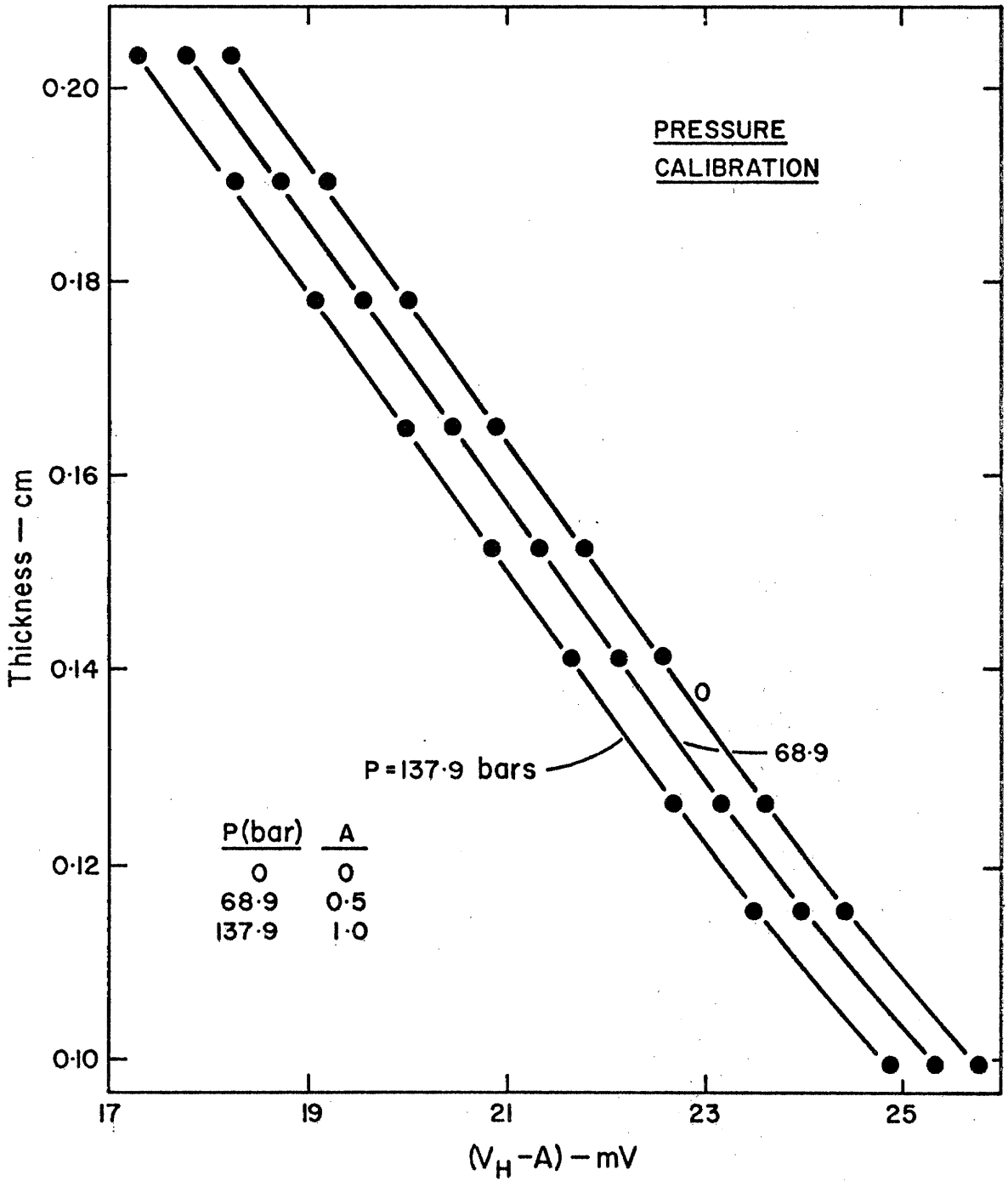

Figure 8 Calibration curves of thickness vs. Hall output voltage at various pressures.

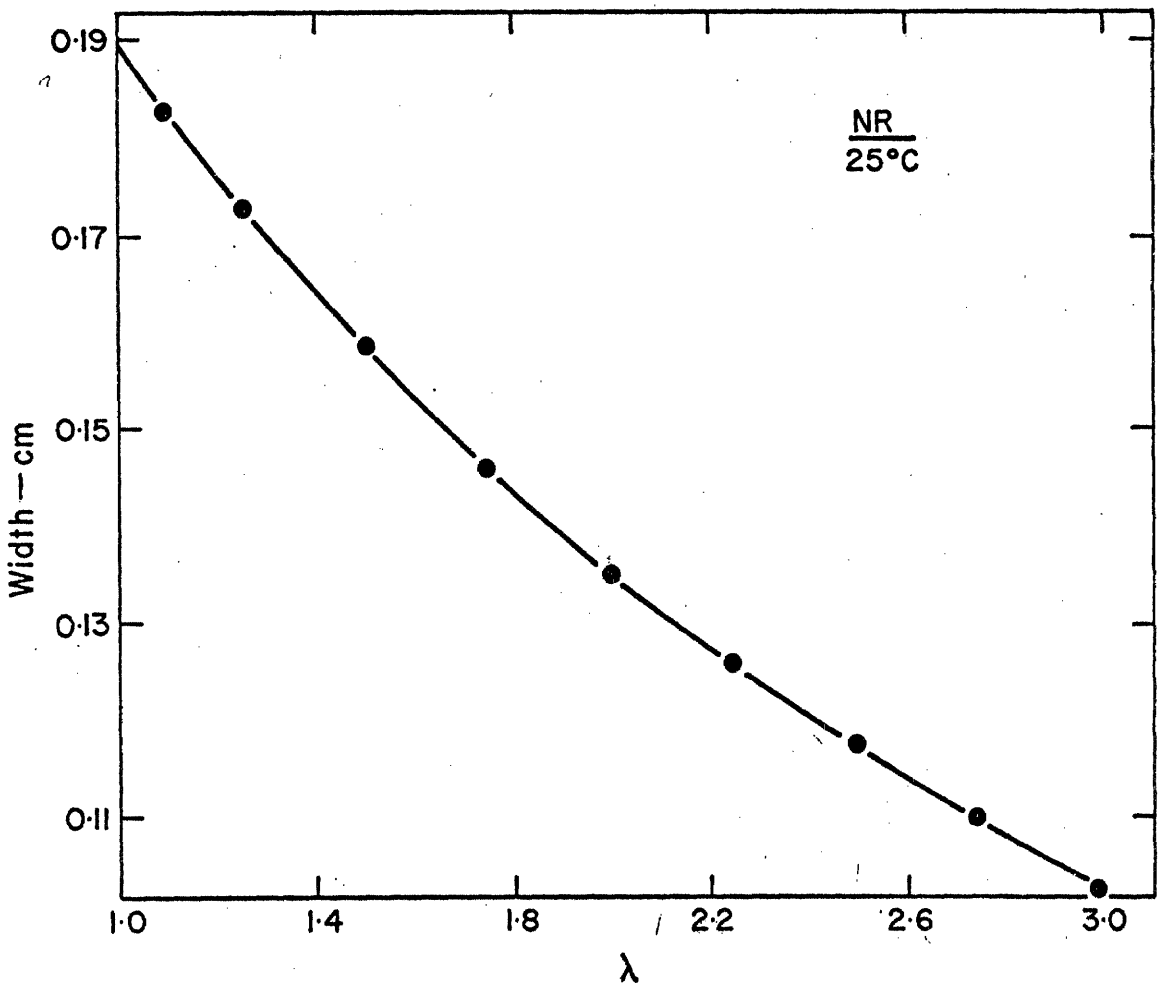

Figure 9 Plot of width of a natural rubber sample against the extension ratio at 25°C.

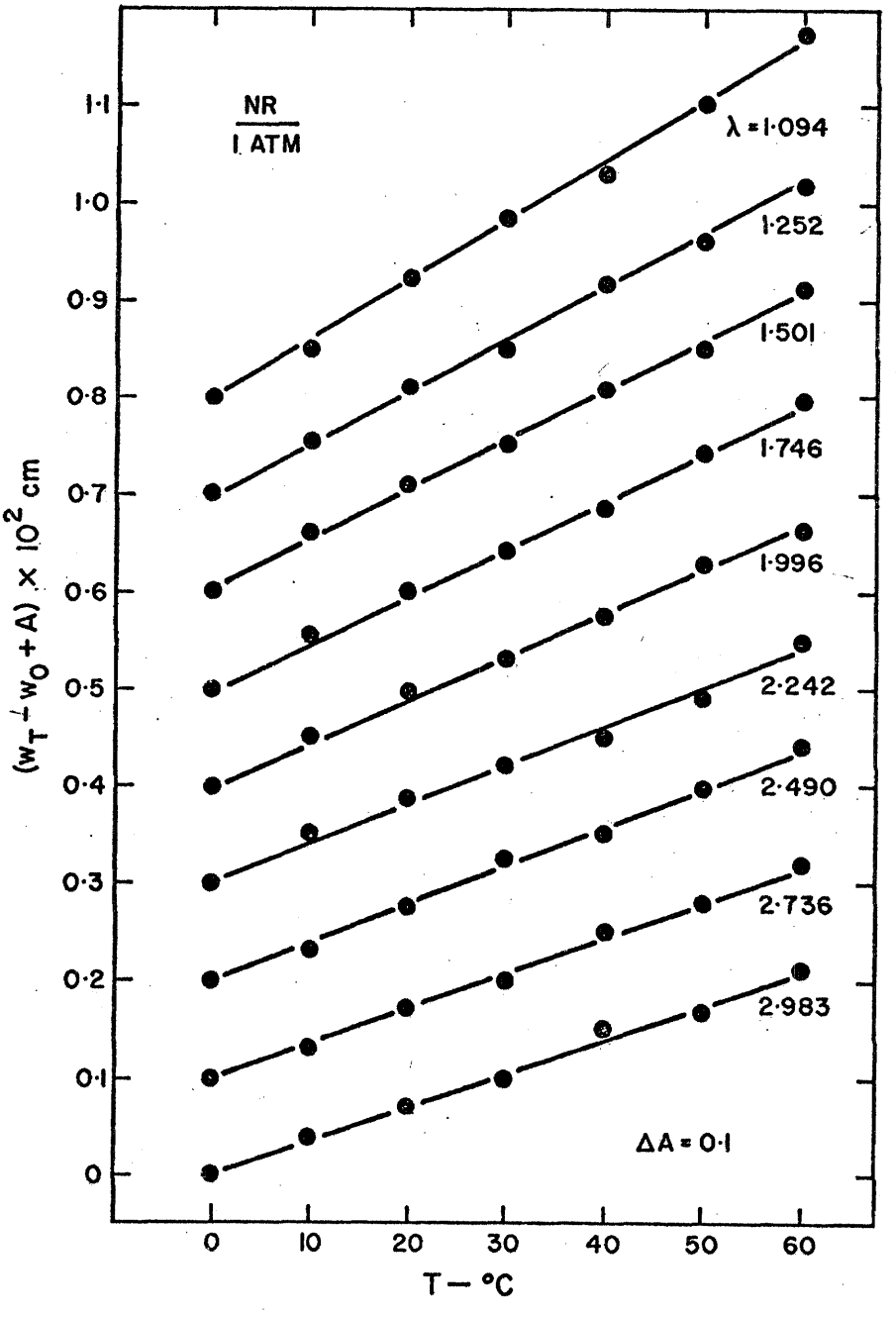

Figure 10 Plot of change in width of a natural rubber sample against temperature at various extension ratios. Note the shift in ordinate.

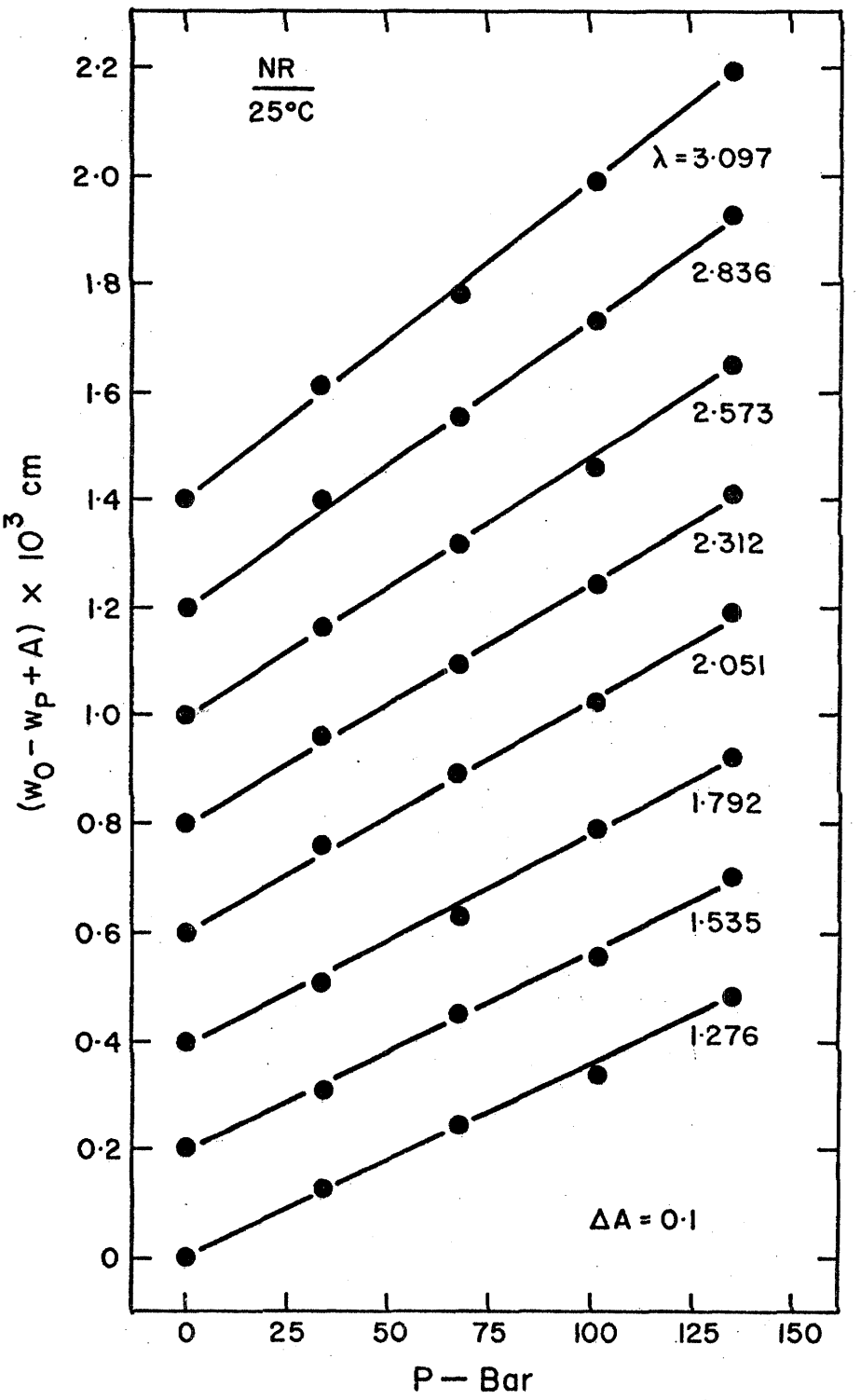

Figure 11 Plot of change in width of a natural rubber sample against pressure at various extension ratios. Note the shift in ordinate.

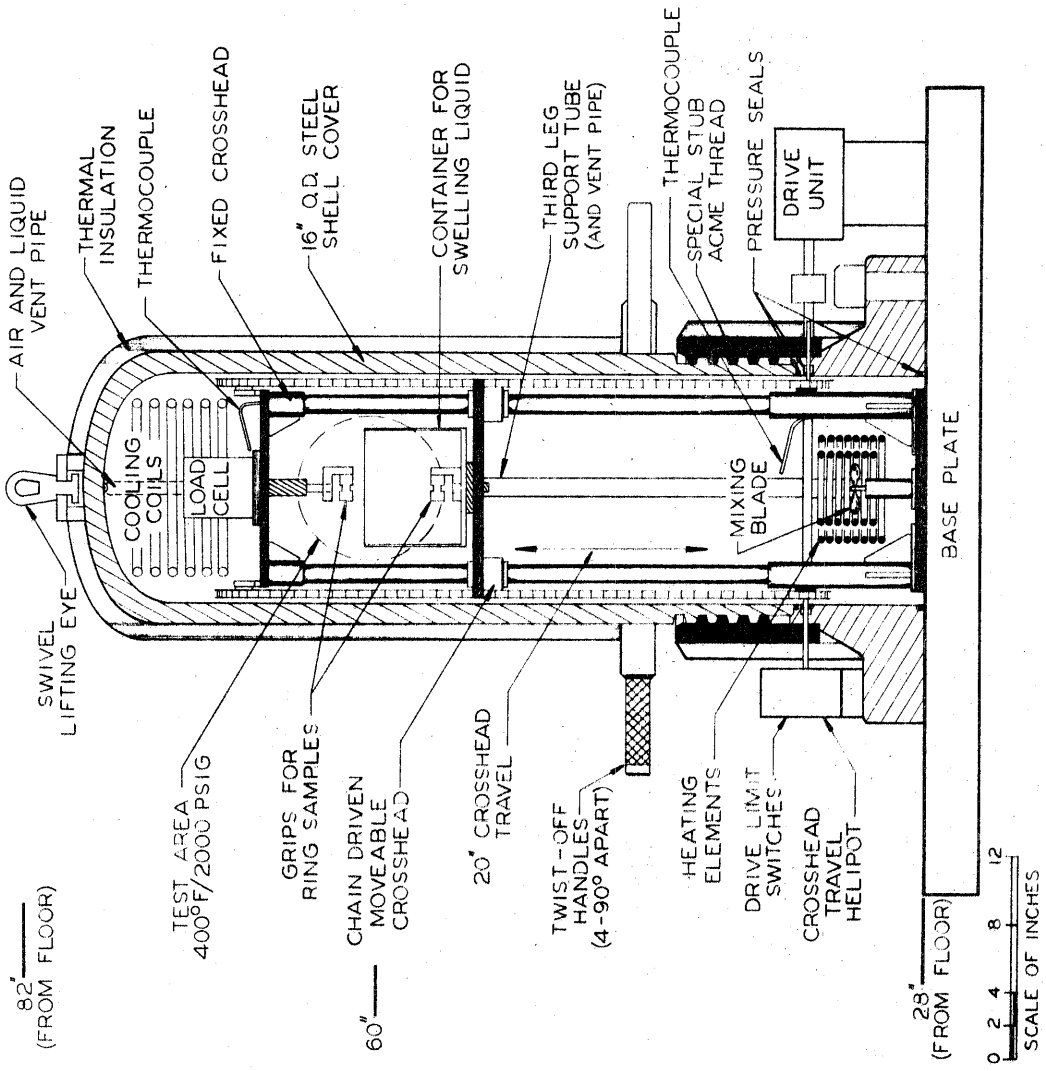

Figure 12 PRESSURIZED TENSILE TESTER

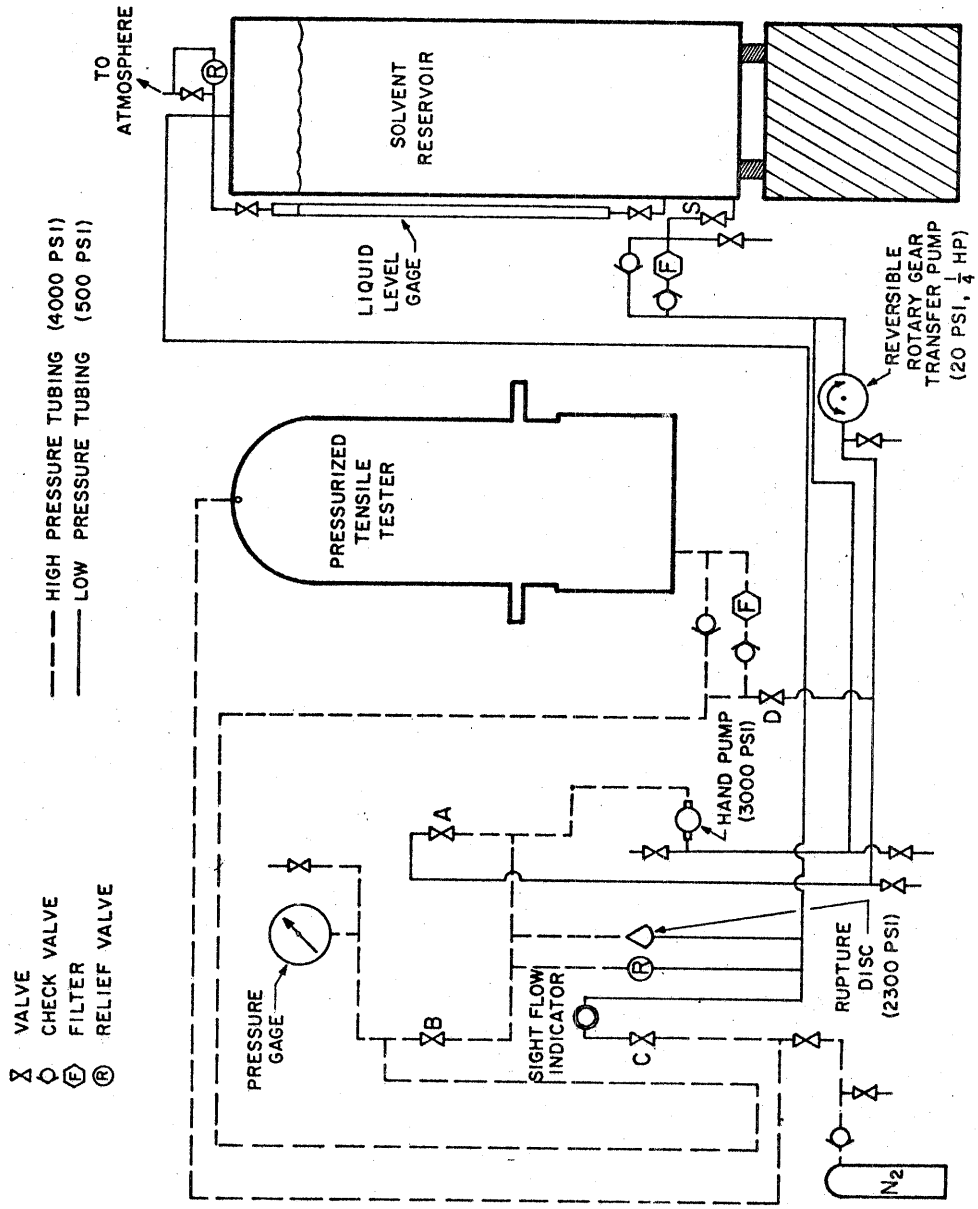

Figure 13 PIPING SCHEMATIC FOR PRESSURIZED TENSILE TESTER

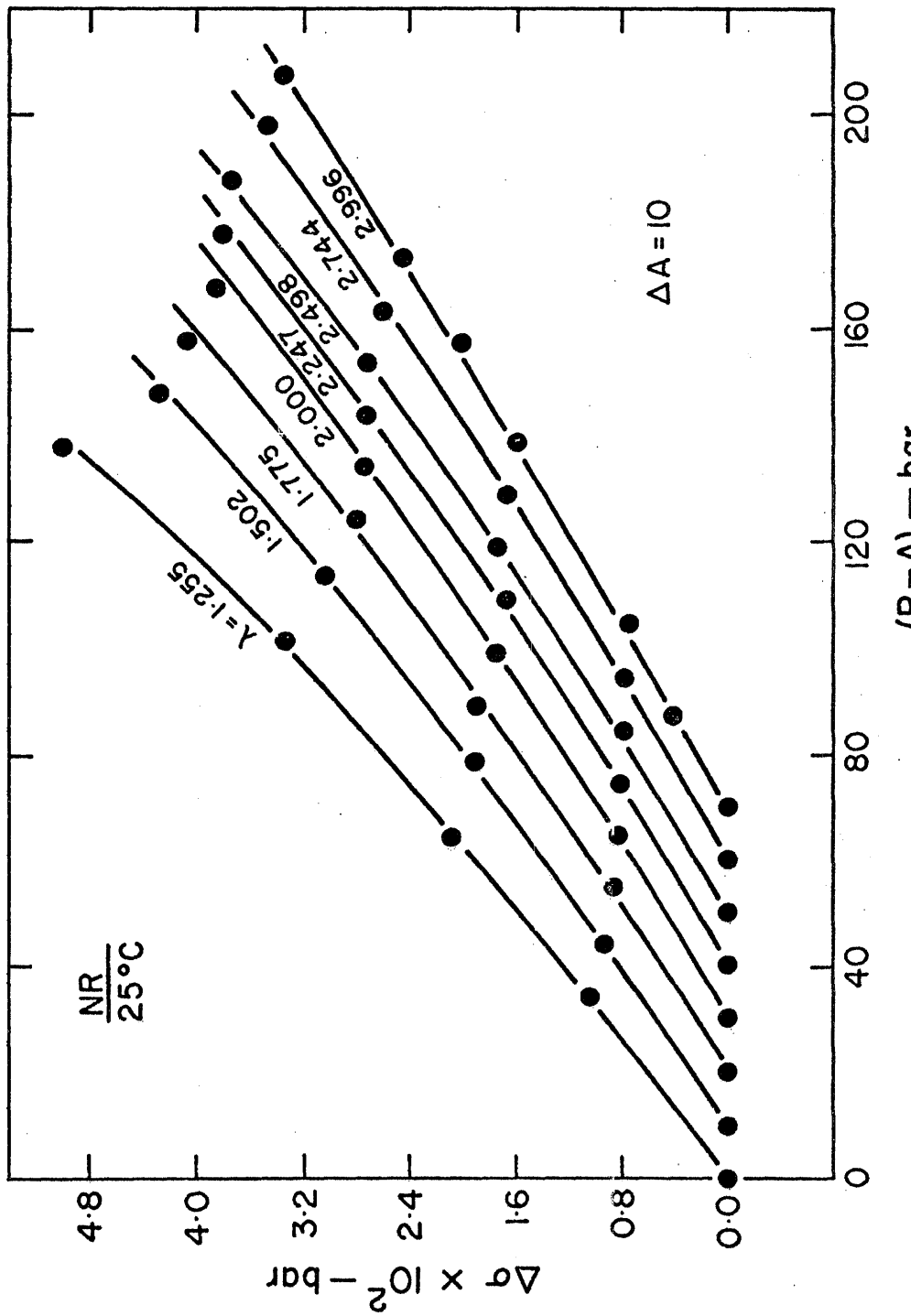

Figure 14 Plot of $\Delta\sigma$ vs. P for various extension ratios. Note the shift in origin.

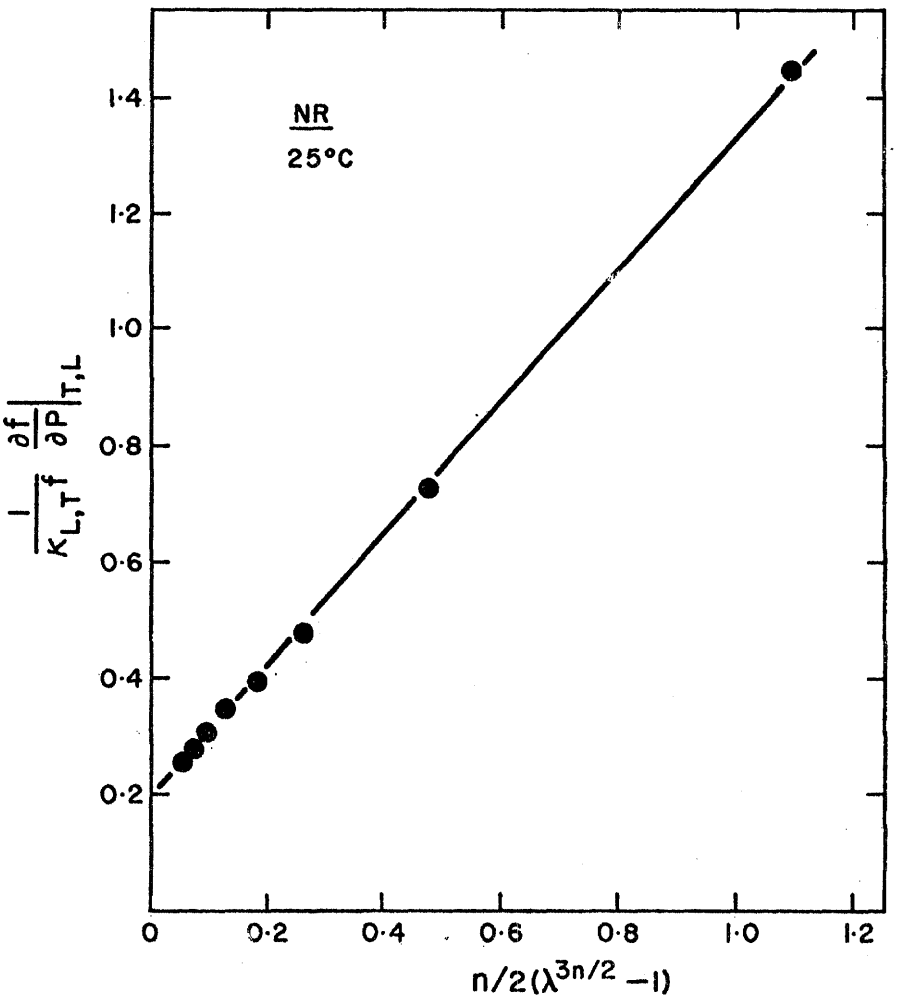

Figure 15 Dimensionless force-pressure coefficients plotted against $n/2(\lambda^{3n/2} - 1)$ according to Eq. (3.40).

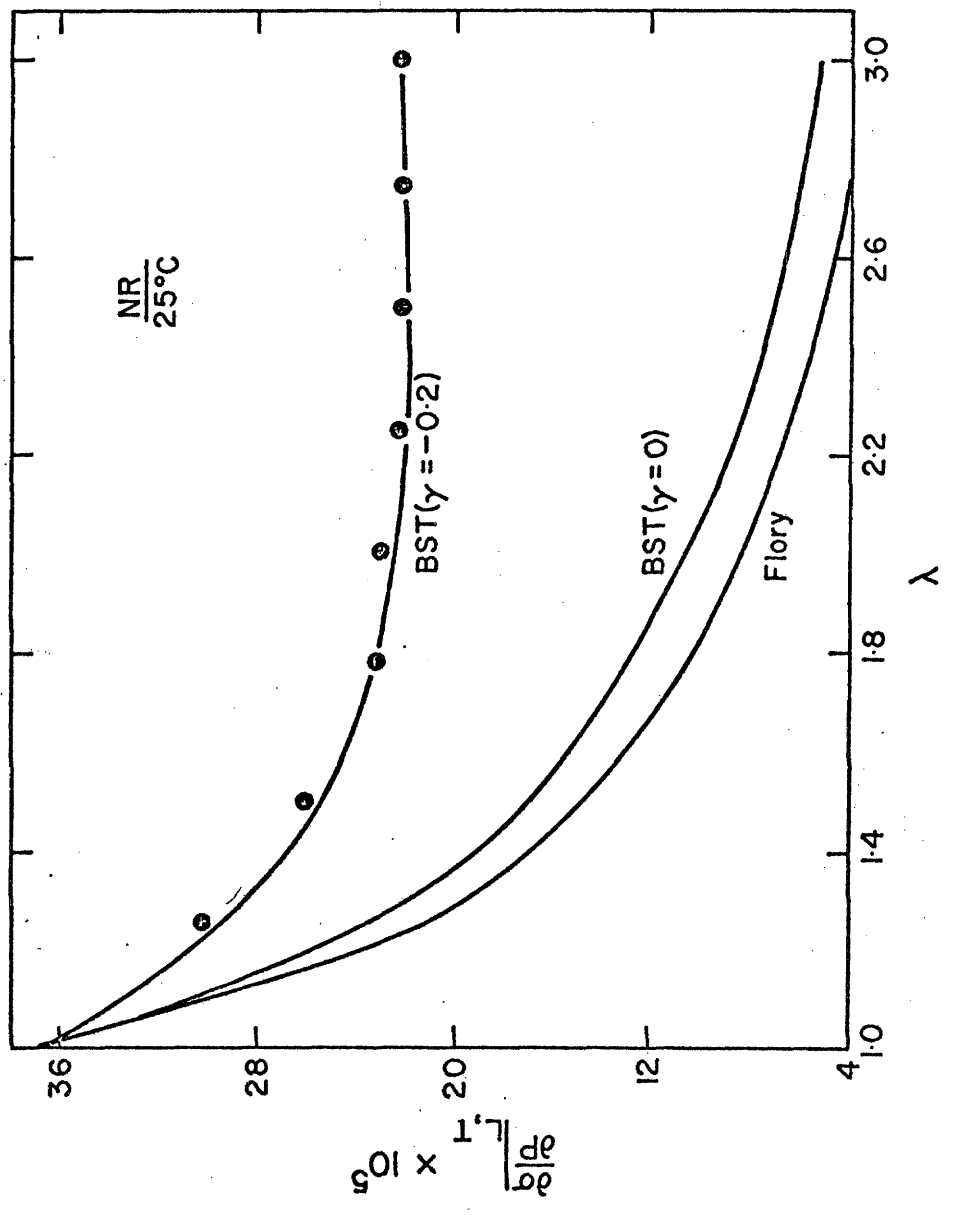

Figure 16 Stress-pressure coefficients of natural rubber.

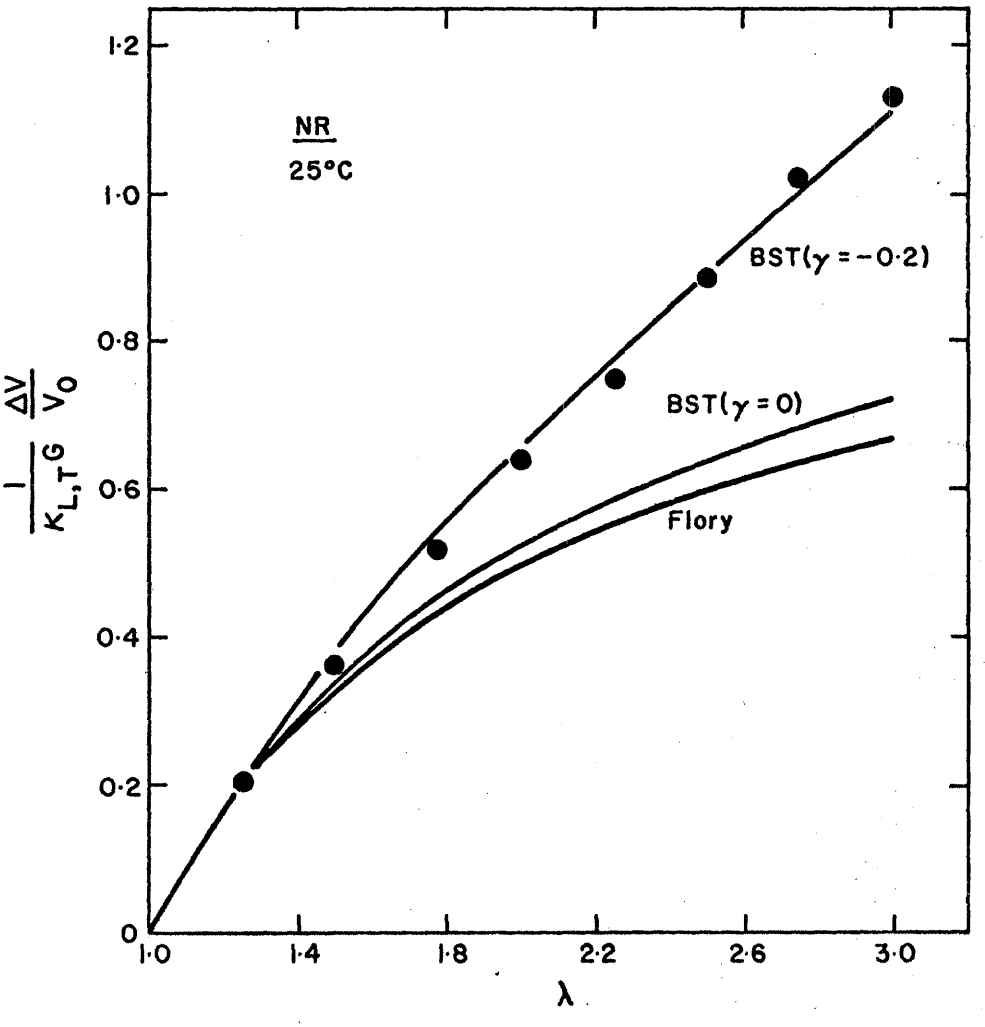

Figure 17 Plot of change in volume against extension ratio.

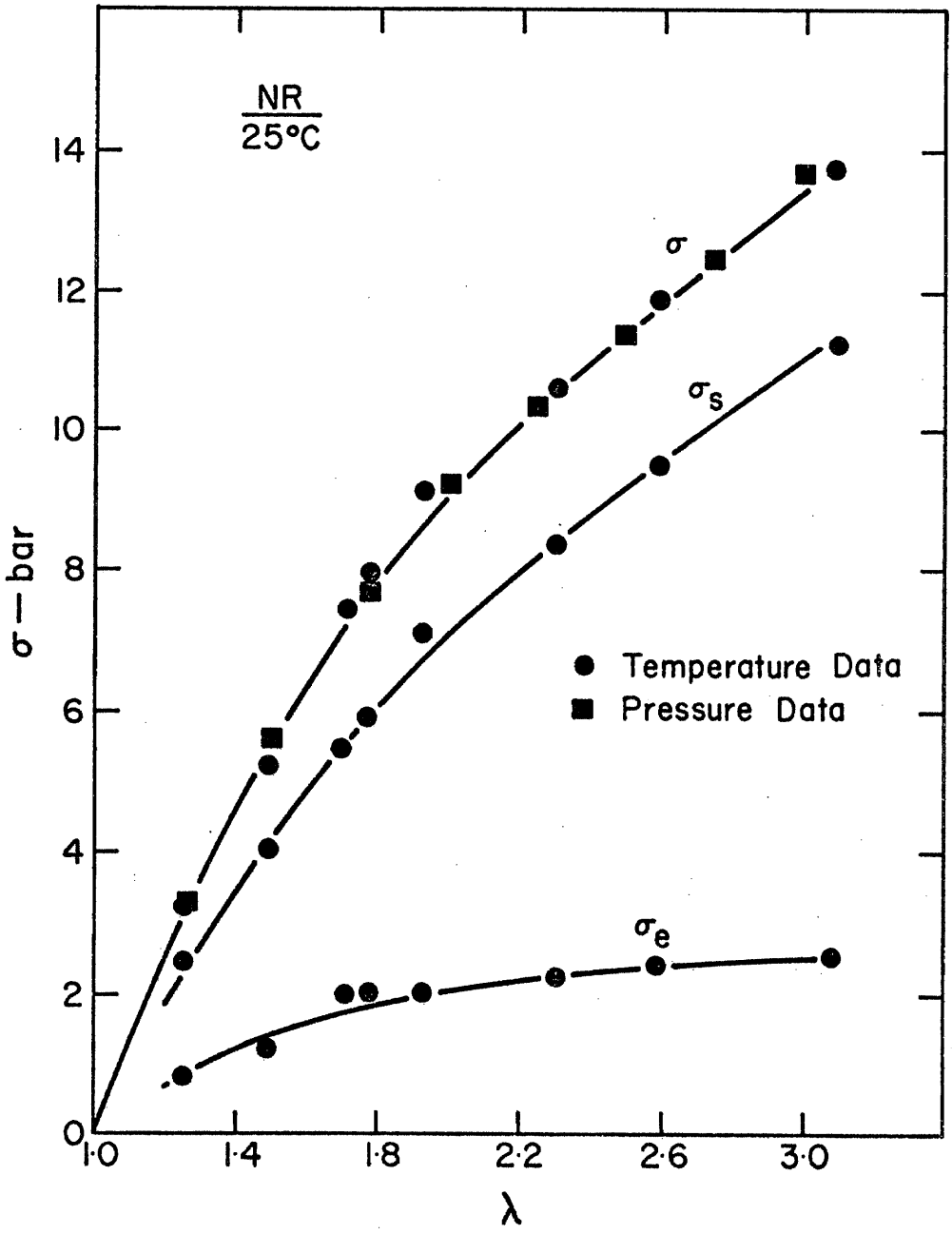

Figure 18 Plots of stress and its entropic and energetic components for natural rubber. Data calculated from Eq. (3.8).

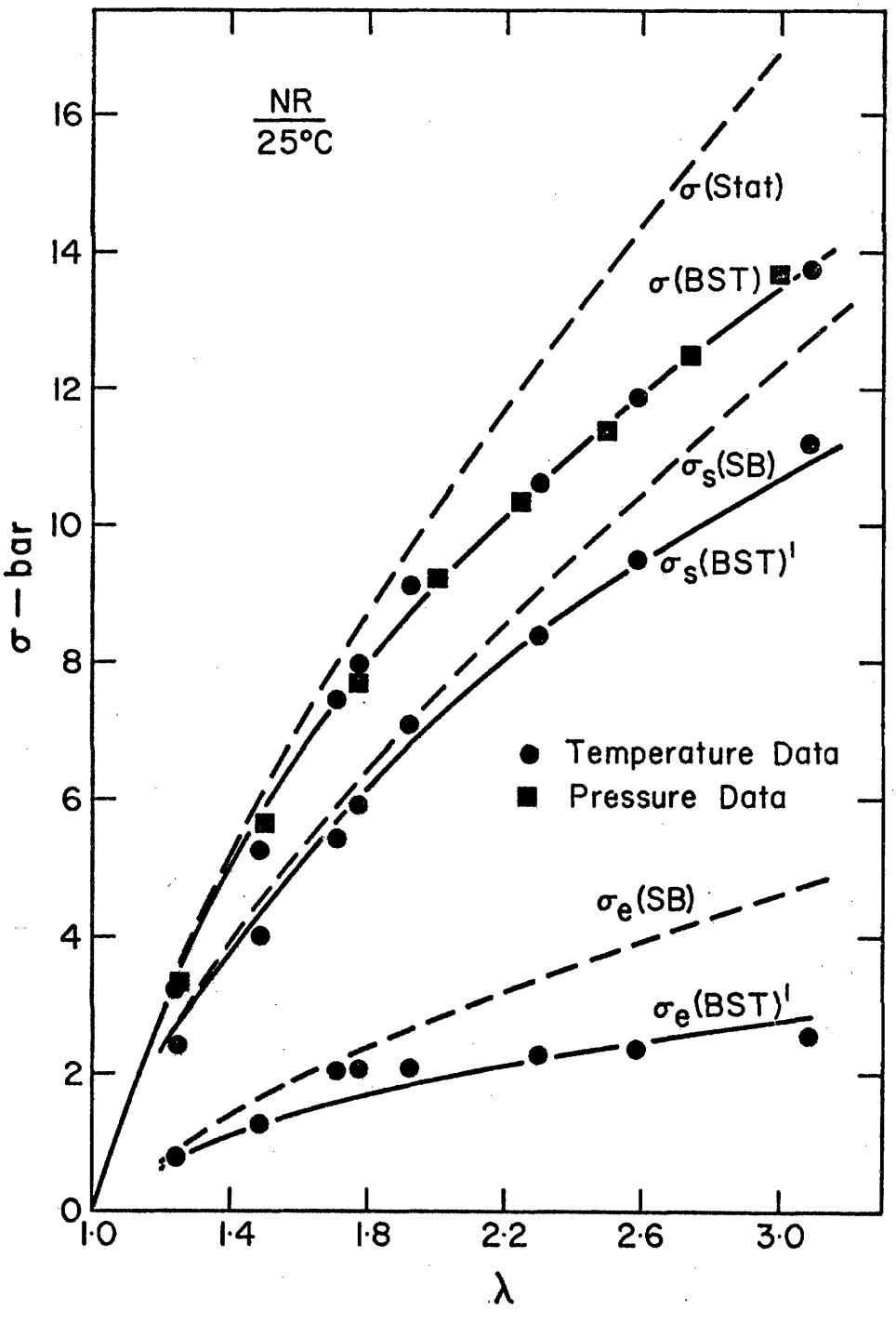

Figure 19 Comparison of experimental data with the predictions of BST[1] and SB equations.

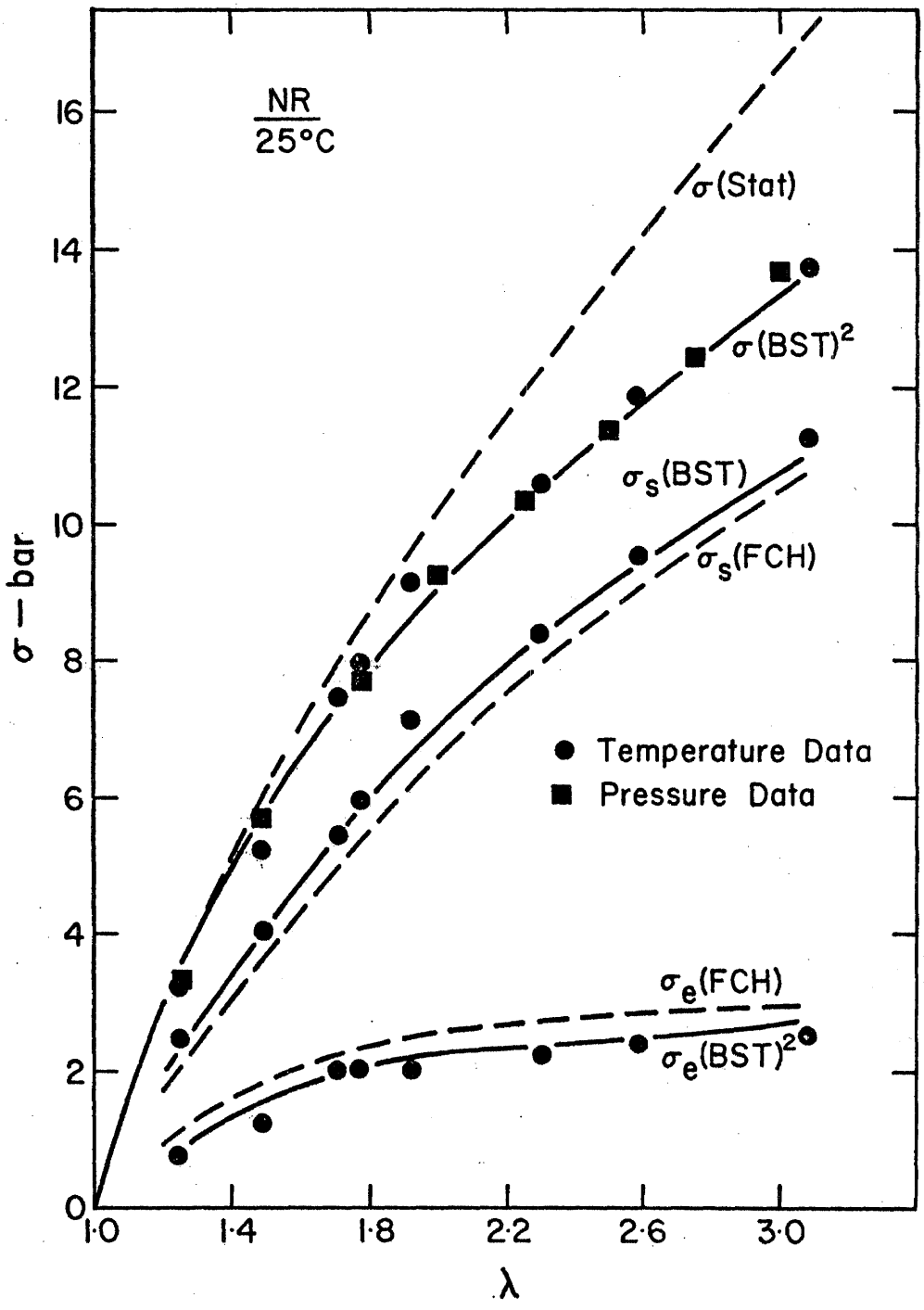

Figure 20 Comparison of experimental data with the predictions of BST^2 and FCH equations.

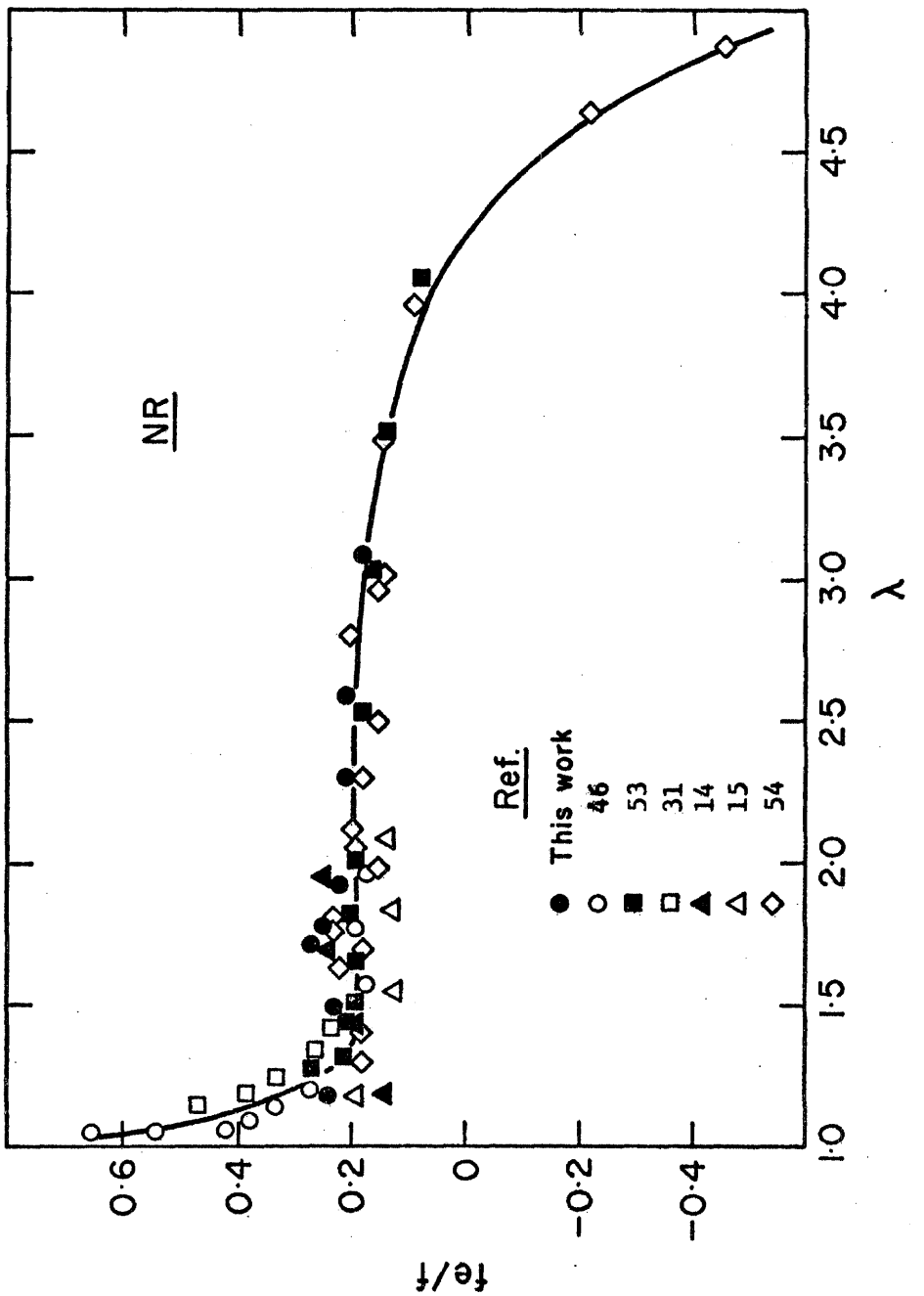

Figure 21 Plot of fe/f vs. λ for natural rubber.

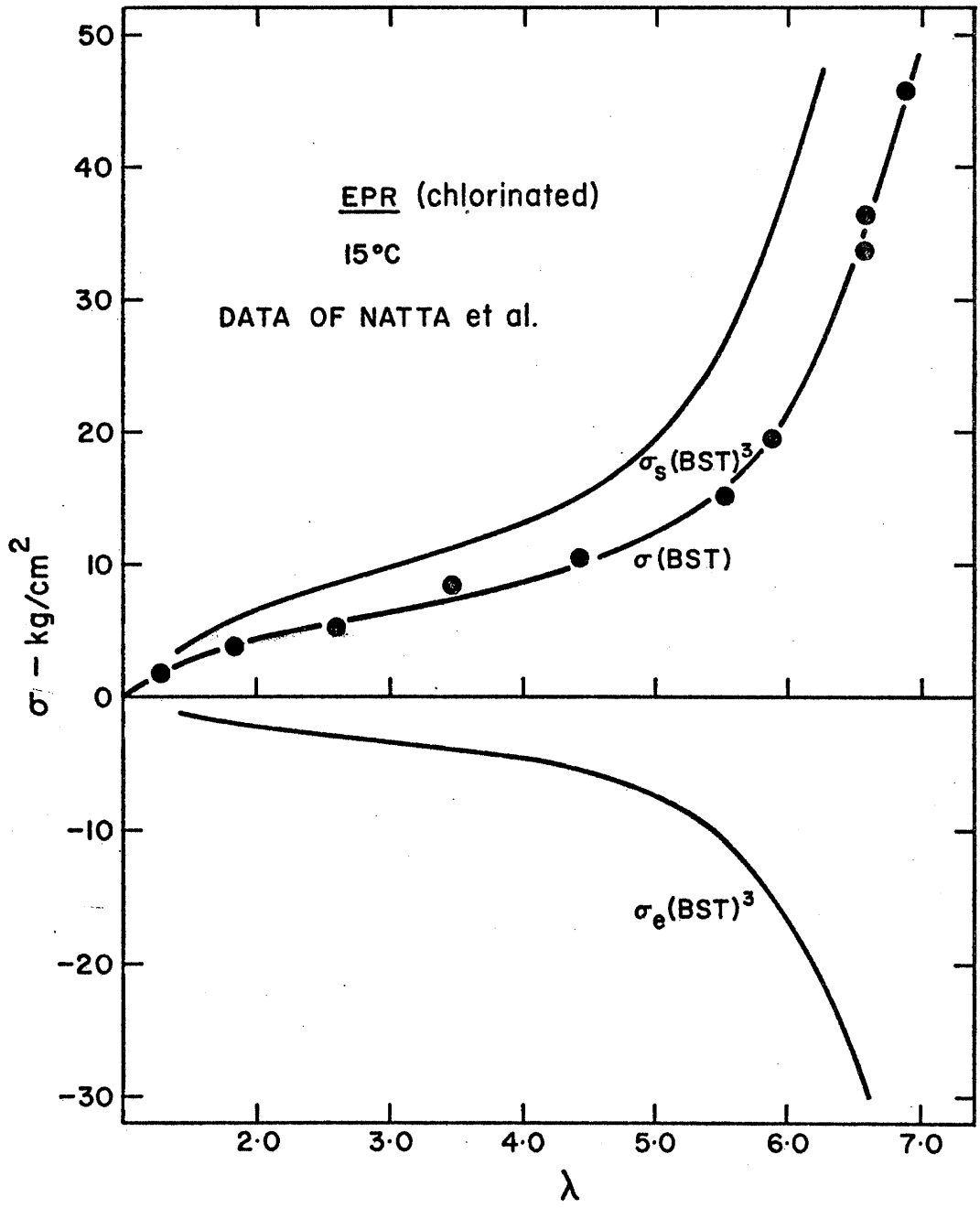

Figure 22 Plots of stress and its entropic and energetic components for chlorinated ethylene-propylene copolymer rubber.

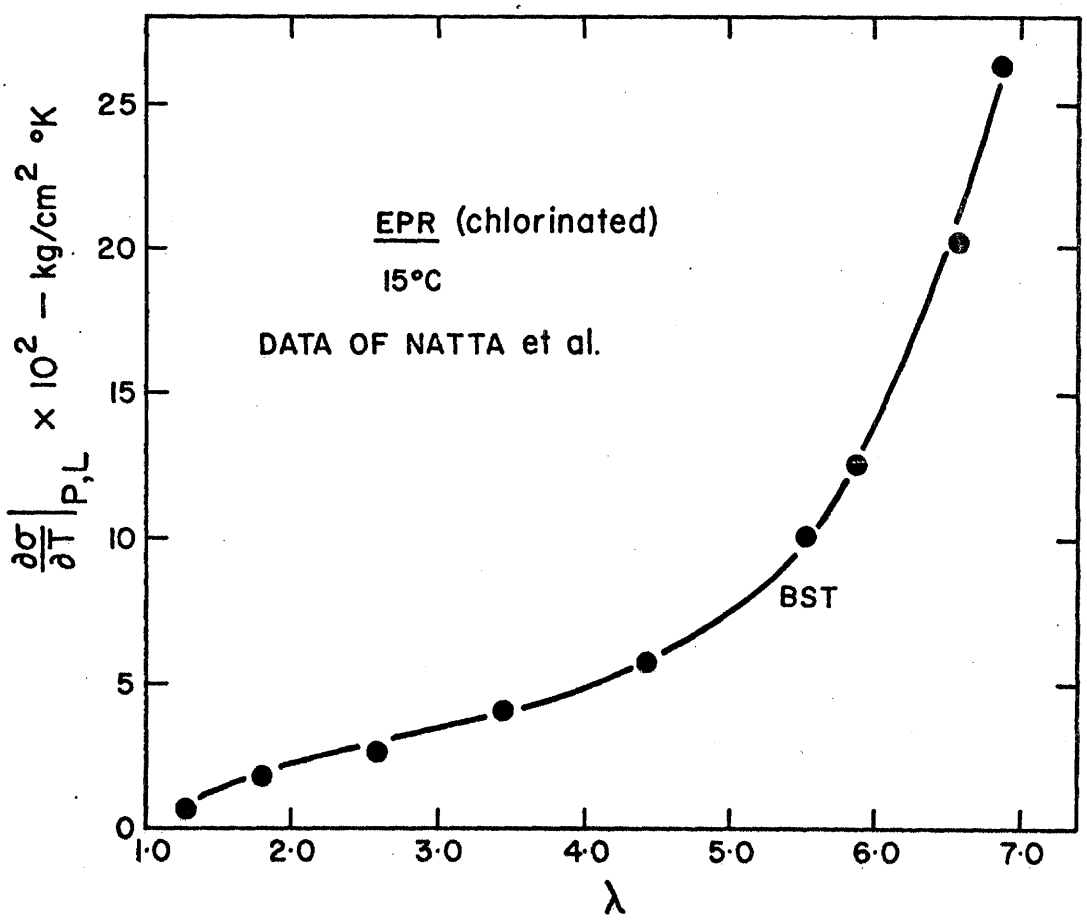

Figure 23 Stress-temperature coefficients for chlorinated ethylene-propylene copolymer rubber.

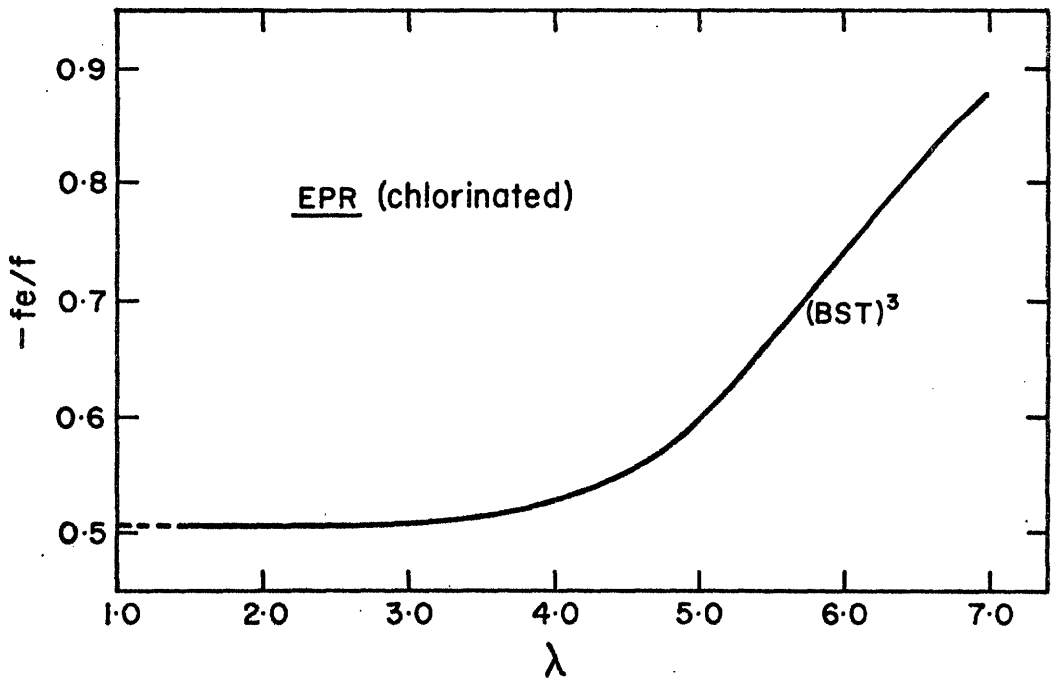

Figure 24 Plot of fe/f vs. λ for chlorinated ethylene-propylene copolymer rubber.

TABLE 1

Stress-Temperature Data

$\lambda = 1.250$		$\lambda = 1.491$		$\lambda = 1.713$		1.776	
T	σ	T	σ	T	σ	T	σ
°C	Bars	°C	Bars	°C	Bars	°C	Bars
5.5	3.129	19.5	5.164	-1.0	7.015	-1.5	7.533
20.0	3.207	31.5	5.292	8.0	7.170	9.0	7.694
35.5	3.282	41.5	5.383	18.0	7.350	18.0	7.845
50.25	3.353	50.5	5.496	29.5	7.476	26.5	7.954
35.0	3.280	61.0	5.589	39.5	7.647	30.0	8.053
19.5	3.200	50.5	5.505	49.0	7.806	39.5	8.210
5.0	3.126	41.5	5.410	60.0	7.952	50.0	8.368
		31.5	5.300			60.0	8.558
		19.5	5.164				

(continued)

TABLE 1 (continued)

λ = 1.925		λ = 2.300		λ = 2.586		λ = 3.083	
T		T		T		T	
°C	Bars	°C	Bars	°C	Bars	°C	Bars
-1.5	8.560	1.0	10.038	-1.5	11.092	-2.0	12.280
8.0	8.750	11.0	10.230	8.5	11.425	8.0	12.900
18.5	8.940	25.5	11.560	24.5	11.862	18.0	13.290
26.5	9.100	42.5	11.000	31.5	12.050	26.0	13.590
39.5	9.440	49.5	11.250	39.5	12.322	39.0	14.020
50.0	9.642	59.5	11.532	49.0	12.593	60.0	15.500
60.0	9.858			59.5	12.880	49.0	14.900
				49.0	12.790	39.0	14.480
				39.0	12.490	27.0	13.890
				27.0	11.980	18.0	13.650
				17.5	11.720	8.0	13.220
				8.0	11.430	-2.0	12.350
				-2.0	11.100		

TABLE 2

λ	$\frac{1}{w}\frac{\partial w}{\partial T}\Big\vert_{P,L}$ /°C	λ	$-\frac{1}{w}\frac{\partial w}{\partial P}\Big\vert_{T,L}$ Bars^{-1}
1.094	3.45×10^{-4}	1.276	32.3×10^{-6}
1.252	3.53	1.535	31.3
1.501	3.51	1.792	31.9
1.746	3.54	2.051	31.6
1.996	3.44	2.312	31.7
2.242	3.46	2.573	31.3
2.490	3.45	2.836	32.9
2.736	3.43	3.097	32.8
2.983	3.53		
Av	3.48×10^{-4}	Av	32.0×10^{-6}

TABLE 3

Change in Stress with Pressure ($\Delta\sigma \times 10^2$ Bars) T = 25°

P Bars (Gage)	λ							
	1.255	1.502	1.775	2.000	2.247	2.498	2.744	2.996
0	0.00	0.00	0.00	0.00	0.00	0.00	0.00	0.00
34.47	1.04	0.92	0.86	0.82	0.80	0.78	0.76	0.74
68.95	2.08	1.86	1.88	1.74	1.70	1.73	1.66	1.57
103.40	3.32	3.03	2.80	2.80	2.74	2.72	2.60	2.45
137.90	5.00	4.24	4.06	3.82	3.80	3.72	3.50	3.35
σ_{25}	3.262	5.610	7.651	9.212	10.316	11.376	12.463	13.690

TABLE 4

Thermodynamic Equation

λ	σ	$\left.\frac{\partial\sigma}{\partial T}\right\|_{P,L}$	$\frac{T}{\sigma}\left.\frac{\partial\sigma}{\partial T}\right\|_{P,L}$	$\left.\frac{\partial\sigma}{\partial P}\right\|_{T,L}$	$\frac{T}{\sigma}\gamma_{V,L}\left.\frac{\partial\sigma}{\partial P}\right\|_{T,L}$	$\frac{f_e}{f}$ or $\frac{\sigma_e}{\sigma}$	
	Bars	x 10^3 Bars/°C		x 10^5			
1.250	3.228	5.00	0.460	30.4	0.300	0.24	
1.491	5.225	10.45	0.596	26.3	0.160	0.24	
1.713	7.426	15.41	0.624	23.9	0.102	0.27	
1.776	7.961	16.66	0.648	23.2	0.091	0.26	
1.925	9.105	21.40	0.700	22.9	0.084	0.22	
2.300	10.600	25.70	0.724	22.1	0.066	0.21	
2.586	11.880	29.20	0.735	22.0	0.057	0.21	Av. = 0.23
3.083	13.720	35.0 ?	0.760	22.2	0.050	0.19	

$T = 25°C$

$\gamma_{V,L} = 10.8$ bars/°C

TABLE 5

Values of Parameters

	NR*	CℓEPR**
T	25°C	15°C
n	1.64	1.71
m	....	4.84
B	....	6.47×10^{-5}
G	5.87	2.71
dG/dT	13.0×10^{-3}	14.2×10^{-3}
dB/dT	....	5.54×10^{-7}
γ	-0.2	....

* Units are Bars or Bars/°C

** Units are Kg/cm^2 or $Kg/cm^2°C$

TABLE 6

FCH and BST Equations of State

λ	σ Bars		$\frac{T}{\sigma}\frac{\partial\sigma}{\partial T}\Big\vert_{P,L}$	$\frac{3\alpha_o T}{\lambda^3 - 1}$	$\frac{f_e}{f}$ (FCH)	$\left[\frac{n}{2(\lambda^{3n/2}-1)} - \gamma\right] 3\alpha_o T$	$\frac{f_e}{f}$ (BST)
	σ(Stat.)	σ(BST)					
1.250	3.58	3.49	0.458	0.220	0.32	0.270	0.27
1.491	6.11	5.79	0.596	0.090	0.31	0.140	0.26
1.713	8.06	7.42	0.624	0.052	0.33	0.100	0.27
1.776	8.57	7.83	0.648	0.045	0.31	0.095	0.26
1.925	9.72	8.72	0.700	0.034	0.27	0.080	0.22
2.300	12.40	10.63	0.724	0.019	0.26	0.065	0.21
2.587	14.28	11.89	0.735	0.013	0.25	0.058	0.21
3.083	17.50	13.80	0.767	0.007	0.22	0.055	0.18
					Av. 0.28		Av. 0.24

References

1. W. R. Krigbaum and R. J. Roe, Rubber Chem. Tech., 38, 1039 (1965).

2. A. Ciferri, J. Polymer Sci., 54, 149 (1961).

3. M. Shen, W. F. Hall and R. E. DeWames, Macromol. Chem., C2(2), 183 (1968).

4. L. R. G. Treloar, "The Physics of Rubber Elasticity", second ed., Oxford University Press, London, 1958.

5. P. J. Flory, "Principles of Polymer Chemistry", Cornell University Press, Ithaca, N.Y., 1953.

6. E. Guth, J. Poly. Sci.: Pt. C, 31, 267 (1970).

7. M. V. Volkenstein, "Configurational Statistics of Polymer Chains", John Wiley and Sons, Inc., New York, 1963.

8. P. J. Flory, C. A. J. Hoeve and A. Ciferri, J. Poly. Sci., 34, 337 (1959).

9. M. V. Volkenstein and O. B. Ptitsyn, Zhur. Tekh. Fiz., 25, 649 (1955).

10. H. B. Callen, "Thermodynamics", John Wiley and Sons, Inc., New York, 1966.

11. P. J. Flory, Trans. Faraday Soc., 57, 829 (1961).

12. F. T. Wall, "Chemical Thermodynamics", W. H. Freeman and Co., San Francisco, 1958.

13. H. K. Livingston and G. P. Reghi, Rubber Chem. Tech., 42, 441 (1969).

14. G. Allen, U. Bianchi and C. Price, Trans. Faraday Soc., 59, 2493 (1963).

15. G. Allen, M. J. Kirkham, J. Padget and C. Price, Trans. Faraday Soc., 67, 1278 (1971).

16. J. E. Mark, Rubber Chem. Tech., 46, 593 (1973).

17. W. Dick and F. H. Mueller, Kolloid-Z. Z. Polym., 172, 1 (1960).

18. K. J. Smith Jr., in "Polymer Science", ed. A. D. Jenkins, North-Holland Publishing Co., Amsterdam, 1972.

19. H. M. James and E. Guth, J. Poly. Sci., 4, 153 (1949).

20. H. M. James and E. Guth, J. Chem. Phys., 15, 669 (1947).

21. A. Ciferri, Trans. Faraday Soc., 57, 846 (1961) and 57, 853 (1961).

22. W. Taylor, J. Chem. Phys., 16, 257 (1948).

23. T. M. Birshtein and O. B. Ptitsyn, "Conformations of Macromolecules", High Polymers, Vol. XXII, John Wiley and Sons, Inc., New York, 1966.

24. P. J. Flory, "Statistical Mechanics of Chain Molecules", John Wiley and Sons, Inc., New York, 1969.

25. P. J. Blatz in "Rheology", Vol. 5, ed., F. R. Eirich, John Wiley and Sons, Inc., New York, 1969.

26. P. J. Blatz, Rubber Chem. Tech., 36, 1459 (1963).

27. P. J. Blatz and W. L. Ko, Trans. Soc. Rheology, VI, 223 (1962).

28. F. Murnaghan "Finite Deformations of an Elastic Solid", John Wiley and Sons, New York, 1951.

29. P. Bridgman, Proc. Am. Acad. Arts Sci., 75, 9 (1944).

30. A. V. Tobolsky and M. C. Shen, J. Appl. Phys., 37, 1952 (1966).

31. M. Shen and P. J. Blatz, J. Appl. Phys., 39, 4937 (1968).

32. P. J. Flory, A. Ciferri and C. A. J. Hoeve, J. Poly. Sci., 45, 235 (1960).

33. M. Okuyama, K. Yagii, S. C. Sharda and N. W. Tschoegl, Polymer Engineering and Science, 14, 38 (1974).

34. M. Shen, Macromolecules, 2, 358 (1969).

35. M. Shen, E. H. Cirlin and M. H. Gebhard, Macromolecules, 2, 682 (1969).

36. P. J. Blatz et al., Polymer Science Report, MATSCIT, PS64-8, California Institute of Technology, Pasadena, California, 1964.

37. K. Yagii, Ph.D. dissertation, California Institute of Technology, Pasadena, California, 1972.

38. P. J. Blatz, S. C. Sharda, N. W. Tschoegl, Proc. Nat'l. Acad. Sci., 70, 3041, 1973.

39. P. J. Blatz, S. C. Sharda and N. W. Tschoegl, Trans. Soc. Rheology (in press).

40. U. Bianchi and E. Pedemonte, J. Poly. Sci., A, 2, 5039 (1964).

41. N. W. Tschoegl et al., Chemical Engineering Polymer Laboratory report CHECIT PL68-1, California Institute of Technology, Pasadena, California, 1968.

42. N. W. Tschoegl et al., Chemical Engineering Polymer Laboratory report CHECIT PL69-1, California Institute of Technology, Pasadena, California, 1969.

43. T. N. Khasanovich, J. Appl. Phys., 30, 948 (1959).

44. R. G. Christensen and C. A. J. Hoeve, J. Poly. Sci., A-1, 8, 1503 (1970).

45. J. C. Goebel and A. V. Tobolsky, Macromolecules, 4, 208 (1971).

46. M. C. Shen, D. A. McQuarrie and J. L. Jackson, J. Appl. Phys., 38, 791 (1967).

47. G. Natta, G. Crespi and U. Flisi, J. Poly. Sci., A, 1, 3569 (1963).

48. H. Wagner and P. J. Flory, J. Am. Chem. Soc., 74, 195 (1952).

49. J. E. Mark, J. Am. Chem. Soc., 88, 4354 (1966).

50. H. Benoit, J. Polymer Sci., 3, 376 (1948).

51. C. W. Bunn, Proc. Roy. Soc. (London), A180, 40 (1942).

52. T. Ishikawa and K. Nagai, J. Poly. Sci., Part A-2, 7, 1123 (1969).

53. R. J. Roe and W. R. Krigbaum, J. Poly. Sci., 61, 167 (1962).

54. K. J. Smith Jr., A. Greene and A. Ciferri, Kolloid Z., 194, 49 (1964).

PROPOSITION I

A NEW KINETIC MODEL FOR THE GLASS TRANSITION INTERVAL IN POLYMERS

Abstract

A new kinetic model for glass transition in polymers is proposed. This describes the sudden change in heat capacity of the polymer in the glass transition interval. The effect of heating rate on the glass transition temperature is studied.

1. Introduction

This proposition presents a model for the change in heat capacity of polymers in the glass transition interval. The heat capacity of a polymer shows a sudden change in value when the material is heated or cooled through the glass transition. The range of temperature in which this change occurs varies with the heating or the cooling rate. The rate dependence of glass transition suggests that the phenomenon can be described by a kinetic rate process. A kinetic description of the glass transition has been presented in the literature (1, 2). This regards the vitrification process (or conversely the softening process) as a first order chemical reaction. It assumes that two energy levels are available to the material near the glass transition temperature. The process of vitrification is accomplished by passage of kinetic particles from one energy state to the other. The theory involves two parameters: (1) the difference in the energies of the two states, and (2) a single relaxation time (or a rate constant). No relation exists between the structure of the polymer and these parameters. Thus, the theory applies to any substance independent of its structure.

In this work, a new kinetic model of glass transition in polymers is proposed. This is based on the various rotational states available to a polymer molecule. A polymer molecule has associated with it a number of spatial conformations, which are due to rotation around single bonds in the chain backbone. A simple molecule such as polyethylene is characterized by three rotational energy minima around the CH_2-CH_2 bond. For more complex molecules such as polyisoprene, polybutadiene etc., other such minima exist due to different

bonds in their chain structure. The conformation of a polymer chain thus arises from a mixture of these rotational states. In this model it is postulated that as the polymer passes from a rubber to a glass or vice versa, the distribution of these rotational states changes (i.e., the number of conformations in different energy states pass from one rotational state to the other). The redistribution is accomplished by a kinetic rate process. The rate of change of the number of conformations in various states and the difference in rotational energies of these states determine the changes in heat capacity of the polymer.

This model differs from the previous model in a number of important aspects:

1) The number of reactions is given by the number of rotational states. In the previous model, only one reaction exists.
2) The various rotational states are determined by the structure of the polymer chain, whereas the structure plays no part in the earlier model.
3) The differences in the energies of the various rotational states now become the structural parameters and can be compared with similar parameters obtained from other studies, such as diffusion, spectroscopy and thermoelasticity, etc.

However, the fundamental principle underlying the two models remains the same. In both the glassy state is distinguished from the rubbery state by the fact that internal chemical equilibrium is not established. In the glassy state the molecules vibrate relative to one another but do not rotate (so called "frozen" state). In the rubbery

state, the rotation increases as the temperature rises. The transformation from vibrational modes to rotational modes accounts for the change in various thermodynamic properties in the glass transition interval. This transformation or the change in the internal configuration of the system can be described in terms of some reaction coordinate which at any time gives the concentration of the rotating units.

In the discussion below, the heat capacity of the polymer is expressed in terms of the change in the internal configuration of the system. In Section 2, a kinetic model with three rotational states is considered, which is then modified to any number of energy states. In Section 3, a sample calculation is presented showing that the model indeed describes the sudden changes in heat capacity. The effect of different rates of heating on the glass transition temperature is shown. This gives rise to a simple relation between the rate of heating and the temperature at which the heat capacity shows a maximum. In Section 4, the results of this study are summarized.

2. Theory

In order to develop a general kinetic theory of glass transition, it is desirable to start with a simple three rotational state model. Let the potential energy curve for a given polymer be represented by three rotational minima:

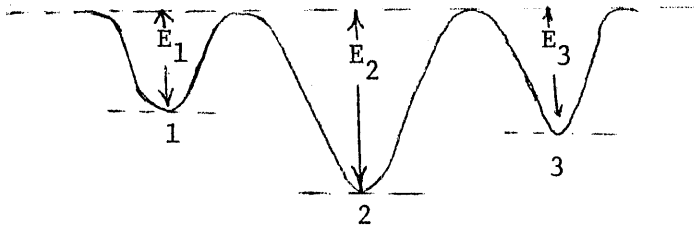

I

The three energy states are designated 1, 2, 3. N_1, N_2 and N_3 are the numbers of conformations in states 1, 2 and 3, respectively. For the purpose of discussion, these conformations are referred to as chemical species. As the polymer is heated or cooled through the glass transition, the number of conformations in states 1, 2 and 3 change. It is convenient to assume that the redistribution is accomplished by a first order reversible reaction. For a chemical reaction of this type, the general kinetic scheme can be represented by (3)

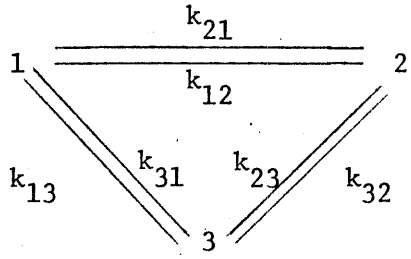

II

where k_{ij} are the rate constants. Let x_i be the composition of the various chemical species:

$$x_i = N_i \Big/ \sum_{j=1}^{3} N_j \qquad i = 1, 2, 3 \tag{1.1}$$

Also,

$$\sum_i x_i = 1 \tag{1.2}$$

Since the difference between E_i and H_i is small (of the order of RT), the enthalpy of the reaction system may be written as

$$H = \sum_i x_i E_i \tag{1.3}$$

Assuming that the E_i remain constant over the range of temperature in which the glass transition is observed (about 10°), the heat capacity of the system at constant pressure is given by

$$C_P = \left.\frac{\partial H}{\partial T}\right|_P \tag{1.4}$$

$$= \sum_i E_i \left.\frac{\partial x_i}{\partial T}\right|_P \tag{1.5}$$

A convenient way of representing E_i is by considering the state 2 (or the state with the lowest energy) as the reference state. Thus, the E_i are then replaced by E_2 and ΔE_i ($i \neq 2$). If the change in composition of the various chemical species is known as a function of temperature, Eq. (1.5) can be used to determine Cp.

The rate equations for the various chemical species in Formula II are given by

$$dx_1/dt = -(k_{21} + k_{31})x_1 + k_{12}x_2 + k_{13}x_3 \quad (1.6)$$

$$dx_2/dt = k_{21}x_1 - (k_{12} + k_{32})x_2 + k_{23}x_3 \quad (1.7)$$

$$dx_3/dt = k_{31}x_1 + k_{32}x_3 - (k_{13} + k_{23})x_3 \quad (1.8)$$

If θ is the rate of temperature change

$$\theta = dT/dt \quad (1.9)$$

Eqs. 6, 7 and 8 are rewritten as

$$dx_1/dT = -\theta^{-1}(k_{21} + k_{31})x_1 + \theta^{-1}k_{12}x_2 + \theta^{-1}k_{13}x_3 \quad (1.10)$$

$$dx_2/dT = \theta^{-1}k_{21}x_1 - \theta^{-1}(k_{12} + k_{32})x_2 + \theta^{-1}k_{23}x_3 \quad (1.11)$$

$$dx_3/dT = \theta^{-1}k_{31}x_1 + \theta^{-1}k_{32}x_2 - \theta^{-1}(k_{13} + k_{23})x_3 \quad (1.12)$$

Thus, the heat capacity is determined by combining Eq. (1.5) with Eqs. (1.10 to (1.12). Since k_{ij} depend on temperature, these may be obtained from the Arrhenius equation or the equation (4)

$$k_{ij} = k^{o}_{ij} T^{\alpha} \exp(- E_j/RT) \tag{1.13}$$

where k^{o}_{ij} are the frequency factors and α is usually of the order 1. For the Arrhenius equation α is zero. Thus the problem has been reduced to solving Eq. (1.5) with the aid of Eqs. (1.10), (1.11), (1.12), (1.13) and the initial conditions:

$$\text{At} \quad t = o, \quad T = T_o \tag{1.14}$$

$$x_i = x_{io} \tag{1.15}$$

All the quantities in Eqs. (1.5) and (1.10-1.13) are in terms of E_i and T. These sets of equations may be solved numerically. Before demonstrating a sample calculation, the structure of these equations leads to an easy generalization to n component system.

Equations (1.5) and (1.13) hold for the n component system whereas the rate equations may be written in a matrix form as follows:

$$\frac{\vec{dx}}{dT} = K\vec{x} \tag{1.16}$$

where $\vec{x}$ is the composition vector

$$\vec{x} = \begin{pmatrix} x_1 \\ x_2 \\ \cdot \\ \cdot \\ \cdot \\ x_n \end{pmatrix} \tag{1.17}$$

and K is a matrix given by

$$K = \begin{Bmatrix} -\sum_{i=1}^{n}(k_{i1} - k_{ii}) & k_{12} & \cdots & k_{1n} \\ k_{21} & -\sum_{i=1}^{n}(k_{i2} - k_{ii}) & \cdots & k_{2n} \\ \vdots & \vdots & & \vdots \\ k_{n1} & k_{n2} & \cdots & -\sum_{i=1}^{n}(k_{in} - k_{ii}) \end{Bmatrix} \quad (1.18)$$

It is being pointed out that the kinetic scheme II is the most general three rotational state scheme. This would imply an unrestricted rotation. The problem simplifies if the rotation is hindered, since in that case the number of reactions may be reduced (see below).

3. Calculations

The potential curve considered in I is the most general three point rotational curve. For a sample calculation it is convenient to consider a polymer with rotational minima at say ± 120° and 0°, where the energies of the ± 120° states are equal. To simplify these sample calculations, it is assumed that the kinetic particles may not pass from the + 120° rotational state to the - 120° rotational state or vice versa. Thus, only the following reaction scheme is allow d:

$$1 \underset{k_{12}}{\overset{k_{21}}{\rightleftharpoons}} 2 \underset{k_{23}}{\overset{k_{32}}{\rightleftharpoons}} 3 \qquad \text{III}$$

where 1 and 3 are the ± 120° states and 2 is the 0° state. Also, we set $k_{12} = k_{32} = \ell$ (say) and $k_{21} = k_{23} = m$ (say). This is quite reasonable since the passage of kinetic particles from state 2 to 1 or 3 now have to overcome the same energy barrier. This is also true for the kinetic particles in states 1 and 3. Thus, the kinetic scheme III simplifies to the following rate equations:

$$dx_1/dT = \theta^{-1}(\ell x_2 - m x_1) \tag{3.1}$$

$$dx_2/dT = \theta^{-1}(m x_1 + m x_3 - 2\ell x_2) \tag{3.2}$$

$$dx_3/dT = \theta^{-1}(\ell x_2 - m x_3) \tag{3.3}$$

If the initial concentrations of the chemical species 1 and 3 are the same, the three rate equations uncouple:

$$dx_1/dT = dx_3/dT = \theta^{-1}(\ell x_2 - m x_1) \tag{3.4}$$

$$dx_2/dT = -2\theta^{-1}(\ell x_2 - m x_1) \tag{3.5}$$

Using

$$2x_1 + x_2 = 1 \tag{3.6}$$

Eqs. (3.4) and (3.5) become

$$dx_1/dT = -\frac{1}{2}\, dx_2/dT = dx_3/dT = \theta^{-1}[\ell - x_1(2\ell + m)] \tag{3.7}$$

From Eq. (1.13), the rate constants ℓ and $m(\alpha = 1)$ are

$$\ell = \ell_o T \exp\ (-E_2/RT) \tag{3.8}$$

$$m = m_o T \exp\ (-E_1/RT) \tag{3.9}$$

Thus, Eq. (3.7) becomes

$$\frac{dx_1}{dT} = \theta^{-1} m_o T \exp(-E_1/RT) \left\{ \frac{\ell_o}{m_o} \exp(-\Delta E/RT) - x_1 \left[1 + \frac{2\ell_o}{m_o} \exp(-\Delta E/RT) \right] \right\} \tag{3.10}$$

with initial condition

$$\text{at} \quad T = T_o, \quad x_1 = x_{10} \tag{3.11}$$

Also, from Eq. (1.5)

$$C_P = - 2\Delta E \frac{dx_1}{dT} \tag{3.12}$$

where $\Delta E = E_2 - E_1$

Now Eqs. (3.10) and (3.12) may be solved numerically. This involves solving the differential Eq. (3.10) and substituting the values in Eq. (3.12). There are four parameters in the present example. These are ℓ_o, m_o, E_1 and ΔE. The difference in rotational energies is of the order of one or two Kcal/mole for most polymers. A convenient way of determining the other parameters is to curve fit the Cp measurements using differential thermal analysis (DTA). Since the number of the parameters is large, it may be necessary to conduct the experiments at a number of heating or cooling rates. However, an initial guess for E_1, ℓ_o and m_o may be obtained from the liquid hole theory. The value of E_1 chosen here is comparable to the hole energy for polystyrene (2).

The results for four heating rates ranging from 0.0001°C/sec to 0.1°C/sec are plotted in Figure 1. Table 1 lists the values of the various parameters. The initial starting temperature for the four heating rates is $T_o = 365°K$. It is desirable that the initial condition be picked close to the start of the heat capacity peak since it was assumed previously that the energies E_i do not depend on T over the small range of the glass transition. The curves shown in Figure 1 are plotted as the change in heat capacity. Since the DTA data is in arbitrary units, one is only interested in the change in the heat

capacity. In this particular example, the material is glassy at T_o.

The maximum of the curves in Figure 1 can be described by a simple relation.

$$T_m = a \log \theta + b \tag{3.13}$$

where a and b for this particular example are 3.2°C and 384.9°C, respectively. T_m for various heating rates are also given in Table 1.

4. Results and Proposal

The glass transition in polymers is discussed in terms of a kinetic rate process. The objective of the calculation given in Section 3 was to establish the feasibility of the proposed kinetic scheme. A sample calculation based on three rotational energy states predicted the shape of the heat capacity curve of polymers in the glass transition region (5). The temperature corresponding to the maximum heat capacity was shown to increase with increase in the heating rate. This is similar to observed behavior in polymers (2).

Based on the preliminary success of this model, a research project is proposed. The aim of this proposal is to experimentally verify the model. This can be achieved in the following manner. A polymer with known rotational energy states should be chosen for the study. The heat capacity measurements at various heating and cooling rates can be made using a differential thermal analyzer. The parameters in the model are then determined by curve fitting the data for a single heating or cooling rate. These parameters should predict the heat capacity data at other heating or cooling rates.

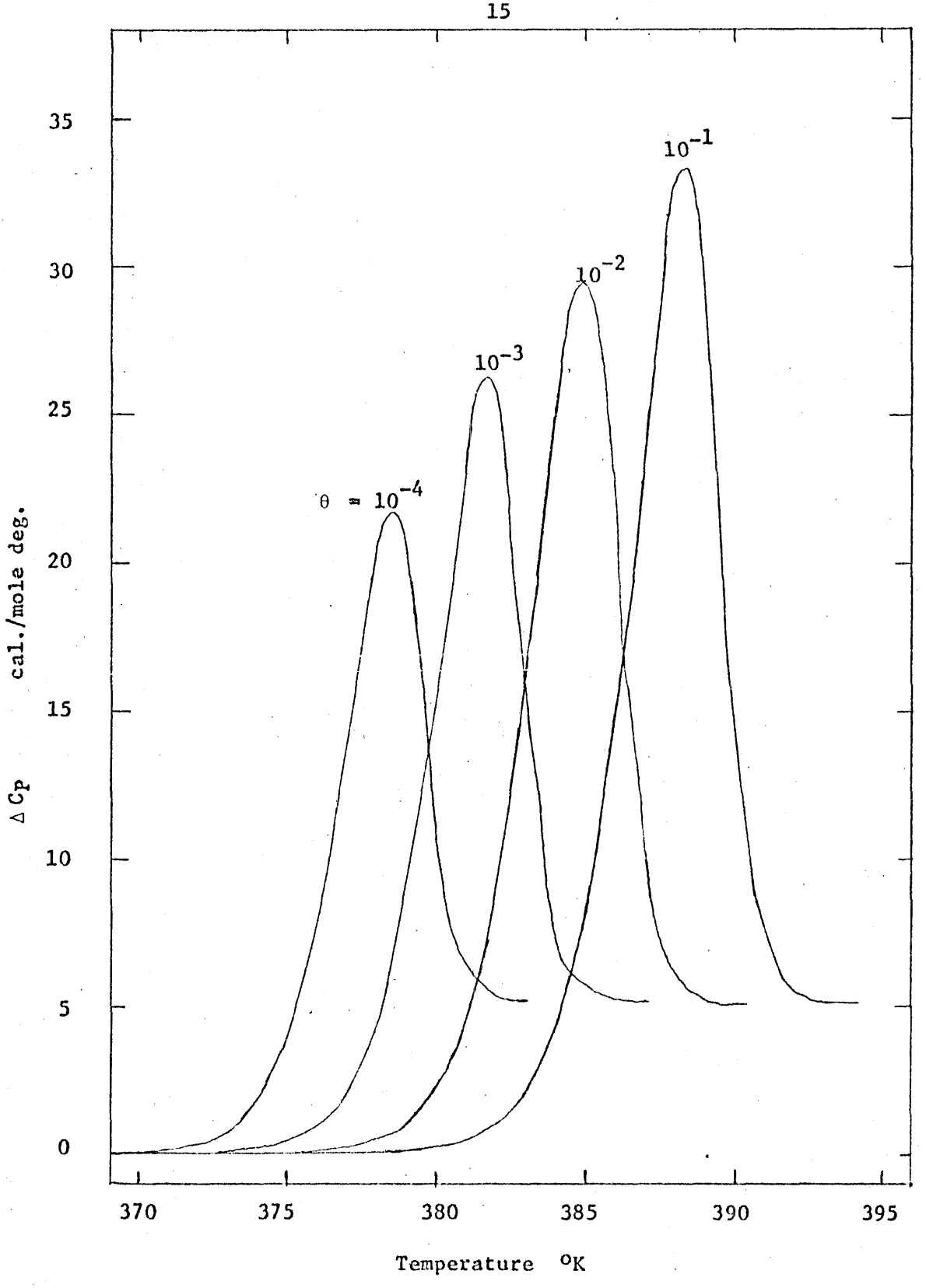

Fig. 1 Change in heat capacity vs. temperature for different heating rates.

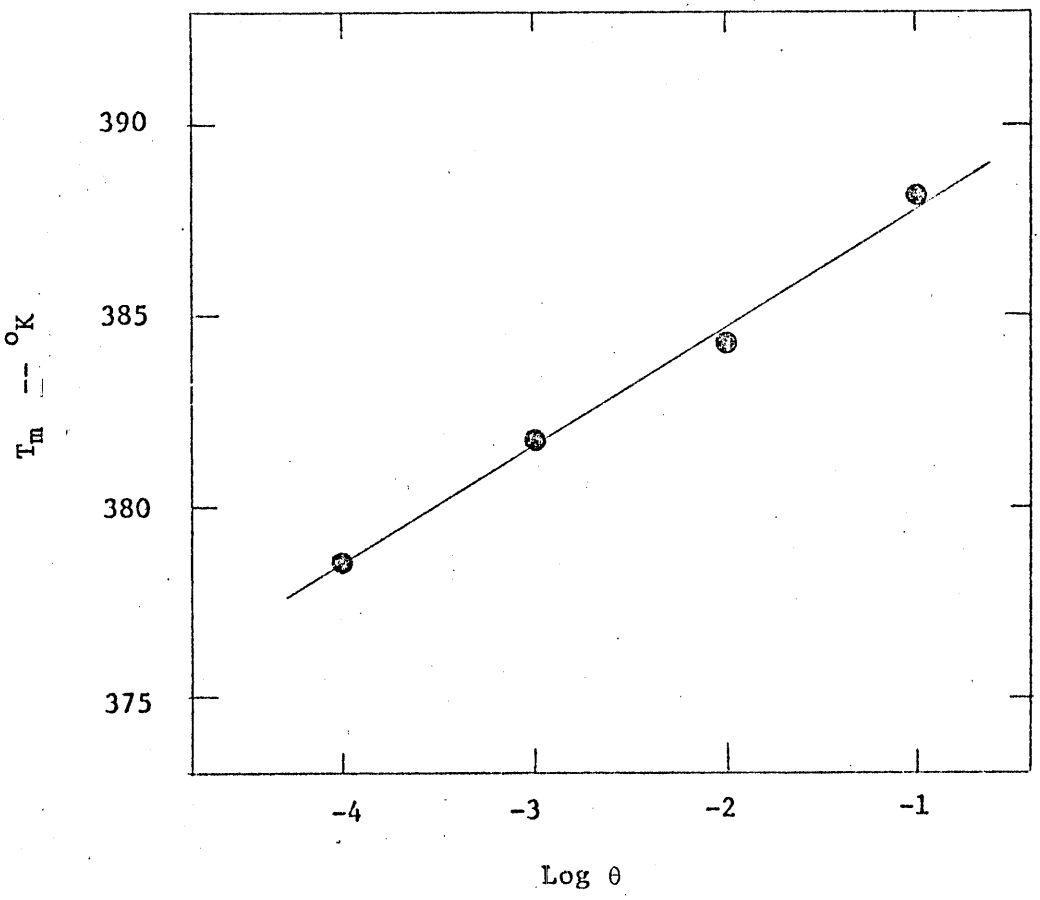

Fig. 2 Maximum temperature vs. logarithm of the heating rate.

TABLE 1

θ = 0.0001, 0.001, 0.01, 0.1 °C/sec

T_o = 365°K

x_{10} = 0.7

E = 1 K cal/mole

E_1 = 300 K cal/mole

$_o$ = 1.06×10^{-110}

m_o = 0.2×10^{-110}

θ	T °K
0.0001 °C/sec	378.5
0.001	381.7
0.01	384.0
0.1	388.3

References

1. M. V. Volkenstein and O. B. Ptitsyn, Soviet Phys.-Tech. Phys., 1, 2138 (1957).

2. B. Wunderlich, D. M. Bodily and M. H. Kaplan, J. Appl. Phys., 35, 95 (1964).

3. J. Wei and C. D. Prater, Advances in Catalysis, 13, 203 (1962).

4. O. Levenspiel, "Chemical Reaction Engineering", John Wiley and Sons, Inc., New York, 1962.

5. M. C. Shen and A. Eisenberg, Rubber Chem. Tech., 43, 95 (1970).

PROPOSITION II

A MODIFICATION TO THE PRESENT SCORING SYSTEM IN BRIDGE

A Modification to the Present Scoring System in Bridge*

Abstract

A modification designed to correct the drawbacks of the present scoring system in bridge is proposed. This assigns 30 points for the first trick and 20 points for the subsequent tricks in the minors. The modified scoring system is shown to be more competitive and fair.

* A summary submitted for publication in the bulletin of American Contract Bridge League.

Introduction

In this proposition a modification to the existing scoring system in bridge is suggested. The need for a modification arises from realizing that the present scoring system does not provide for the higher difficulty factor in making higher level contracts. In certain situations, the scoring system is even unfair and discourages competition. Also, there does not exist any clear scoring order in this system.

A highly desirable feature of any scoring system is the simplicity with which it can be used. It is an important criteria since the majority of the bridge players would not accept or approve any complex system, however fair and competitive it may be. It is perhaps possible to devise a very sound scoring system but it is very doubtful that such a system would be simple and easily adaptable. Thus, with simplicity as the most important objective, a modification to the present scoring system is being proposed.

Present Scoring System

This scoring system is based on the following. It assigns

1) 20 points for each trick* in the minor suits, i.e. in Clubs (C) or Diamonds (D);
2) 30 points for each trick* in the major suits, i.e. in Hearts (H) and Spades (S) and
3) 30 points for each trick* in no trump with the exception of the first trick which is assigned 40 points.

The steps 1, 2 and 3 are based on the ranking in the order Clubs, Diamonds, Hearts, Spades and No Trump, with the Clubs assigned the lowest rank. The following table gives a part of the scoring system of interest here:

Table 1

Level	# of Tricks	Minors	Majors	No Trump	
1	7	20	30	40	I
2	8	40	60	70	
3	9	60	90	100	
4	10	80	120	130	II
5	11	100	150	160	
6	12	120	180	190	III
7	13	140	210	220	

The first column in this table gives the level at which the contract is

* Points are counted for tricks over a minimum of six.

being played, the second column gives the number of tricks required in a given level and the remaining three columns give the scores depending on the suit in which the contract is being played. For the purpose of this discussion, bonuses, penalties, etc. will be omitted since these remain unchanged in both the present and the modified scoring systems.

In order to realize the drawbacks in the present scoring system, it is convenient to divide Table 1 in three sections. In section I the scores are less than 100 and are called "part scores". In section II the scores are equal to or greater than 100 and are called "game scores". In section III the scores are also greater than 100 but are called "slams" and are assigned high bonus points. Since in the new system the significant differences lie only in sections I and II, the discussion for section III will be omitted.

Considering the part scores first, an order based on the increasing scores may be written (m = Minor, M = Major and N = No Trump):

Order:	1m	1M	1N	2m	2M	2N	3m	3M	4m	A
Score:	20	30	40	40	60	70	60	90	80	

As is evident from A, the order breaks down beyond 2M. For example, a 4m contract is worth less points than a 3M contract, although one requires an extra trick to fulfill the 4m contract. This is like a double penalty. The 4m contract not only requires an extra trick, it is also worth 10 less points. A difference of 10 points may not make any difference in rubber (social) bridge but may result in getting a top score or a bottom score in the duplicate (competitive) bridge. The

same arguments apply when one compares the 3m contract with the 2N contract.

Thus, from I it is observed that there are two drawbacks as far as the part scores are concerned. These are the lack of any specific order and the neglect of the higher difficulty factor.

Now considering the game scores, the following order similar to A exists:

Order:	3N	4M	4N	5m	5M	5N	B
Score:	100	120	130	100	150	160	

In addition to lack of order, these scores have one major drawback. This is seen by comparing 3N and 5m, which are the minimum game scores. This system discourages playing the contracts in 5m. As a matter of fact, whenever possible it is preferred to play in 3N rather than 5m. No incentive or award is given for making two extra tricks in 5m.

Modified Scoring System

This scoring system is based on the following. It assigns

1) 20 points for each trick in the minor suits except the first trick which is assigned 30 points;
2) 30 points for each trick in the major suits and
3) 30 points for each trick in no trump with the exception of the first trick which is assigned 40 points.

A comparison with the existing scoring system reveals that the difference in the two systems exists only in step 1. The first trick in the minors is now assigned 30 points instead of 20 points.

Thus, in the modified system the format of the minor suits is made the same as the format of the no trump.

This modification originated when it was realized that in most bidding systems 1C and 1D (i.e. 1m) bids are artificial. Even when these are not artificial, very few contracts, if any, are ever played at the one level in the minors. As a matter of fact, in competition or duplicate bridge contracts of 1 in the minors or 1 in the majors are extremely rare. This implies that nothing will be lost if one were to modify the scores for the tricks at the first level. This observation suggests the modification proposed here.

The following table gives the modified scores. The old scores are given in parenthesis for comparison.

Table 2

Level	# of Tricks	Minors	Majors	No Trump	
1	7	30(20)	30	40	I
2	8	50(40)	60	70	
3	9	70(60)	90	100	
4	10	90(80)	120	130	II
5	11	110(100)	150	160	
6	12	130(120)	180	190	III
7	13	150(140)	210	220	

Once again considering the part scores first the following order is obtained:

Order:	1m	1M	1N	2m	2M	2N	3m	3M	4m	C
Score:	30	30	40	50	60	70	70	90	90	

Comparing A and C reveals that the drawbacks in A are corrected in C as far as the order in the part scores are concerned. Unlike the present scoring system this does not penalize twice. The scores are still simple to work with and always increase or remain equal to the scores at a lower level.

Another very interesting feature of the modified system is that it provides more competition in the following contracts:

1) 1N against 2m.

2) 2M against 3m.

Such a competition does not exist in the present scoring system. There is no incentive for playing the more difficult 2m or 3m contracts at present. Thus, the modified system attempts to correct this unfairness.

Now considering the game scores the following order may be written:

Order:	3N	4M	4N	5m	5M	5N	D
Score:	100	120	130	110	150	160	

Similar to B the order in the game scores in D is still not correct, but it does attempt to correct the drawback as far as the minimum game scores are concerned. It suffices to say that there is more competition between 3N and 5m. The higher difficulty factor in 5m is now awarded an additional 10 points.

In summary, the modification suggested here is an extensive

improvement on the existing scoring system. In addition to being fair and more competitive it maintains the simplistic nature of the present system.

PROPOSITION III

APPLICATION OF THE HEIL-PRAUSNITZ SOLUTION THEORY TO OSMOTIC PRESSURE DATA

Abstract

The solution theory of Heil-Prausnitz is applied to osmotic pressure data in polymers. A comparison with the well known Flory-Huggins theory is made. It is demonstrated that the Heil-Prausnitz theory applies over a much wider range of concentrations. It is also shown that unlike the parameter in the Flory-Huggins theory the parameters in the Heil-Prausnitz theory do not depend on concentration.

Introduction

The lattice theory of fluids has been derived for liquid mixtures where the molecules of the components of the mixture are approximately of the same size. One of the most useful applications is its extension to polymer solutions. The most widely known treatment of polymer solutions was derived independently by Flory(1,2) and Huggins(3,4,5). This theory has found wide applications in the physical chemistry of macromolecules. The basic concepts of the Flory-Huggins theory are quite similar to that of the lattice theory except that here the polymer molecule is assumed to behave like a chain consisting of a large number of segments, each segment being equal to the size of a solvent molecule. The theory itself suffers from objections arising out of physical considerations, since it does not account for intermolecular forces.

Many modifications(6,7,8) to the Flory-Huggins theory have been suggested, but the complexities of the results render them difficult to use. In addition, these require extensive data to determine numerous parameters. Recently Heil and Prausnitz(9,10) have derived a two parameter semi-empirical equation. The main objective of this work was to obtain an improved description of the thermodynamic properties of binary polymer solutions which would employ a relatively small number of parameters and could easily be extended to describe multicomponent behavior. No data were presented

comparing their results with other theories. At present, an obvious advantage of this treatment is a description of multicomponent systems based entirely on the knowledge of binary systems.

In this paper a study of the osmotic pressure of polymer solutions is intended and the existing data will be utilized to compare the Flory-Huggins and Heil-Prausnitz theories.

Flory-Huggins Theory

The polymer molecules in solution may be several thousand times larger than the sovent molecule. The Flory-Huggins theory assumes the polymer molecule to consist of s chain segments such that each segment occupies one site in the lattice. Thus the total number of sites are n_1+sn_2, where n_1 and n_2 are number of solvent and solute molecules. The main idea here is to calculate first the total configurational entropy of the polymer solution arising from the number of possible lattice configurations for a mixture of polymer molecules occupying s sites each and solvent molecules occupying single sites. Flory and Huggins have developed a theoretical expression for entropy of mixing:

$$\Delta S_m = -R(n_1 \ln \phi_1 + n_2 \ln \phi_2) \qquad (1)$$

where ϕ_1 and ϕ_2 are volume fractions of the solvent and the solute respectively. To obtain the free energy of mixing a semiempirical formula was assumed for heat of mixing

$$\Delta H_m = \chi \phi_1 \phi_2 (n_1 + sn_2)RT \qquad (2)$$

where χ is called the Flory interaction parameter. Equations (1) and (2) yield an expression for Gibbs free energy of mixing

$$\Delta G_m = RT(n_1 \ln \phi_1 + n_2 \ln \phi_2 + \chi \phi_1 \phi_2 (n_1 + s n_2) \qquad (3)$$

The main reason for the wide use of this expression is its simplicity coupled with only one experimentally determinable parameter. The theory requires that all the polymer molecules be identical with respect to the chain length, or molecular weight. This is hardly the case in most polymers. Also Flory and Huggins originally implied that the parameter χ had a single value for a particular system. Since then it has been realized that a unique value for the parameter χ may not be used due to its strong dependence on polymer concentration.

Heil-Prausnitz Theory

As already mentioned the theory of Flory-Huggins does not consider the intermolecular forces. In order to describe the properties of a solution in which the components differ not only in molecular size but also in intermolecular forces Wilson(11) developed the concept of local volome fractions. This idea was recently used by Heil and Prausintz to develop a semi-empirical solution theory.

The local volume fraction of solvent molecules about a central solvent molecule is

$$\epsilon_{11} = \frac{x_1}{x_1 + A x_2} \qquad (4)$$

The local volume fraction of polymer segments about a central polymer segment is

$$\epsilon_{22} = \frac{x_1}{B\,x_1 + x_2} \tag{5}$$

The local volume fraction of solvent molecules about a central polymer segment is

$$\epsilon_{12} = \frac{B\,x_1}{B\,x_1 + x_2} \tag{6}$$

The local volume fraction of polymer segments about a central solvent molecule is

$$\epsilon_{21} = \frac{A\,x_2}{x_1 + A\,x_2} \tag{7}$$

where A and B are given by

$$A = (V_2/V_1)\ \exp\ (-(g_{12} - g_{11})/RT) \tag{8}$$

$$B = (V_1/V_2)\ \exp\ (-(g_{12} - g_{22})/RT) \tag{9}$$

and x_1 and x_2 are the mole fractions of solvent and solute respectively. V_1 and V_2 represent the molar volumes of the solvent and solute respectively. The quantity g_{ij} is the molecular interaction energy between an i-j pair. These interaction energies give rise to two adjustable parameters for each binary system. These are $(g_{12}-g_{11})$ and $(g_{12}-g_{22})$. For convenience the following parameters will be used here:

$$G_1 = (g_{12} - g_{11})/RT \tag{10}$$

$$G_2 = (g_{12} - g_{22})/RT \tag{11}$$

Heil and Prausnitz expected the interaction energies to be

very weak functions of temperature and polymer concentration, but this has never been shown. However, it was found(9,10) that these two parameters were independent of polymer molecular weight. A new equation for the Gibbs free energy of mixing was proposed, based on the concept of local volume fraction

$$\Delta G_m = RT(n_1 \ln \epsilon_{11} + s\, n_2 \ln \epsilon_{22} + (1-s)\, n_2 \ln \phi_2 + n_1 \epsilon_{21} G_1 + s\, n_2 \epsilon_{12} G_2) \qquad (14)$$

Values of interaction energies g_{ij} are reported for a large number of systems. The above expression was proposed to meet the following requirements:

1) It was expected to give a reasonably accurate description of the chemical potential relative to polymer concentration.

2) It may be easily extended to polymer solutions of mixed solvents.

3) The parameters were expected to be uniquely defined and might be used over a wide range of polymer concentrations.

Heil and Prausnitz have extended the theory to multi-component behavior and have provided experimental data to meet the second requirement. The remaining objectives of this theory need to be assessed. This proposition yields information towards fulfilling the third requirement.

Data Analysis

A comparison of the aforementioned theories will be made utilizing osmotic pressure data of Flory and Krigbaum(12) for the polystyrene-toluene system. The chemical potential of the solvent on mixing is related to the osmotic pressure π by

$$\Delta\mu_1 = -\pi V_1 \tag{15}$$

From the definition

$$\Delta\mu_1 = \left(\frac{\partial \Delta G_m}{\partial n_1}\right)_{T,P,n_2} \tag{16}$$

theoretical expressions for chemical potential may be easily obtained:

A. Flory-Huggins Theory

$$\Delta\mu_1 = -\pi V_1 = RT\left[\ln (1-\phi_2) + (1-\frac{1}{s})\phi_2 + \chi\phi_2^2\right] \tag{17}$$

B. Heil-Prausnitz Theory

$$\Delta\mu_1 = -\pi V_1 = RT\left[\ln \frac{x_1}{x_1 + Ax_2} + \frac{Ax_2}{x_1 + Ax_2} - \frac{sBx_2}{Bx_1 + x_2} + (s-1)\frac{x_2V_1}{x_1V_1 + x_2V_2} + \frac{AG_1x_2}{x_1 + Ax_2} - \frac{AG_1x_1x_2}{(x_1 + Ax_2)^2} + \frac{sBG_2x_2}{(Bx_1 + x_2)} - \frac{sB^2G_2x_1x_2}{(Bx_1 + x_2)^2}\right] \tag{18}$$

The numerical evaluations made in this proposition consist of two major steps:

1. Evaluation of parameters in equations (17) and (18).
2. Use of these parameters for calculating the osmotic

pressure curves.

The parameters $(g_{12}-g_{11})$ and $(g_{12}-g_{22})$ for the polystyrene-toluene system have been reported by Heil and Prausnitz(9). Being independent of molecular weight, these parameters may be applied to different molecular weight samples of polystyrene in toluene. The values for $(g_{12}-g_{11})$ and $(g_{12}-g_{22})$ were obtained as follows. The vapor pressure of the solvent in solution is related to its chemical potential by

$$\Delta\mu_1 = RT\left[\ln \frac{P_1}{P_1^o} + \frac{B_1}{RT}(P_1 - P_1^o)\right] \qquad (19)$$

where P_1 = observed vapor pressure of the solvent in solution at equilibrium.

P_1^o = vapor presure of the pure solvent

B_1 = second virial coefficient

Equations (18) and (19) yield an expression which contains only two parameters at a constant temperature. Heil and Prausnitz used the vapor pressure data of Bawn and Freeman (13) to determine the two parameters. The data are shown in figure 1. The range of concentration for which the data were fitted are given in a later section. The same data are being used in this work to determine the Flory interaction parameter χ. From equations (17) and (19), one gets

$$\ln \frac{P_1}{P_1^o} + \frac{B_1}{RT}(P_1-P_1^o) = \ln (1-\phi_2) + (1-\frac{1}{s})\phi_2 + \phi_2^2 \qquad (20)$$

This equation may now be used to solve for χ. The results are given in figure (2). Contrary to the original theory(1)

χ is a very strong function of the polymer concentration in solution. The parameters so obtained are now used to illustrate the ability of equations (17) and (18) to represent the experimental data.

Flory and Krigbaum (12) obtained osmotic pressure data on various molecular weight samples of polystyrene in toluene. It is customary to present the osmotic pressure data as a plot of the quantity π/C_2 against C_2, where C_2 is the polymer concentration. The numerical procedure consists of picking different values of C_2 form the original data of Flory and Krigbaum and then evaluating π/C_2 using equations (17) and (18). As far as the Heil-Prausnitz theory is concerned the calculataions are trivial if we assume that the theory involves unique parameters. On the other hand in Flory-Huggins theory where the interaction parameter χ is a known function of ϕ_2 (figure 2), one of the following procedures may be used.

1. For each value of C_2 a different value of χ is employed according to figure 2.
2. Since the purpose of the calculaion is of a comparative nature, the limiting values of χ may be used.

The values of C_2 considered here correspond to a polymer fraction of less than 0.1. The value of χ is almost constant in this range (fig. 2) and is approximately the maximum value of χ. Hence, the second procedure, may be used since it will also give the information that would be obtained from the first.

Figures 3 to 5 were constructed in this manner for various molecular weight samples of polystyrene in toluene. A complete tabulation of all variables desired for the numerical calculation is provided in table 1.

Results

The results calculated for six different polystyrene samples are shown in figures 3,4 and 5. The dotted lines result from the Flory-Huggins theory for the limiting values of interaction parameter χ. The experimental results of Flory and Krigbaum(12) are represented by the points, through which a smooth curve has been drawn. The remaining line has been obtained from Heil-Prausnitz theory.

Heil and Prausnitz had expected their parameters to be independent of polymer concentration. As stated earlier, this has never been shown. The parameters for polystyrene-toluene system have been taken from the original work(9). These parameters were fitted for the concentration range of 0.26 to 0.89 weight fraction of the polystyrene in toluene. The same values are being used here to describe a concentration range of less than 0.1. Figures 3,4 and 5 clearly indicate that the parameters in the Heil-Prausnitz theory may be used for any concentration range with a reasonable reliability. The theory yields similar results in all six cases investigated. This emphasizes the generality of parameters in Heil-Prausnitz equation. On the other hand, the Flory-Huggins equation, where the concentration dependence of χ has been taken account of, does not give a good quantitative description of the osmotic pressure data. A value of the interaction parameter χ lying between the limiting values

might fit the experimental data, but would have no physical significance. Such a value will ignore the concentration dependence of χ and consequently would become a function of polymer molecular weight, since in such a case, different fractions of the polymer will require different χ values and will be a contradiction of the original Flory-Huggins theory.

It should also be realized that the same parameters in both theories yield similar results for different polymer molecular weights. For the success of any polymer solution theory, it is desirable that the parameters be either independent of the size of the polymer molecule or a very weak function of it. The author does not know of any work where χ was reported to be a function of the molecular weight. Concerning the parameters in Heil-Prausnitz theory, these have been shown independent of polymer molecular weight(9). This work supports the original conclusion.

In summary, the definite advantage of the Heil-Prausnitz theory over the Flory-Huggins theory has been demonstrated. It was also shown for the first time that the parameters in Heil-Prausnitz theory may be reliably used to describe the solution behavior over a wide range of concentrations.

Table 1

Polystyrene-toluene system

T	= 30°C
$(g_{12}-g_{11})$	= -53.03 cal/g.-mole
$(g_{12}-g_{22})$	= 158.4 cal/g.-mole
$\mathcal{S}_1$	= 0.857
$\mathcal{S}_2$	= 1.083
P	= 1 atm.
V_1	= Mol. wt. of solvent/$\mathcal{S}_1$
V_2	= Mol. wt. of polymer/$\mathcal{S}_2$
s	= Mol. wt. of polymer/Mol. wt. of repeating unit
R	= 1.987 cal/(g.-mole)(°K)

Concentration range for which $(g_{12}-g_{11})$ and $(g_{12}-g_{22})$ were fitted = 0.26 to 0.89 weight fraction of the polystyrene in toluene?

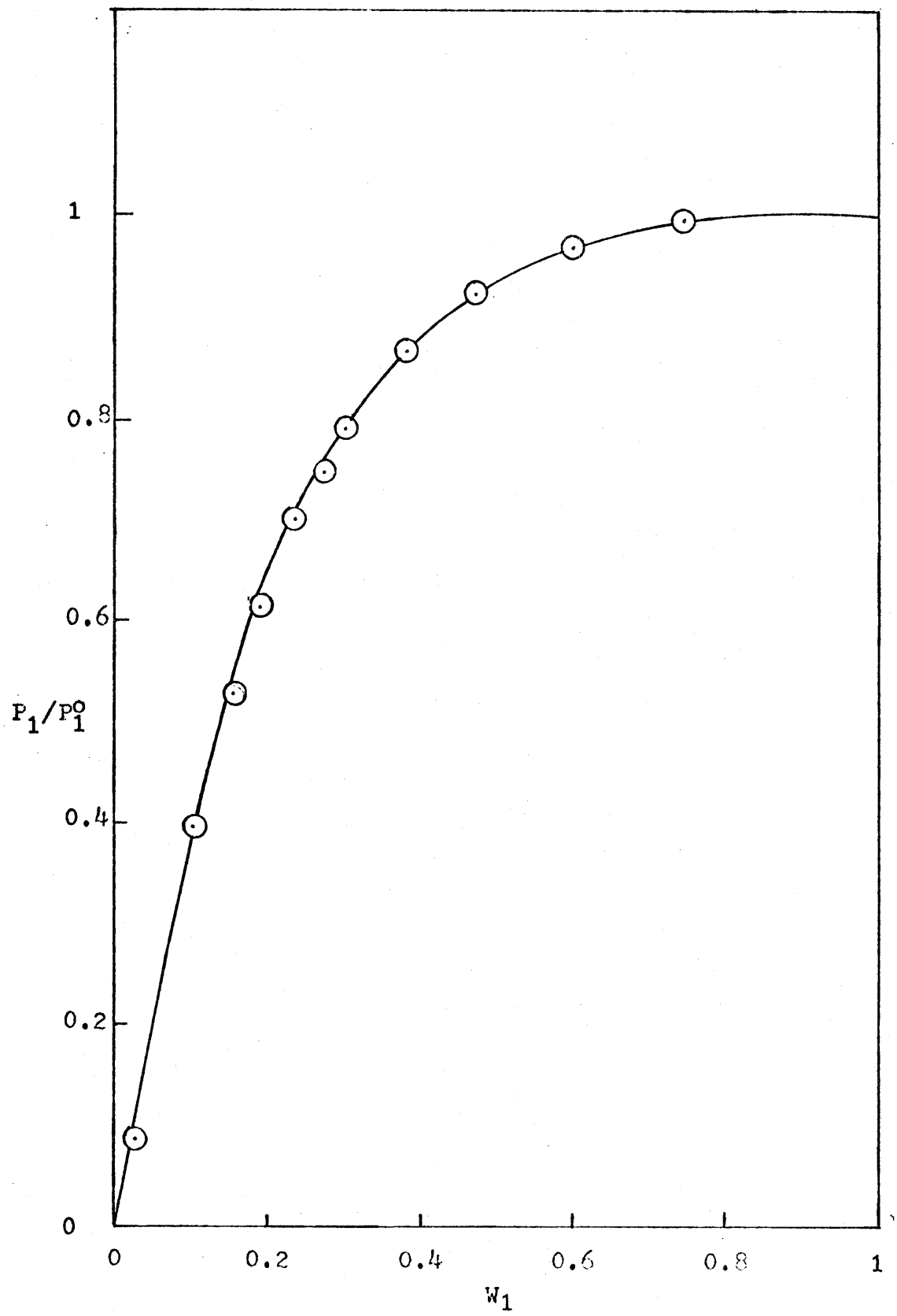

Fig. 1 Vapor pressure- weight fraction plot for polystyrene-toluene system

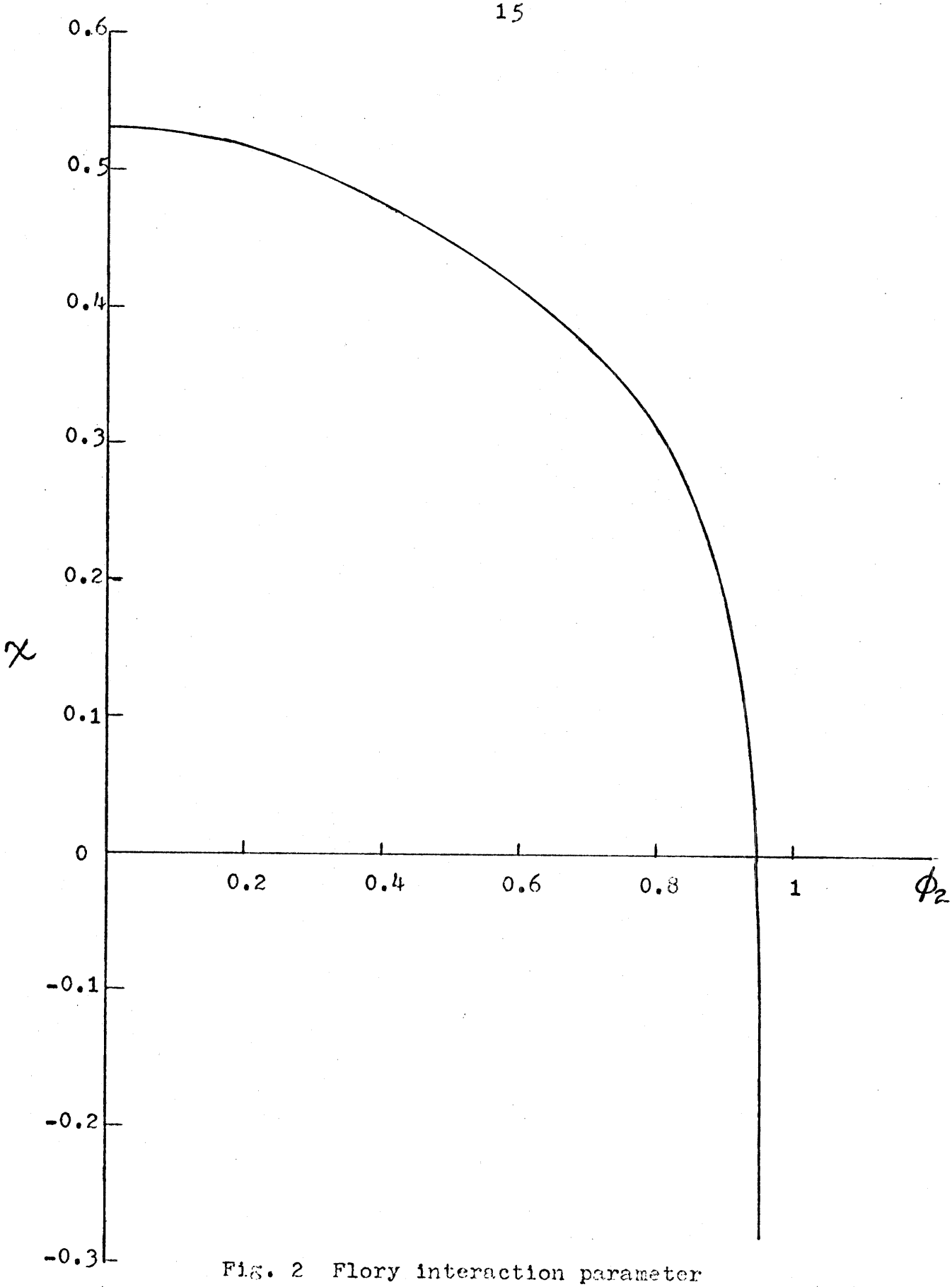

Fig. 2 Flory interaction parameter

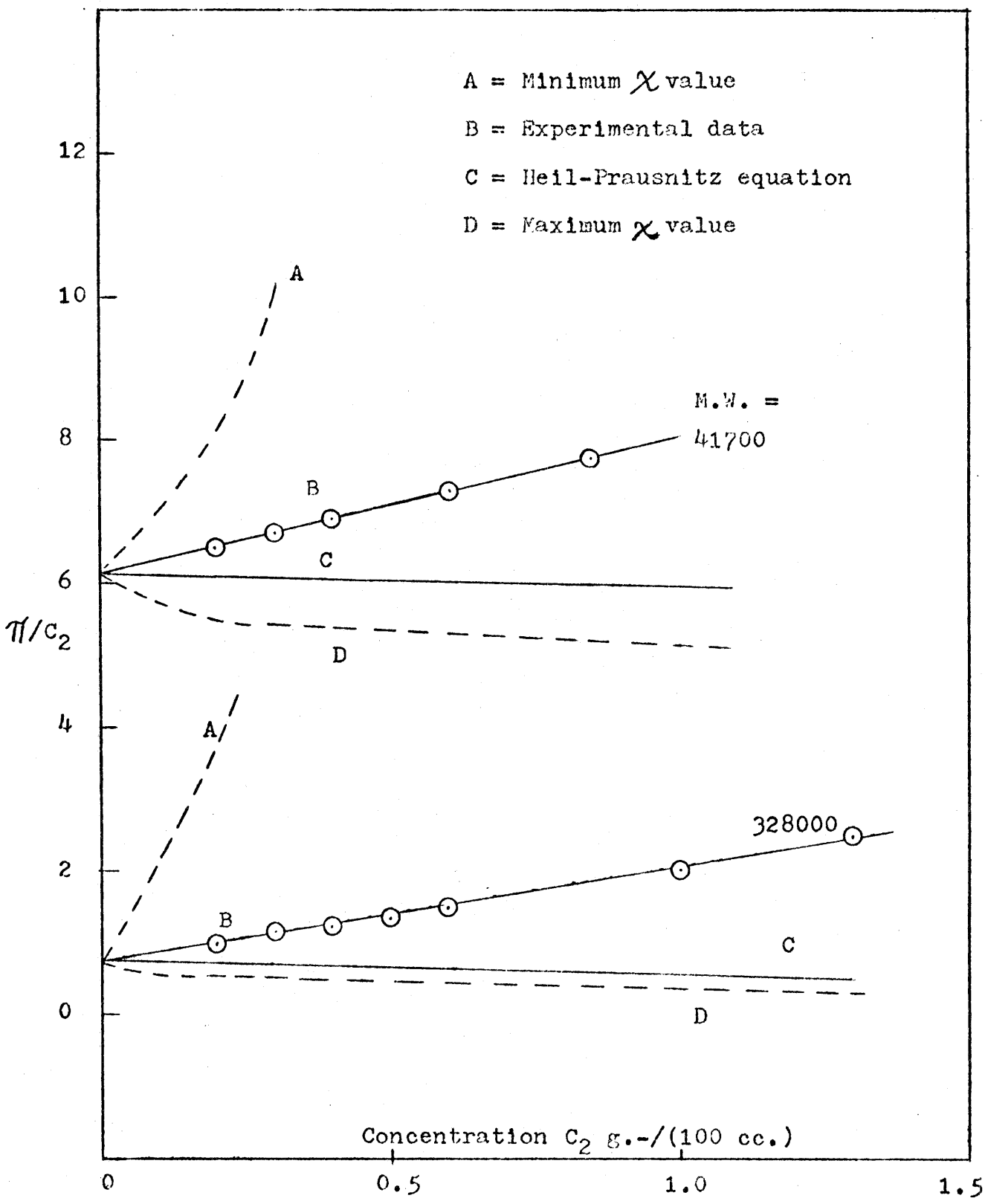

Fig. 3 Osmotic pressure plot

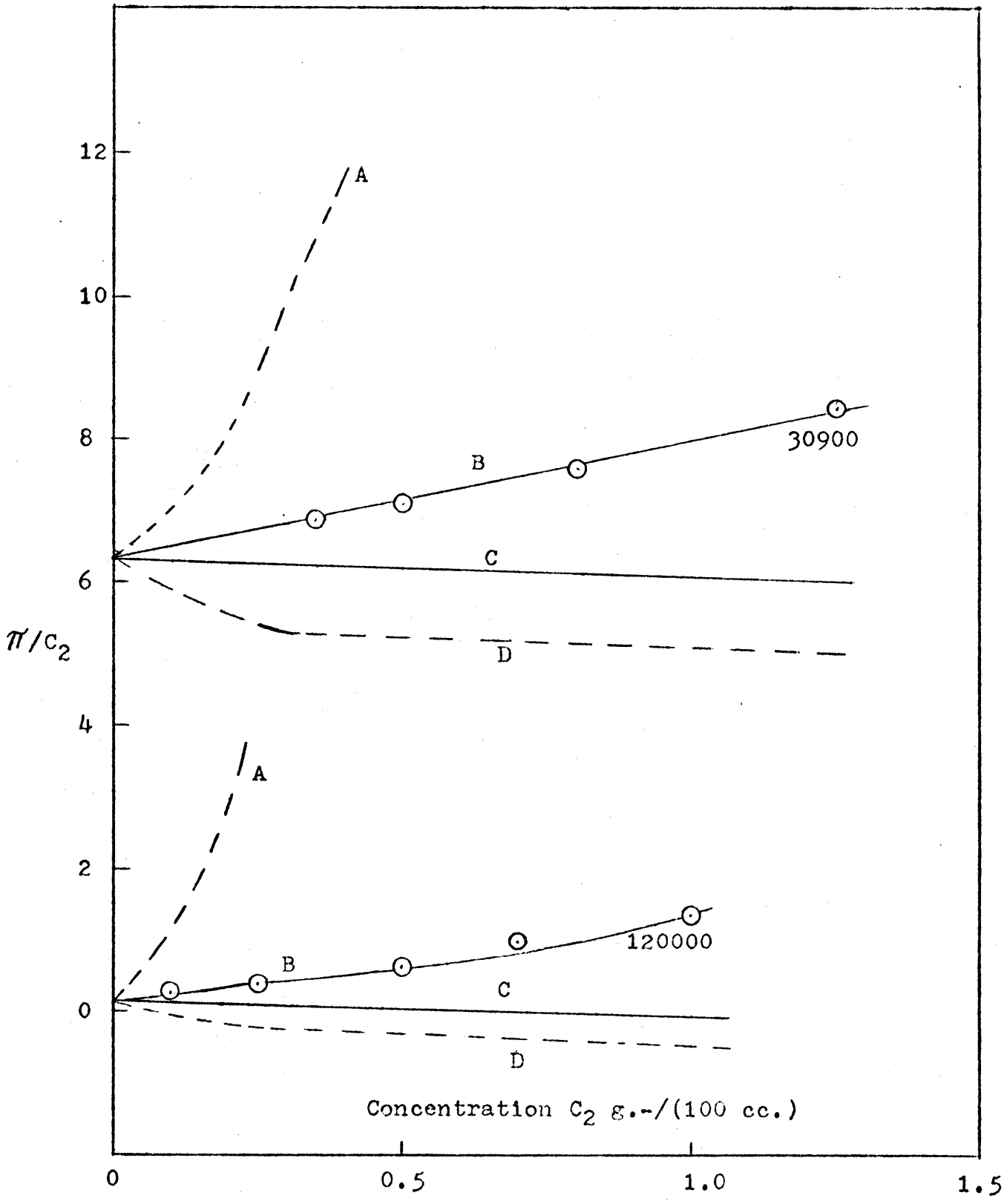

Fig. 4 Osmotic pressure plot

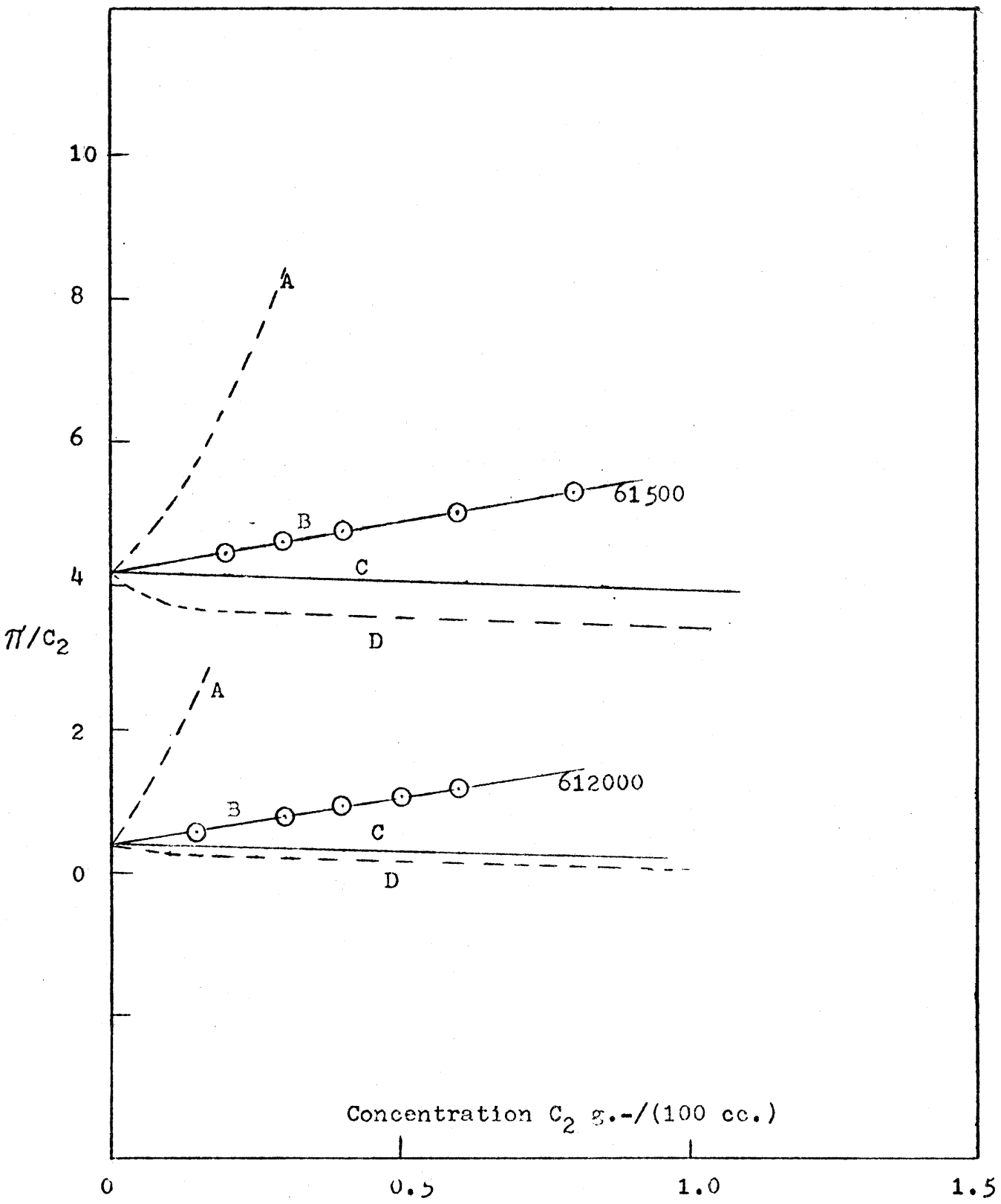

Fig. 5 Osmotic pressure plot

Notation

1 = subscript for solvent

2 = subscript for polymer

ϕ = volume fraction

χ = Flory interaction parameter

ε_{ij} = local volume fraction

μ = chemical potential

π = osmotic pressure

ρ = density

B_1 = second virial coefficient

C = concentration

H_m = heat of mixing

S_m = entropy of mixing

G_m = Gibbs energy of mixing

P = pressure

P_1 = observed vapor pressure of solvent in equilibrium with the solution

P_1^o = vapor pressure of pure solvent

g_{ij} = energy of i-j molecular interaction

V = molar volume

T = temperature

x = mole fraction

R = universal gas constant

s = number of segments per polysegmented molecule

n = number of molecules

References

1. P. J. Flory, J. Chem. Phys., 10,51(1962).
2. P. J. Flory, J. Chem. Phys., 9,660(1941).
3. M. L. Huggins, J. Am. Chem. Soc., 86,3535(1964)
4. M. L. Huggins, J. Chem. Phys., 9,440(1941).
5. M. L. Huggins, Ann. N.Y. Acad. Sci., 43,1(1942).
6. M. L. Huggins, Physical Chemistry of High Polymers, J. Wiley & Sons. New York(1958).
7. J. H. Hildebrand and R. L. Scott, The solubility of Non-electrolytes, Reinhold, New York(1950).
8. E. A. Guggenheim, Mixtures, Oxford Press, 1958.
9. J. F. Heil and J. M. Prausnitz, A.I.Ch.E. Journal,12,678 (1966).
10. J. F. Heil, Doctrol dissertation, Univ. California, Berkeley(1965).
11. G. M. Wilson, J. Am. Chem. Soc., 86,127(1964).
12. W. R. Krigbaum and P. J. Flory, J. Am. Chem. Soc., 75,1775(1953).
13. C. E. H. Bawn and R. Freeman, Trans. Faraday Soc., 46,677(1950).